

# A review on the oldest known gas-hydrate - The chemistry of chlorine hydrate

László Kótai<sup>1,2,\*,#</sup>, István Gács<sup>1</sup>, Szabolcs Bálint<sup>1</sup>, Györgyi Lakatos<sup>2</sup>, Andras Angyal<sup>3</sup>  
and Raj N. Mehrotra<sup>4,\*,§</sup>

<sup>1</sup>Chemical Research Center, Hungarian Academy of Sciences, Pusztaszeri u. 59-67, Budapest, H-1025, <sup>2</sup>Deuton-X Ltd., Selmei u. 89., Érd, H-2030, <sup>3</sup>Axial-Chem Ltd., Sajóbáony-Gyártelep, H-3792, Hungary. <sup>4</sup>Department of Chemistry, J. N. V. University, Jodhpur 342 005, Rajasthan, India

## ABSTRACT

In the last century a lot of new findings were reported in the field of chlorine hydrate - the oldest known compound belonging to the so called gas hydrates. Chlorine hydrate was a very interesting compound which engages an elemental chlorine molecule in a water clathrate cage causing changes in the reactivity of the chlorine and ensuring storage in solid phase at room temperature even at mild overpressures (6 atm). Chlorine hydrate, however, decomposes at atmospheric pressure around 8°C. It therefore acts as a solid phase carrier for chlorination with gaseous chlorine in aqueous medium, e.g. as battery chlorine electrode material, chlorinating and disinfecting agents etc. This review summarizes the investigation results from the oldest publication of Davy in 1811 up to the beginning of the decade, and some unpublished new results as well.

**KEYWORDS:** chlorine hydrate, non-stoichiometric clathrate hydrates

## 1. INTRODUCTION

The chlorine hydrate - a non-stoichiometric clathrate compound having elemental chlorine molecule

encaged in water molecules - was discovered a little over 200 years ago by *Humphry Davy* when he investigated the so-called “oxymuriatic acid gas” (chlorine) formed by the action of hydrochloric acid on pyrolusite (MnO<sub>2</sub>) [1]. Although the formation of “oxymuriatic gas” (chlorine) was first observed by *Scheele* in 1774, who believed that the gas was a mixture containing oxygen [2], *Gay Lussac* and *Thénard* considered the possibility that it might be an element, after their attempt to separate the oxygen by reacting it with charcoal failed [3, 4]. *Davy* repeated the experiment in 1811 and declared it an element naming it chlorine. Since *Davy* cooled the gas over an aqueous solution, he was credited with producing the first synthetic solid gas hydrate at 10°C. Ever since, chlorine hydrates, popularly called “chlorine ice” has been the subject of consistent investigations. *Davy* reported that the aqueous solution of chlorine freezes more readily than pure water, but the pure gas dried over calcium chloride underwent no change whatever, at temperatures below -30°C. The intensive development of the chemistry of chlorine hydrate started from this point.

## 2. General description and properties

*Thénard* [4] described chlorine hydrate as a solid formed during the cooling of the aqueous solution of chlorine. The bright yellow coloured crystals liquefied at slightly increased temperature releasing

---

\*Corresponding authors

# kotail@chemres.hu

§ raj\_n\_mehrotra@yahoo.co.uk

the chlorine gas in abundance. Faraday studied the chlorine hydrate in detail, and determined not only its composition (see section 5) but studied its properties as well [5, 6, 7]. Although the dry chlorine hydrate has high chlorine content, it has a much weaker chlorine smell than a 0.7 per cent aqueous chlorine solution. This was explained by the reduced vapour pressure of the chlorine captured in the hydrate state [8].

Chlorine hydrate was formed as crystallised crust or dendritic crystalline mass when chlorine gas was introduced in less than the sufficient amount of water to convert it into hydrate [5]. Crystals left below 0°C for a few days sublimed with the formation of large brilliant crystals which are delicate prismatic needles extending from 1.25 cm to 5 cm. The shorter ones were also formed as flattened octahedral, and the three axes of the octahedron had different dimensions [5].

Biewend observed formation of chlorine hydrate from water and chlorine gas at around 0°C as thin slurry of lamellar crystals [9]. These crystals decomposed on heating. The chlorine hydrate formed from liquid chlorine and water at 0°C, formed feather-like crystals [9]; however, at room temperature large beautiful crystals were obtained [9, 10].

Nordenskjöld left a chlorine hydrate filled bottle on a cold window during a winter period (when high temperature gradient takes place between the parts of the bottle). The chlorine hydrate then gradually deposited well-framed crystals on the cooler part of the bottle by slow sublimation. These crystals belonged to the rhombic system,  $a:b:c = 1:0.7038:0.6924$ . Beside the rhombic crystals, there were other crystalline forms. Nordenskjöld found the following crystallographic parameters:  $b:x = 134^{\circ}32'$ ,  $x:x^1 = 90^{\circ}56'$ ,  $a:y = 124^{\circ}42'$ , and  $y:y^1 = 110^{\circ}36'$  [11]. The shape of the formed crystals can be seen in Figure 1.

Rammelsberg repeated Nordenskjöld experiments and studied the large chlorine hydrate crystals under polarized light using a microscope. These crystals were orthorhombic or clinorhombic [12].

The crystallization process of the chlorine hydrate was studied by Ditte [13] in detail using the Faraday method [5-7] to prepare liquid chlorine from the hydrate. Chlorine hydrate containing

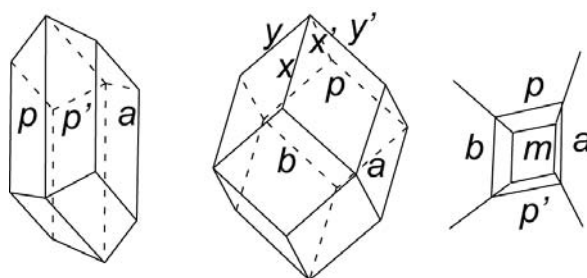


**Figure 1.** The shape of chlorine hydrate crystals found by Nordenskjöld [11].

excess water was placed into one of the arms of a closed large V-shaped tube which was then heated to decompose the hydrate. The liquefied chlorine condensed in the other arm which was kept cold. Re-formation of a small amount of hydrate in water could be observed after slow cooling for 24 h. The bulk of the liquefied chlorine remained in the arm where it had condensed. The small crystals of hydrate produced in the middle of the water had a shape of grouped in clusters or feather-like fern leaves. The materials inside the tube changed slowly when the branch containing the mixture of water and hydrate was immersed in a vase filled with water, while the other part containing the liquid chlorine was left exposed to the ambient air. The amount of the hydrate formed in the water first increased and then after about a month the hydrate formed cakes and a kind of crystallised membrane on the surface of the liquid, twisted and folded. A certain amount of the hydrate had deposited on the walls of the curved portion of the V tube. The reason for the appearance of the hydrate at the curved part between the two layers of the liquid chlorine was that this part was in contact with the atmosphere of chlorine gas at temperatures between 8 and 12°C. Under these conditions, the hydrate deposition had spread over a length of the tube (0.20-0.25 part) and the fern leaf gradually changed into isolated crystals. Most of these reached a size of >3 mm in length by the end of one year.

All the crystals, smaller and larger, were found to be crisp and perfectly transparent, and had dark greenish yellow colour. The crystals were relatively refractive because these showed some iridescent colours when viewed in sunlight; their

shape seemed to have been derived from the regular system. Perfect octahedral or other modification of the crystals where the general shapes have been altered could be observed. These crystals are plates with very developed appearance of both sides, which are completed with a regular hexagonal contour [13].

Depending on the synthesis conditions, Maumene [14] found cubic chlorine hydrate crystals prepared directly by introducing chlorine gas into water or a mixture of liquefied chlorine and water. However, octahedral but orthorhombic chlorine hydrate crystals were formed when a warm chlorine saturated solution was left to evaporate and condense into a cold part of the apparatus (reaction of chlorine gas and water vapour). The faces of these crystals showed that these developed very irregularly. However, the hydrate was formed with variable composition when a warm solution of dissolved chlorine was placed in a large branch of a tube and was left to escape slowly into the cooled small branch of the same tube [14].

Chlorine hydrate induces the crystallizations of cubic  $\text{SO}_2 \cdot 6\text{H}_2\text{O}$ ,  $\text{CH}_3\text{Cl} \cdot 6\text{H}_2\text{O}$  and the crystallization of the chlorine hydrate at  $0^\circ\text{C}$  [15]. This shows their isomorphous character. The polarized light does not act on chlorine hydrate crystals, but other crystalline forms often appear which could not be observed in the case of other gas hydrates [16].

### 2.1. Solubility of chlorine hydrate

Faraday observed that during the preparation of chlorine hydrate by cooling the chlorine solution, a portion of the chlorine remained in the solution and the crystals formed had dissolved slowly as well. The latter could be attributed to the higher solubility of the chlorine hydrate compared to that of the chlorine [5]. Gay-Lussac [17] observed an inflection point on the solubility curve of chlorine at  $8^\circ\text{C}$ . This indicated increased dissolution of the chlorine hydrate in water with rising temperature. However, above  $8^\circ\text{C}$  (the upper limit for the existence of the hydrate at atmospheric pressure), it was only the chlorine that dissolved in water and the solubility decreased with increasing temperature and became zero at  $100^\circ\text{C}$  [18]. This justified the observations of Isambert [19] and Roozeboom [20]. At temperatures lower than  $9^\circ\text{C}$

**Table 1.** The solubility (g/100 g of water) of chlorine and chlorine hydrate.

Temperature	$^\circ\text{C}$ Solubility [22]	g/100g $\text{H}_2\text{O}$ [20, 21]
0	0.5598	0.507
1	0.6017	-
2	0.6444	-
3	0.6878	0.615
4	0.7320	-
5	0.7770	-
6	0.8228	0.714
7	0.8694	-
8	0.9167	-
9	0.9648	0.908
12.5	1.112	-
20	1.853	-
28.5	3.627	-
$\text{Cl}_2$ gas solubility	g/100 g of $\text{H}_2\text{O}$ [23]	
10.00	1.00	
20.00	0.72	
25.00	0.64	

only the hydrate was formed and dissolved in water, but above this temperature at normal pressure only the dissolution of the chlorine gas in water was observed [20, 21].

The numerical solubility values of the chlorine hydrate were determined by Winkler [22] and Roozeboom [20] as a function of temperature. These results are given in Table 1.

Winkler found [22] that the dissolved amount of chlorine did not change with the chlorine pressure above the hydrate crystal containing chlorine solutions. Thus, the chlorine did not follow the Henry Dalton law between  $0$  and  $9^\circ\text{C}$  if chlorine hydrate was present in a closed system. In this system the excess of the chlorine hydrate dissolved and decomposed when the pressure was decreased to supply the solution with fresh chlorine. On the other hand, chlorine hydrate crystallised out when the pressure was increased (see section 3). It meant that the dissolved

chlorine content (between 0 and 9°C) can be considered to be the chlorine content of the dissolved chlorine hydrate. The solubility of the chlorine hydrate in water was expressed by equation 1 [22].

$$s = 0.5598 + 0.04154t + 0.0003842t^2 \quad (1)$$

where  $t$  is the temperature in °C,  $s$  is the solubility in g of chlorine hydrate in 100 g of water.

## 2.2. Density of chlorine hydrate

Faraday, by floating the hydrate crystals over calcium chloride solutions of various concentrations, found that the density of the plate like hydrate was  $d = 1.2 \text{ g cm}^{-3}$  [5]. Since he observed continuous slight liberation of gas, and the imperceptible bubbles could have adhered to the hydrate surface, therefore, the density could be presumed to be less than  $d = 1.2 \text{ g cm}^{-3}$ . Using the methods of Kótai *et al.* [23], the formula of these type of chlorine hydrate crystals prepared by Faraday should have  $\text{Cl}_2 < 7.63\text{H}_2\text{O}$ . The highest experimentally determined density ( $1.31 \text{ g cm}^{-3}$ ) of the isolated chlorine hydrate was reported by Smirnov and Kleshchunov [24]. This density provided the composition of the hydrate to be  $\text{Cl}_2.6.01\text{H}_2\text{O}$  [23], which was close to the  $\text{Cl}_2.6.2\text{H}_2\text{O}$  obtained by the authors [24].

In capillaries the density of the hydrate showed a value of  $1.37 \text{ g cm}^{-3}$ . This value was too large even in case of complete occupation ( $8\text{Cl}_2.46\text{H}_2\text{O}$ ) which would give  $d = 1.325 \text{ g cm}^{-3}$ . It means that the lattice of the chlorine hydrate in the capillaries is to be contracted ( $a = 1.192 \text{ \AA}$ ) or the difference between the molar volumes of the empty clathrate cage and the ice should be diminished from the average  $3.1$  to  $2.5 \text{ cm}^3/\text{mol}$  (see section 5.2.3) [23]. These differences in the lattice constant and molar volume values are too high. No example for this magnitude of contraction among the clathrates, even at higher pressures than the observed 10-12 atm in the capillaries, could be found. The perfect filling of the cavities should cause dilatation rather than contraction. Therefore, the hydrate formed in the capillaries probably does not belong to the clathrate type [23].

Roozeboom [20] experimentally determined the density of two samples of crystalline hydrate to be

$d = 1.220$  and  $1.237 \text{ g cm}^{-3}$ . Based on these values, the calculated formula [23] proved to be  $\text{Cl}_2.7.24\text{H}_2\text{O}$  and  $\text{Cl}_2.6.97\text{H}_2\text{O}$  respectively. This indicated that the water content might have been less than what Roozeboom had observed experimentally [20].

The chlorine hydrate prepared in zinc chloride solutions can be compacted and stabilised with 60-80 atm pressure. If the pressure is less than 60 atm, the density falls below  $1 \text{ g cm}^{-3}$ , but at 70 atm the value increases to  $1.1-1.15 \text{ g cm}^{-3}$  and becomes  $1.1-1.2 \text{ g cm}^{-3}$  at 80 atm. Above 800 atm the value of the density was  $d = 1.21-1.22 \text{ g cm}^{-3}$ . Further increase in the pressure does not result in significant increase in the density value [25]. The hydrate prepared in water has a higher chlorine content and its density at 800 atm was found to be  $d = 1.23 \text{ g cm}^{-3}$  [25].

## 2.3. Stability and decomposition of chlorine hydrate

The stability of the hydrate was strongly dependent on its composition, the more chlorine fills the cavities, the more stable was the hydrate formed [23]. The hydrate was a thermally unstable compound, it has an upper temperature existence limit (incongruent melting, see section 3). The chlorine molecule in the hydrate behaves as elementary chlorine and was therefore sensitive to hydrolysis which was an equilibrium reaction (see section 2.5.1). One of its hydrolysis products was the unstable hypochlorous acid which easily decomposed thermally or by light. Therefore the equilibrium can be shifted to complete decomposition.

### 2.3.1. Stability of the chlorine hydrate

The hydrate decomposed when it was in contact with metal chloride solutions at lower temperatures than in pure water [25]. The stability can be increased easily by compressing the hydrate at high pressures. At around 115 atm not only the bulk density increased but the stability as well. A body of chlorine hydrate (86 cm of diameter, 1.6 cm of height and  $61 \text{ cm}^2$  of surface area) completely decomposed at room temperature in 6 hours. The decomposition rate was not completely linear: roughly 50 or 60% of the decomposition took place after 2.5 or 3.5 h, respectively [25].

### 2.3.2. Thermal decomposition of the hydrate

Solid and dried hydrate decomposes on heating to liquid chlorine containing dissolved water and liquid water containing dissolved chlorine as was first observed by Faraday [5-7] and studied by Biewend [9]. Faraday heated the chlorine hydrate in a closed ampoule up to 37°C when a bright yellow gas formed together with two fluid phases, among which the lower phase was the liquid chlorine, the amount of which increased as the mixture was cooled [6, 7]. The reaction was found to be reversible [6, 7, 9]. The first experiment by using the hydrate as a chlorine source was performed in 1838, when Biewend made chlorine hydrate from water and chlorine gas at 0°C in a sealed tube, then warmed the tube to 30-40°C [9]. During the effervescent melting of the chlorine hydrate, the empty part of the tube was filled with the dark yellow chlorine gas, while the crystal scales dissolved with the formation of dark yellow oily drops of anhydrous condensed chlorine falling to the bottom as a yellowish liquid. The chlorine separated from the water combined again with the water below 0°C to form chlorine hydrate to a small extent (if mixing was avoided). This hydrate formed fine feather-shaped material, thus the remaining chlorine was enclosed by water. Crystalline chlorine hydrate can be obtained at ordinary temperatures by using the same glass tube without heating. Only a small portion of the chlorine hydrate melts, the rest was gradually produced as beautiful crystals [9].

The results were confirmed by Wöhler [10], who observed that in a sealed glass tube the hydrate maintained itself even at summer temperature due to the overpressure of the compressed chlorine liberated by the partial decomposition of the hydrate. If the tube containing this mixture was immersed into water at 30 to 40°C, the hydrate decomposed into water, and the liquid chlorine was sedimented. If the tube was placed back to normal air temperature, the hydrate was gradually regenerated. Even summer turns the liquid chlorine into crystallised hydrate again [10].

### 2.4. Chemical reactions of the chlorine hydrate

Depending on the pressure and temperature relationship, the hydrate decomposes into chlorine in water or liquefied chlorine containing water.

Hence, the main chemical reaction of the hydrate was definitely the same as the chemical reactions of the chlorine in the presence of water (aqueous solution).

#### 2.4.1. Decomposition by hydrolysis

Faraday had observed some negative effect of the light on the yield of the hydrate [5]. At atmospheric pressure the hydrate was partially decomposed by light with the evolution of some oxygen [10]. There was no diminution in volume of the liquid chlorine when the hydrate in a sealed tube was exposed to sunlight for a whole day and then heated to decompose into water and liquid chlorine. When the tube was brought back to ordinary temperatures the liquid chlorine gradually reunited with the water and crystalline hydrate was formed [10].

Normally, the dissociation of the chlorine hydrate in dilute solutions was represented by equation (2).



The electrical conductivity of such solutions at 0°C was equal to that of a water solution containing the same amount of hydrogen chloride, because hypochlorous acid was not considered to be an electrolyte. In more concentrated solution, the conductivity of the chlorine was much less. Since the dissociation of the chlorine takes place with the absorption of heat, dissociation increases with the temperature. The addition of 0.1-0.5 M solution of hydrochloric acid prevents the formation of chlorine hydrate. An addition of 1-2 M HCl, however, induces a stronger absorption of the chlorine on account of the formation of  $\text{HCl}_3$  [26, 27].

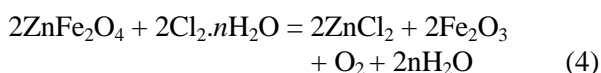
#### 2.4.2. Reactions with inorganic substances

Chlorine hydrate reacts with ammonia or ammonium salts with the formation of nitrogen gas, hydrochloric acid and a small amount of nitrogen chlorides [5]. Faraday also observed that the amount of nitrogen chlorides are less in the reaction of ammonia than in the reaction of ammonium salts [5].

The hydrate reacted with elementary mercury with the formation of a large amount of  $\text{HgCl}_2$  [8, 28] due to the chlorination effect of the highly

condensed chlorine toward primarily formed mercurous chloride ( $\text{Hg}_2\text{Cl}_2$ ) [28].

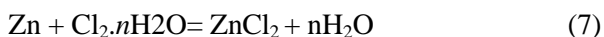
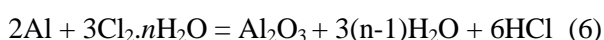
Aqueous solution of the hydrate (which was more concentrated than the chlorine solution) reacted easily with zinc oxide, equation (3), and zinc ferrite, equation (4). However, it did not react with  $\text{Fe}_2\text{O}_3$ ,  $\text{Al}_2\text{O}_3$  or  $\text{MnO}_2$  [29].



In contrast with  $\text{Fe}_2\text{O}_3$ ,  $\text{FeO}$  easily reacted with the hydrate forming  $\text{FeCl}_2$  [30]. The free enthalpy change in this reaction was negative (see section 7.2.2), and the primarily formed  $\text{FeCl}_2$  was easily chlorinated into iron(III) chloride as in equation (5).



Metallic aluminium and elementary zinc are oxidized into aluminium oxide, equation (6), and zinc(II) chloride as in equation (7) [29].



These reactions proceed easily between 0 and 9°C in the existence range of the hydrate solution [29].

Its reaction with iodides liberates a quantitative amount of elementary iodine which can be used for the determination of the chlorine content of the hydrate [20, 31, 32, 33].

#### 2.4.3. Reaction with organic substances

Chlorine hydrate reacts with ethyl alcohol when the temperature of the reaction mixtures is raised up to 45-65°C. Diethyl ether and hydrochloric acid are formed together with some chlorinated hydrocarbon compound. The reaction was strongly exothermic [5].

### 3. Phase relations of the chlorine hydrate

The chlorine hydrate neither decomposes nor dissolves completely below 9°C in a closed tube at normal pressure. It was, however, destroyed at ~9°C when the tension of the dissociation was roughly equal to the atmospheric pressure.

However, it was reformed under pressure at temperatures higher than 9°C as a ball-like solid even at 13 or 14°C [19]. Therefore the knowledge of its dissociation pressure as a function of temperature becomes essential [19].

#### 3.1. Experimental dissociation pressure of the chlorine hydrate

The dissociation pressure of the chlorine hydrate was measured first by Isambert [19], later by Le Chatelier [34], Roozeboom [20], Bouzat [35], Tamman and Krige [36] and Bozzo *et al.* [37, 38, 39], whereas Wilms and Van Haute studied the decomposition process in detail [40, 41].

##### 3.1.1. The dissociation in pure water

Le Chatelier measured the dissociation tension of the hydrate around the lower quadruple point (between -14 and +9°C). During gradual cooling of the hydrate in contact with chlorine atmosphere, the tension decreased simultaneously with the temperatures varied from one experiment to another but in general it was between -4 and -7°C. At this point, pressure of the chlorine increased sharply then dropped quickly and became constant. Further cooling caused steady fall in the pressure. This phenomenon resulted in the sudden freezing of the water that has been in super cooled condition. The temperature rose momentarily due to this change of state and brought a corresponding increase in the pressure. When the temperature equilibrium was restored, the tension of the chlorine resumed its normal value corresponding to the dissociation of the hydrate with the formation of solid water. However, this pressure was higher than the corresponding value in case of formation of water [34]. Roozeboom also observed the supercooling phenomenon in a HCl free system, but the lowest temperature reached was only -3°C [42].

During heating of the hydrate, the pressure increased steadily until about -1°C and the temperature near to this point remained stationary during the melting. No change was observed in the pressure during this process, indicating that the transition at the equilibrium temperature did not lead to appreciable change in either of the dissociation or the vapour pressures [34]. The dissociation pressure values are given in Table 2.

**Table 2.** Experimental dissociation pressure values\* of the hydrate in the region of supercooling.

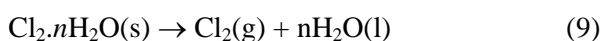
T, °C	Pressure, Torr water	Ice
-1	290	290
-2	230	-
-3	210	-
-3.5	-	262
-4	205	-
-5	146	-
-6	153	-
-7	-	230
-14	-	175

\*The vapour pressure data in this temperature range were measured in water containing HCl and the curves for ice and water cut each other around -1°C. Thus, at this point the hydrate, ice, water and chlorine gas are in equilibrium.

The analytical expression (see equation 8) for the measured values was derived by Kass [39], Wilms and Van Haute [38, 40].

$$\log P = A - B/T \quad (8)$$

where P was pressure in mm of Hg and T was in K. The values of coefficients ( $A = 16.67$  and  $B = 3899.4$ ) are valid for the entire range of the measurements [38, 40]:



The values of  $A = 17.78$  and  $B = 4213.7$  were reported for the process described in equation (9) from 1 atm to the upper quadruple point [38, 40], whereas the values by Iskenderov and Musaev were 16.57 and 3834 respectively for A and B [43].

The  $\log p-1/T$  relationship for the solubility of chlorine in water and the vapour pressure of the water above the solution in contact with the solid hydrate, as given in (equation 9), was not completely linear. Therefore, Wilms and Van Haute suggested another relation expressed in equation (10) [38, 40].

$$\log p = -107.5476 + 1325.6/T + 43.1318 \log T \quad (10)$$

**Table 3.** The dissociation pressures (in Hgmm) of the chlorine hydrate in water, 100 g dm<sup>-3</sup> NaCl and 200 g dm<sup>-3</sup> HCl solutions.

T, °C	H <sub>2</sub> O	NaCl 100g dm <sup>-3</sup>	HCl 36.5 g dm <sup>-3</sup>
0	247	375	340
2	307	452	405
4	395	570	500
6	495	615	-
7	-	770	-
9.8	770	-	-

### 3.1.2. The dissociation in solutions

The dissociation pressure of the hydrate in contact with various solutions containing dissolved salts or acids changes rapidly [44]. The dissociation pressure of the hydrate in aqueous NaCl (100 g dm<sup>-3</sup>) and HCl (g dm<sup>-3</sup>) solutions are shown in Table 3.

It can be seen that a dissociation pressure of 770 mm of Hg was reached in water at 9.8°C, and at 7°C in NaCl solution with a concentration of 100 g dm<sup>-3</sup> and at 3.8°C in the more concentrated (200 g dm<sup>-3</sup>) NaCl solution [44]. Thus, the dissociation pressure of the hydrates formed or kept in these solutions reached the outer environmental pressure at lower temperature than in water, which was consistent with the experiences of Goodwin [45] about the destabilising effect of metal chloride solutions on the chlorine hydrate. Similarly, the inhibiting effect of HCl on the hydrate formation [26, 27] can be the consequence of the increased vapour pressure and the decomposition of the hydrate at lower temperature in HCl solutions [44].

The dissociation pressure of the chlorine hydrate above 0°C was measured in detail by Roozeboom [20], who determined the critical decomposition temperature (9.6°C) in an open vessel [20, 21], and pointed out that the hydrate can be stabilised at higher temperatures by pressure. However, the highest value of temperature that could be achieved was when the pressures of the hydrate and the liquid chlorine saturated with water have become equal with each other [20].

Roozeboom also determined the lowest angular point as quadruple point at -0.24°C, (Le Chatelier

had found  $-1^{\circ}\text{C}$  in the HCl containing system [34]) and the highest quadruple point was given as  $28.7^{\circ}\text{C}$  [21, 42].

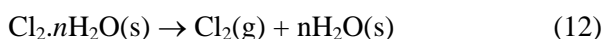
### 3.1.3. Dissociation into ice

Decomposition of solid hydrate into ice and chlorine gas was evaluated as an univariant solid hydrate  $\rightarrow$  gas + liquid type system and can be characterised by the law that the ratio of the absolute temperatures at two different pressures was constant. Calculated from the  $p$ - $T$  data at 300 and 900 Hg mm, a value of 1.032 for the hydrate was obtained [35].

The dissociation pressure in the chlorine gas-ice-chlorine hydrate system was described by Tamman and Krige and is given in equation (11) [36]:

$$T = 49.0 (\log p + 0.4707) \quad (11)$$

where  $T$  is the temperature in  $^{\circ}\text{C}$ , and  $p$  is the pressure in atm. The reaction can be expressed by equation (12).



The coefficients  $A$  and  $B$  of equation (8) calculated from the values of Roozeboom were 7.684 and 1446.6 respectively [38, 40]. However, Wilms and Van Haute reported values of 8.22 and 1595.2 for  $A$  and  $B$  respectively [38, 40].

Kótai *et al.* suggested the equation (13) where  $p$  is the pressure in kPa and  $T$  is the absolute temperature and the coefficients  $A^*$  and  $B^*$  had the values 11.43 and 0.046 respectively.

$$\ln P = A^* - B^*/T \quad (13)$$

### 3.2. The phase diagram of the chlorine hydrate

The phase diagram of the hydrate was partially drawn and evaluated by Le Chatelier [34] and Roozeboom [21, 46]. They interpreted the decomposition processes (equations 9 and 12) and gave the parameters of two invariant points. The phase diagrams of the chlorine hydrate-aqueous metal salt solution-chlorine systems are very similar; the invariant points, however, are markedly changed (see section 3.2.2).

#### 3.2.1. The phase diagram of the chlorine-water-hydrate system

The phase diagram of the chlorine hydrate was evaluated by Roozeboom [21, 46] and supplemented

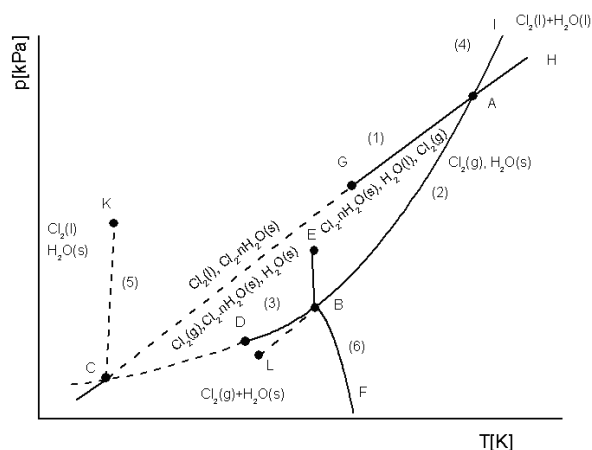


**Figure 2.** The phase diagram of the chlorine hydrate-water-chlorine system.

by Kótai *et al.* [47]. The complete phase diagram contains a new quadruple point and was drawn by using all of the available dissociation pressure data including the hydrate tension in the presence of super cooled water. The complete  $p$ - $T$  phase diagram of the hydrate-water-chlorine system is shown in Figure 2.

There are four coexisting phases in equilibrium with each other at the A, B and C invariant points. Point A represents the decomposition temperature of the hydrate, or the critical temperature according to Stackelberg [48, 49], or the upper temperature of existence according to Van der Waals and Platteeuw [50] if  $dT/dp < 0$ . In this case ( $dT/dp > 0$ ) the meaning of the two previous statements can not be the same, because the melting point of the hydrate increases with increasing pressure [47]. This phenomenon, however, might be the result of increasing occupation and stabilising effect of the chlorine capped in the cavities (increasing pressure increases the amount of the capped chlorine in the hydrate [51, 52]). At point A the four phases in equilibrium with each other are the hydrate, the solution of water in liquid chlorine, the solution of chlorine in water, and the vapour [21, 24, 37, 39, 46, 47, 53, 54].

Point B represents eutectic point of the hydrate, ice, water containing dissolved chlorine, and the vapour phases which are in equilibrium with each other [21, 24, 46, 55].

**Table 4.** The parameters of the invariant quadruple point of the chlorine hydrate-water-chlorine system.

Invariant point	T, K	P, kPa	Ref.
A	301.85	607.95	[47]
B	272.91	32.53	[47]
C	173.16	0.322	[47]

Invariant quadruple point C represents the equilibrium between chlorine gas, liquid chlorine, ice and the hydrate. The parameters of point C were calculated by extrapolation of the saturated vapour pressure curve of the chlorine and the dissociation pressure curve of the hydrate (dotted lines in Figure 2) [47]. There is no equilibrium between the ice, chlorine gas and its aqueous solution because the equilibrium curve should start at the point for which the heat of transformation,  $\Delta H$ , would pass through zero and would become negative [21, 46]. Barrer and Edge experimentally confirmed the possibility of the formation of the hydrate at 90 K via the reaction of solid ice and condensed phase chlorine [56]. This invariant point corresponds to this equilibrium. Parameters of the invariant point are given in Table 4.

These invariant points belong to the hydrate at a given composition, thus on the phase diagram of  $p$ - $T$ - $x$  ( $x$  means the chlorine mole fraction in the hydrate  $x = 1/(1+n)$ ) the curve AB (AC) shifts to the left with increasing  $x$ , consequently, with increasing water content (decreasing the chlorine content), the temperatures and pressures of the invariant points are decreased [40, 41]. The same situation was observed in the case of aqueous solutions kept in equilibrium with the chlorine hydrate [37, 39] (section 3.2.2). This result easily explains the results of Bjorkman [57] about the stability of dense hydrate, because during densification the chlorine content of the hydrate increased [57].

For example, the parameters of the invariant points of the hydrate with a composition of  $\text{Cl}_2 \cdot 6.2\text{H}_2\text{O}$  [24] (the calculated composition from the density value was  $\text{Cl}_2 \cdot 6.01\text{H}_2\text{O}$  [23]) or the parameters of some other chlorine hydrates without the knowledge of the exact composition

**Table 5.** Invariant point parameters for various hydrates.

n	Temperature, °C		Pressure, bar	
	A	B	A	B
6.01[24]	28.0	+0.22	8.3	0.35
6.97[20]	28.7	-0.24	6.08	0.33
6.20[37]	28.3	-0.24	8.52	0.32
6.97[40]	28.3	-0.22	8.42	0.32

are a bit different from the values given in Table 4. The values of the parameters A and B, both in temperature and pressure, corresponding to various n values given in Table 5 were derived from experimental densities [23].

Curve AB (line 2 corresponding to the temperature dependence of the dissociation of the saturated vapour (dissociation) pressure of the hydrate) shows the experimental equilibrium of the the hydrate in the presence of coexisting solution and  $\text{Cl}_2$  gas. Point B belongs to the hydrate, and continuing the cooling along the BD (BC) curve. Ice could be formed below 0°C. Curve BC (line 3) represents the equilibrium of the hydrate in the presence of ice and gaseous  $\text{Cl}_2$ , LBA represents a supercooled solution and the presence of  $\text{Cl}_2$  gas [47].

During decomposition of the hydrate by heating at a pressure above the critical decomposition point two liquid phases ( $\text{Cl}_2$  and  $\text{H}_2\text{O}$ ) are formed increasing the volume. This corresponds to a positive slope of the melting pressure curve AI (Figure 2) i.e., the decomposition temperature (of the incongruent melting point) was increasing with increasing pressure [53]. Declination of line 4 was determined by Byk and Fomina [54]. The  $dT/dp$  value for the hydrate was found to be  $0.80 \times 10^{-2} \text{ °C atm}^{-1}$  [54].

Curve BF represents the pressure of  $\text{Cl}_2$  gas above a solution that was in equilibrium with the ice, or in other words, line 6 shows the change in the freezing point of the water in the presence of dissolved chlorine [21, 46, 47]. The concentration of chlorine in this solution decreases regularly from B to F. Therefore F is the melting point of the ice that has zero concentration of  $\text{Cl}_2$  gas ( $p = 0$ ).

The heat of transformation reduces from F to B, and at point F (0°C) it is the heat of fusion of the pure ice. Beyond this point it was reduced by the absorption heat of Cl<sub>2</sub> which increases as B was being approached. There is no doubt that the heat of transformation of the ice was still positive close to point B. However, its value was low due to the small amount of chlorine contained in the solution at the intersection of curves FB and AB [21, 46].

Curve AG (AC) shows the saturated vapour pressure of liquid chlorine. Along line 1, the hydrate and the solution of H<sub>2</sub>O in the liquid Cl<sub>2</sub> are in equilibrium with each other. The AH section of line 1 represents the presence of two solutions, the solution of water in liquid chlorine, and the solution of the chlorine in water. Along curve AI (line 4) not only these solutions, but the solid hydrate also exists [47].

Curve BE means the co-existence of the ice, the hydrate and the solution of chlorine in water, while curve CK (line 5) represents the presence of the ice, the hydrate and the liquid chlorine.

### 3.2.2. The phase diagrams of the aqueous metal chloride-chlorine-chlorine hydrate systems

The dissolved metal chlorides affect the stability and the composition of the chlorine hydrate. The chlorine hydrate decomposes in contact with concentrated salt solutions, and its composition depends on the concentration of the metal chlorides used during its preparation. Generally, with the more concentrated metal salt solution, the lower decomposition temperature and chlorine content in the hydrate could be observed.

The shift in the numerical value of the critical temperature depends on the chemical nature of the salt used, however, the shift was independent of the concentration of each salt in the solution. The difference between the critical temperatures and the freezing temperature of the given salt solution, equation (14), at a given concentration was constant.

$$T_c^* = T_c - T_f \quad (14)$$

where  $T_c^*$  is the temperature difference for a given salt, and  $T_c$  is the critical temperature of the chlorine hydrate in contact with a given concentration of the salt, while  $T_f$  is the freezing point of the salt solution at the given

**Table 6.** Relationships between the freezing points of the sodium chloride solutions and the  $T_c^*$  values calculated from the average  $T_c$  values of the hydrate, in °C.

$W_{\text{NaCl}}$ , % w/w	$\Delta T_c$	$T_f$	$T_c^*$
2	0.95	1.52	0.57
4	1.95	3.00	1.05
6	3.05	4.51	1.46
8	4.25	5.98	1.73
10	5.50	7.44	1.94
15	9.25	10.80	1.55

concentration [58]. The dependence of the  $T_c^*$  values on the concentration is shown in Table 6 [59].

The Karsten's formula, equation (15), could be used for the calculation of the freezing point of sodium chloride solutions,  $T_f(\text{NaCl})$ , at different concentrations  $W$  expressed in % (w/w) [59].

$$T_f(\text{NaCl}) = 0.0022244W^2 - 0.7663855W \quad (15)$$

The correlation of the critical temperature  $T_c$  and the concentration of NaCl is expressed by equation (16).

$$T_c = 28.3 - 0.4324W - 0.0111W^2 \quad (16)$$

However, for the concentration of the NaCl between 0-15 % w/w the correlation is expressed by equation (17) [58].

$$T_c = 28 - 0.4780W - 0.0209W^2 \quad (17)$$

The dependence of the  $\Delta T_c$ ,  $T_f$  and  $T_c^*$  on the concentration of the sodium chloride in solution is shown in Table 6.

#### 3.2.2.1. The aqueous sodium chloride-chlorine-the hydrate system

The formation of the chlorine hydrate in sodium chloride solution has been studied in detail [37, 38, 39, 58]. The pressure-temperature-salt concentration relationships are evaluated between 1-8 atm and from 0-15% NaCl concentration in the temperature range of 12-24°C [38].

By the addition of sodium chloride to water in contact with the hydrate, line *AB* of the phase diagram shifts to the left so that the boundaries of

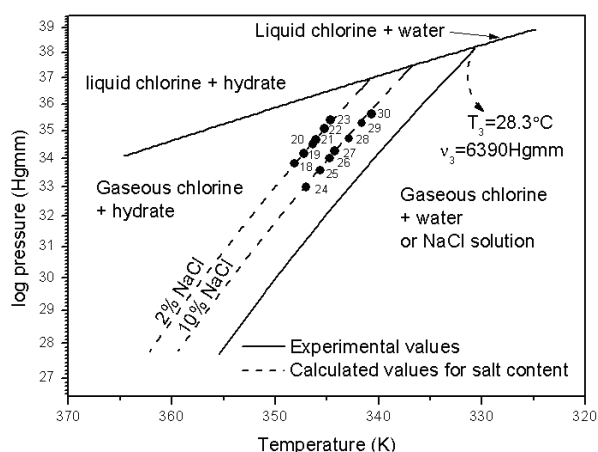


**Figure 3.** The log  $p$ - $1/T$ - $x$  phase diagram of the aq. sodium chloride-chlorine-chlorine hydrate system.

the existence of the chlorine hydrate becomes parallel to the existence of the chlorine hydrate in water. Therefore, based on the phase diagram of the chlorine-water-chlorine hydrate system, and knowing the change in critical temperature of the hydrate formation by changing the salt content of the solution, the phase diagram of the chlorine-salt-water system can easily be constructed [58]. The phase diagram in the aq. NaCl-chlorine-hydrate system is given in Figure 3.

Figure 3 shows that the equilibrium lines between 0 and 15% NaCl content are parallel, and the temperatures of the invariant points decreased with increasing NaCl concentration. The composition of the chlorine hydrate prepared in pure water was  $\text{Cl}_2 \cdot 6.2\text{H}_2\text{O}$ , the parameters of the invariant point were  $T_c = 28.3^\circ\text{C}$  and  $p_c = 8.41 \text{ atm}$  [37, 39]. That the lower eutectic point ( $T_e = -0.24^\circ\text{C}$ ,  $p_c = 0.32 \text{ atm}$ ) decreased with increasing NaCl concentration is shown in Table 7.

If NaCl concentration is increased further, the eutectic point will contain solid NaCl, solid hydrate, liquid chlorine, chlorine gas and aqueous solution, the calculated temperature was  $7^\circ\text{C}$ , the pressure is 4.7 atm and the NaCl concentration is 26.3% [38-40].

The hydrate formation in the presence of NaCl has great importance due to the desalination experiments with sea water. As seen in Table 7, the critical temperature changes in the presence of sodium chloride and the sea salt is almost the same. This aspect of the hydrate formation in

**Table 7.** The depression of critical point temperatures of the chlorine hydrate ( $\text{Cl}_2 \cdot 6.2\text{H}_2\text{O}$ ) by NaCl and sea salt.

Salt wt. %	T <sub>c</sub> , Upper		T <sub>c</sub> , Lower	
	NaCl	Sea salt	NaCl	Sea salt
2	0.9	0.8	1.0	0.9
4	1.9	1.7	2.0	1.9
6	3.0	2.8	3.1	2.9
8	4.2	3.8	4.3	4.0
10	5.4	5.0	5.6	5.1
15	9.0	8.2	9.5	8.5

sea water is of interest because there have been serious accidents when chlorine containing tanks sank into the sea, and chlorine got released due to corrosion of the tank [60]. The phase diagram of chlorine-sea water system has been studied and the existing range of the chlorine hydrate in the temperature range of 0-30°C at 1 and 9 bar (~90 m depth) are shown in Figure 4 and Figure 5 [60].

Mixing the chlorine even with only 0.01 mol% water can result in the formation of solid hydrate if the temperature is below 8°C. If the temperature is low enough [60] further dilution does not cause any phase change until the molar ratio of water to chlorine exceeds 6.2:1 (around 10 g/dm<sup>3</sup> of chlorine content in sea water at 8°C).

It is seen in Figure 5 that at 9 bar pressure one does not expect gaseous phase over the 0-30°C temperature range. Following the dilution of chlorine, a liquid chlorine phase is expected initially. With sufficient water, chlorine hydrate starts to form (below 26°C) or chlorine and water will coexist above 26°C. Further dilution results in the dissolution of the hydrate [60].

### 3.2.2.2 The aqueous $\text{MCl}_2$ ( $\text{M} = \text{Ca, Ba}$ )-chlorine-chlorine hydrate systems

The low freezing point of concentrated calcium chloride solution allows studying the hydrate formation process at low temperature, and it forms as a by-product in the reaction of chlorinated lime with cold HCl during industrial scale synthesis of the hydrate [61]. The aqueous calcium chloride-chlorine-hydrate system is a very important one. The  $\text{CaCl}_2$ - $\text{Cl}_2$ - $\text{H}_2\text{O}$  phase diagram at 0°C and the enlarged water corner of

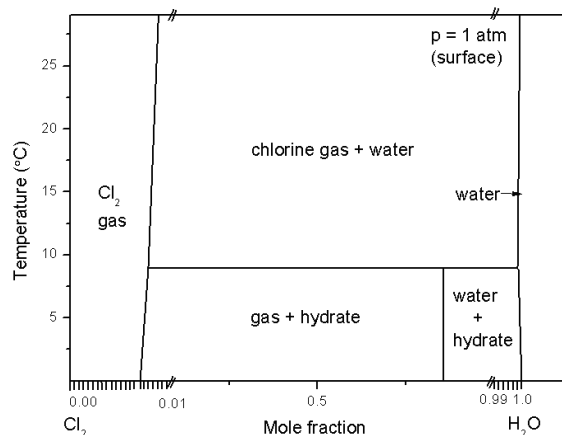


**Figure 4.** The phase diagram of chlorine-sea water system at 1 bar pressure.

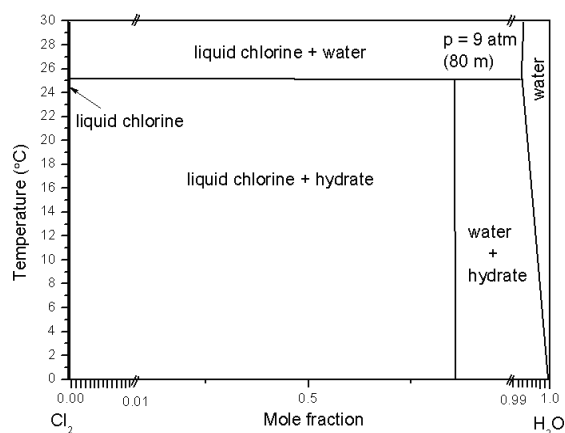


**Figure 5.** The phase diagram of chlorine-sea water system at 9 bar pressure.

this diagram can be seen in Figure 6 and Figure 7 [62].

The compositions (in % w/w) of the marked area are the following [62].

Cl <sub>2</sub>	Components		Phase
	CaCl <sub>2</sub>	H <sub>2</sub> O	
-	34.19	65.81	CaCl <sub>2</sub> ·6H <sub>2</sub> O
-	37.3	62.7	satd. CaCl <sub>2</sub> soln.
0.15	34.19	65.66	variant liq. B
0.45	15	84	variant liq. A
0.5	-	99.5	satd. Cl <sub>2</sub> soln.
35.15	-	64.85	Cl <sub>2</sub> ·7.27H <sub>2</sub> O

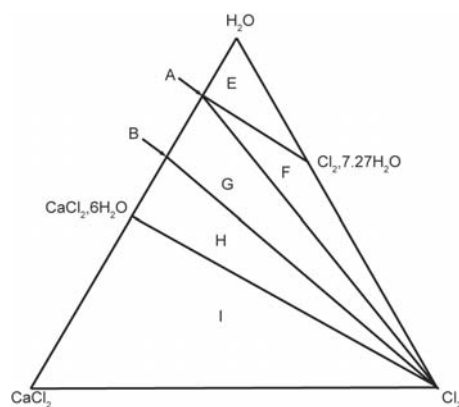


**Figure 6.** The phase diagram of the CaCl<sub>2</sub>-Cl<sub>2</sub>-H<sub>2</sub>O system at 0°C (Reproduced by the permission of the Royal Society of Chemistry).

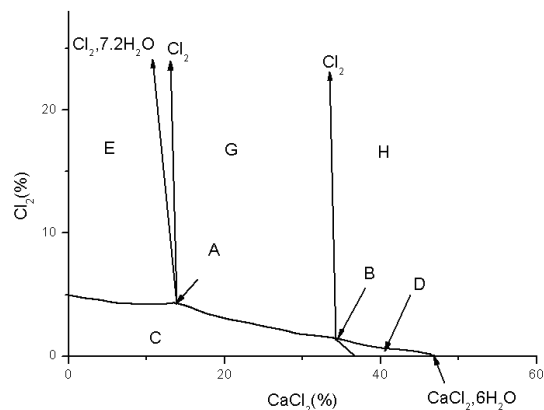


**Figure 7.** The water corner is shown in the phase diagram of CaCl<sub>2</sub>-Cl<sub>2</sub>-H<sub>2</sub>O system at 0°C, where C = unsaturated solution, D = solutions and solid CaCl<sub>2</sub>·6H<sub>2</sub>O, E = solutions and solid hydrate, F = invariant liquid A, solid hydrate and gaseous chlorine, G solutions and gaseous chlorine, H = invariant liquid B, solid CaCl<sub>2</sub> and gaseous chlorine, I = solid CaCl<sub>2</sub>·6H<sub>2</sub>O, solid CaCl<sub>2</sub> and gaseous chlorine [62]. (Reproduced by the permission of the Royal Society of Chemistry).

The analogous system of barium chloride was also studied in which the region of the equilibrium between gaseous chlorine and solution was missing, and the invariant points A and B were coincident [62].

### 3.2.2.3. The aq. zinc chloride-chlorine-chlorine hydrate system

The zinc chloride solution, formed in the electrochemical reaction of the zinc and chlorine

in batteries, acts as a medium for the synthesis of the hydrate during the regeneration of the zinc and the chlorine hydrate. The zinc chloride concentration varies during the synthesis, because the concentrated zinc chloride solutions are electrolysed into zinc and chlorine which transforms into chlorine hydrate. The  $\lg p-1/T-c_{\text{salt}}$  phase diagram [63, 64] has similar character as in the case of sodium chloride, and the critical temperature decreased with increasing zinc chloride concentration. The numerical value of the decreasing critical temperature is different from the values found in the case of the sodium chloride at the same concentration [23]. The upper critical decomposition temperature of the chlorine hydrate formed in aqueous 25%  $\text{ZnCl}_2$  solution is roughly  $16^\circ\text{C}$  [63]. The invariable eutectic point in 16% zinc chloride solution is  $4^\circ\text{C}$ .

The dense hydrate (0.32 g  $\text{Cl}_2/\text{g}$  of hydrate) prepared from liquid chlorine in various zinc chloride solutions [57] showed a decrease in the temperature of the upper critical point with the increasing zinc chloride concentration, namely 16% and 40% of zinc chloride solutions gave dense hydrate at  $24$  and  $22^\circ\text{C}$  upper critical temperatures [23]. Although it is higher than the  $16^\circ\text{C}$  found for the hydrate prepared in a chilled 25% aqueous zinc chloride solution [63], the decomposition temperature is unambiguously dependent on the chlorine content of the hydrate [23], and the densification process decreases the water and increases the chlorine content compared to the hydrate prepared at  $9.6^\circ\text{C}$  in water [65]. Since the increasing occupation increases the stabilising effect on the clathrate phase and the melting point [23], the dense hydrate (1.32 g  $\text{Cl}_2/\text{g}$  hydrate) [57] should be more stable even at higher zinc chloride concentrations than 0.15-0.17 g chlorine/chlorine hydrate prepared in chilled  $\text{ZnCl}_2$  solutions [63]. The stabilising effect of the pressure of the liquid chlorine in this synthesis can also play an important role in the formation of the chlorine hydrate with higher chlorine content. Overpressure applied in the preparation of the hydrate in chilled zinc chloride solutions is the usual technique to obtain more stable (and consequently more chlorine containing) hydrates [25].

#### 4. Preparation of the chlorine hydrate

The chlorine hydrate is one of the most stable gas hydrates. It has the highest melting point and

relatively low dissociation pressure at room temperature. Therefore, it can be prepared easily from chlorine and water under strong cooling to conduct the evolved heat in the exothermic reaction (equations 9 and 12).

##### 4.1. Preparation from the reaction of chlorine gas and water vapour

The chlorine hydrate was discovered as the reaction product formed by cooling of wet chlorine gas [1]. This reaction was repeated many times to produce the hydrate from gaseous chlorine and water vapour under cold conditions [15, 51, 52, 66, 67, 68, 69, 70, 71]. Sometimes, the reaction caused problems, e.g. by clogging the pipeline [66] or by depositions on the reactor walls during chlorine's manufacture or purification [68, 72].

Chlorine formed in electrolytic cells contains water depending on the temperature of the cell operation. This moist gas in contact with the water surface yields a liquid-gas mixture which is cooled by rapid expansion to  $-4^\circ\text{C}$ . Ice and the hydrate are formed, and organic impurities such as  $\text{CCl}_4$ ,  $\text{CHCl}_3$ , and  $\text{Cl}_3\text{CCCl}_3$  are separated though these are partly absorbed in the hydrate [72].

Based on the observation of Tammann and Krige [36] on the formation of gas hydrates from gas and ice at the surface of solid ice, Nikitin [73, 74] used the mass action law to evaluate the experimental parameters of the hydrate found by Faraday [5] and Roozeboom [20, 42].

Nikitin supposed that the formation of the gas hydrates proceeds exclusively in the gas phase because the energy conditions and the equilibrium of the reaction do not depend on the reaction paths, otherwise this situation would contradict the second principle of thermodynamics [73, 74]. In the equilibrium, solid hydrate  $\rightleftharpoons$  ice  $\rightleftharpoons$  gas, the gas phase was considered to be "hydrate vapour" and water vapour saturated phase. The hydrate vapour is in dynamic equilibrium with the gases and the water vapours. Considering the solid hydrate alone, its vapour in the gas phase is partly decomposed. The resulting excess of the water vapour condenses because each temperature corresponds to a specific water vapour pressure. As a result, the gas pressure will increase until the gas phase is saturated with the vapour of the

undissociated hydrate. Thus, there is an equilibrium not only between the solid hydrate and its vapour, but also between the formation and decomposition of the chlorine hydrate molecules in the gas phase.

If the hydrate formed in the gas phase is  $\text{Cl}_2 \cdot 6\text{H}_2\text{O}$  according to equation (18).



The equilibrium constant for the reaction in terms of the mass law at 1 atmospheric pressure (without the consideration of the activity coefficients) is given by equation (19).

$$K = \frac{[\text{Cl}_2 \cdot 6\text{H}_2\text{O}]}{[\text{Cl}_2][\text{H}_2\text{O}]^6} \quad (19)$$

Roozeboom [5, 20] determined the equilibrium dissociation pressures of the chlorine hydrate in the presence of hydrate and ice phases, and in the presence of hydrate and super cooled water phases at the same temperatures. The saturated water vapour pressure above the super cooled water is greater than that over the ice. In the presence of supercooled water the dissociation pressure of the hydrate has to be lower than that in the presence of ice. The product of the gas pressure and the water vapour pressure is in the sixth power. The dissociation of hydrate into gas and ice (E) is similar to the dissociation of the hydrate into gas and water (W) as shown in equation (20).

$$[\text{Cl}_2]_E [\text{H}_2\text{O}]_E^6 = [\text{Cl}_2]_W [\text{H}_2\text{O}]_W^6 \quad (20)$$

The dissociation pressure of the hydrate into gas and water can be calculated if the vapour pressure of the gas and the ice in the hydrate dissociation, and the vapour pressure of the water over the ice and the super cooled water are known. The calculated vapour pressures at -1, -2 and -3°C are 224, 202, and 185 mm Hg respectively. The experimental values at these temperatures by Roozeboom were 223, 200 and 183 mmHg respectively [20]. This demonstrated that the mass action law given in equation (19) could also be used for the determination of the molecular formula of the hydrate accurately [73, 74].

Finally, there is an experimental indication that the undissociated gas hydrates have an appreciable vapour pressure near 0°C. For example, Faraday used large excess of chlorine in the preparation of the hydrate from water and chlorine [5]. Thus, all

the water taking part in the reaction was bound to the hydrate, so the pressure of chlorine was higher than its equilibrium pressure. Faraday had observed very little recrystallization of the chlorine hydrates by sublimation in the absence of ice [5]. The possibility of sublimation and crystallization of the gas hydrates from the gas phase suggests that the hydrate is formed in the gas phase immediately near the ice surface [73, 74].

The alternative method for preparing the hydrate is to attach a flask containing chlorine dissolved in water to a vacuum system when rapid evaporation of the water and the chlorine starts and the hydrate is formed as observed by Faraday [5] and interpreted by Nikitin [73, 74]. Cady prepared chlorine hydrates by the reaction of a known amount of water vapor with an excess of chlorine gas in a cooled reactor at various pressures and compositions. The hydrate had deposited on the wall of the reactor quantitatively under controlled conditions of pressure and temperature [51, 52].

A special way of preparing the hydrate is by reacting the chlorine gas and the water vapour within a capillary. The hydrate is adsorbed on the walls under the influence of uncompensated surface charges. The hydrate molecules are under attractive forces in the capillary walls, which are 10-12 atmospheres in magnitude at a distance of 10-12 Å from the wall. This pressure is more than enough to keep the hydrate stable in condensed phase. Formation of several layers of the hydrate by the condensation of vapours in the three-dimensional system is very probable. The stability of the gas hydrate is ensured by the walls of the capillary.

The hydrate formation was confirmed by the density ( $1.37 \text{ g cm}^{-3}$ ) of the solid formed, or by the decomposition of the solid hydrate by heating the capillary up to a temperature where the hydrate is decomposed and the chlorine can not be rehydrated at temperatures until the dissociation temperature (400°C) of the chlorine in the pores, because density increase can be obtained due to the liquid chlorine ( $d = 1.532 \text{ g cm}^{-3}$ ) [75].

#### 4.2. Preparation from the reaction of chlorine gas and water

Since the chlorine is gas at atmospheric pressure and room temperature and the water is liquid

under these conditions, the most common reaction to form the hydrate is to react chlorine gas with water under intensive cooling [1, 4, 5, 9, 14, 32, 33, 35, 76-79]. Instead of water, metal salt solutions can also be used. Both the chlorine and the metal salts can be prepared in situ by the reaction of metal hypochlorite or other oxidizing metal salts and hydrochloric acid.

#### 4.2.1. Preparation in pure water

Faraday observed that the hydrate formation from the reaction of chlorine gas and water is more efficient in dark than in the presence of light [5]. On passing a large amount of chlorine gas into water around 0°C, the larger part of the water is transformed into hydrate with lamellar crystals settling as thin slurry. The lamellar crystal mass freezes and adheres to the filter at around -3°C. Therefore, the separation of the hydrate mass from the filter becomes difficult even with the harsh handling [11].

Anwar-Ullah [33] prepared the hydrate by various methods and studied the effect of the reaction time on the composition of the hydrates. The Cl<sub>2</sub>:H<sub>2</sub>O ratio in the hydrate prepared from water and chlorine gas at 0°C converged to the Cl<sub>2</sub>.6H<sub>2</sub>O if sufficient time was allowed for the completion of the reaction. A variation of the reaction time from 1.5 h to 9 months led the composition to change from Cl<sub>2</sub>.9.6H<sub>2</sub>O to Cl<sub>2</sub>.5.97H<sub>2</sub>O.

The yield of the hydrate from the reaction of water and chlorine gas at 0.25°C was 25.14% of the added chlorine [79]. It completely disappeared within 42 min when it was purged with a gas mixture containing 5% Cl<sub>2</sub> in N<sub>2</sub> at 0.5°C because of the stripping action of the nitrogen. No hydrate was formed when the chlorine concentration was 28.6 vol. % and 75 vol. %, respectively after 1.4 and 2 h. However, with a 93% Cl<sub>2</sub> containing mixture, the hydrate formation could be observed at 0.5°C after 23 min, which completely disappeared when it was purged with 20.9% chlorine containing mixture for 55 min [79].

More stable hydrate could be prepared by diffusing chlorine gas into water between 0 and 9°C and separating the hydrate with centrifugation at 800 atm pressure. The hydrate, Cl<sub>2</sub>.9.2H<sub>2</sub>O, contained 33% of chlorine, and the

apparent bulk density was found to be between 0.5 and 0.6 g cm<sup>-3</sup> which increased under pressure, but the chlorine content did not alter at all [35].

#### 4.2.2. Preparation in salt solutions

Goodwin first observed that chloride salts have important effect on the formation and stability of the hydrate [45]. A potassium chloride solution (20 g/100 cm<sup>3</sup>) saturated with elementary chlorine and cooled, prevented the formation of the solid hydrate between 2 and 10°C [45]. The hydrate formed at negative temperatures decomposed between 7 and 8°C which is lower than that measured for the hydrate prepared in pure water. The solubility character of the hydrate is the same in KCl solutions as it is in water up to 7°C [45].

Similar behaviour was observed in case of NaCl, LiCl, SrCl<sub>2</sub>, CdCl<sub>2</sub>, and MnCl<sub>2</sub>, or with a mixture of KCl and NaCl, but the hydrate was formed at lower temperatures and in a lesser amount than if it were prepared from pure water. In this concentration (20 g/100 cm<sup>3</sup>) the chlorides of calcium, magnesium, iron(II) and cobalt(II) prevented the formation of the hydrate even in the negative temperature range up to -5°C (in several cases even up to -7°C) and the chlorine hydrate dissolved with effervescent decomposition in these salt solutions [45]. The chlorine hydrate could be formed at decreasing temperatures even if the Cl<sub>2</sub>/HCl ratio was 8-9:1, or even in the presence of NaCl, KCl or CaCl<sub>2</sub> containing solutions as well [80]. A lot of metal salts can be used in the hydrate preparation [25] between -25 and 9°C, but the concentration of the metal chlorides employed should not be so high that the hydrate formation would be prevented. For example, barium chloride [62], calcium chloride [61, 62, 81] or zinc chloride [25, 65] can also be used.

##### 4.2.2.1. Preparation in zinc chloride solutions

Formation of the chlorine hydrate in the presence of zinc chloride solutions with various concentrations is a basic reaction in the charging of high energy density zinc-chlorine batteries.

The use of 10, 20 and 35 w/w % zinc chloride solution lowered the temperature for the formation of the hydrate to 3, -4, and -20°C respectively [25]. With increasing zinc chloride concentrations

the decomposition temperature of the chlorine hydrate decreased [25]. Since the batteries operate at room temperature, therefore the regeneration of batteries (formation of the hydrate) was also studied at various concentrations of the zinc chloride (0-40 w/w %) at room temperature. The vapour pressure measurements of the chlorine hydrates formed in concentrated zinc chloride solutions unambiguously showed that lower pressures are needed to prepare the hydrate in these solutions than in pure water (see section 3.2.2.3). Thus the studies at ambient temperature were carried out at 1-5 atm pressure [65]. Interestingly, the decomposition of the hydrate crystals removed from zinc chloride solution started at 9°C as in the case of samples prepared in pure water [25].

#### 4.2.2.2. Preparation in calcium chloride solutions

The hydrate could be prepared in 5% aqueous calcium chloride solution by passing chlorine into the solution even at 0°C [81, 82]. Starting from 5-14% calcium chloride, the synthesis of the hydrate could be performed and the composition of the formed hydrate could be expressed as  $\text{Cl}_2 \cdot 7.27\text{H}_2\text{O}$  [82]. The calcium chloride is a very useful agent to decrease the freezing point of aqueous solutions, thus the calcium chloride can be used as a low temperature media for the preparation of the chlorine hydrate both from gaseous and liquid/solid chlorine up to -50°C [23].

#### 4.2.2.3. Preparation in the presence of mixed metal chlorides

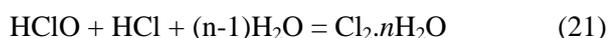
The salts like iron(II), cobalt(II) or manganese(II) chlorides can be oxidized with chlorine or the chlorine hydrate to their higher chloride states especially in the presence of a third complex forming component. It is well known that the mixture of NaCl and  $\text{PbCl}_2$  absorb a lot of chlorine due to the formation of  $\text{Na}_2\text{PbCl}_6$  [45]. In order to study analogous reactions, mixtures of  $2\text{NaCl} + \text{CoCl}_2$  and  $2\text{NaCl} + \text{MnCl}_2$  were studied in the hydrate forming reaction. Although hydrate had formed at -4°C it did not oxidize the manganese (II) into manganese dioxide up to 7.5°C which is the decomposition point of the formed hydrate in this system [45].

#### 4.2.3. Preparation with *in situ* generated chlorine

The first method for the *in situ* preparation of the hydrate by decomposing a solution of hypochlorous

acid cooled to 2 or 3°C with hydrochloric acid was developed by Pelouze [83]. The released chlorine combined with the water and the result was a large quantity of hydrate crystals. Thus the method provided an excellent way to obtain plenty of crystals of the hydrate.

In the treatment of hypochlorous acid with hydrochloric acid solution added drop by drop to obtain the hydrate deposition as a jelly like mass, equation 21, some chlorine was released at the same time. If the solution was cooled by ice, the gas evolution was diminished and the hydrate had formed almost completely [84].



The hypochlorous acid may generally be prepared *in situ* from hypochlorite salts with hydrochloric acid. The hypochlorous acid is a weak acid and its reaction with HCl, equation (22), is an equilibrium reaction.



The opposite reaction is the hydrolysis of the chlorine formed. The shift of the equilibrium is essential. The  $K$  value for the reaction is low ( $K = 1.45 \times 10^{-4}$ ), therefore the extent of hydrolysis of the chlorine is low. The formation of the chlorine is favoured, but some of the conditions are to be optimized to satisfy the requirements for completing the reaction between the hydrochloric acid and hypochlorous acid [61, 85, 86].

Formation of the chlorine hydrate in itself shifts the equilibrium immediately because of the removal of chlorine from the solution. Although the addition of excess hydrochloric acid or chloride ion is favourable; yet too much HCl inhibited the hydrate formation by decreasing the chlorine content in the hydrate by forming trichloride ion ( $\text{Cl}_3^-$ ). Formation of too concentrated hypochlorous acid solution (>25 wt. %) is followed by its fast decomposition with oxygen evolution and with the formation of  $\text{Cl}_2\text{O}$ . The most valuable starting material is the commercial sodium hypochlorite solution which consists of NaOCl, NaCl and NaOH. Addition of HCl results in the formation of large amounts of dissolved NaCl and liberation of the HOCl which produces chlorine in the subsequent reaction with HCl (equation 21). The formation of chloric acid from HOCl did not occur due to the low temperature (around 0°C) of

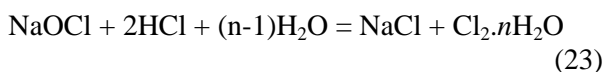
**Table 8.** The distribution of the chlorine containing species in zinc chloride (M) solutions used for the chlorine hydrate preparation ( $\Sigma\text{Cl}_2=2\text{M}$ ).

M	pH	Cl <sub>2</sub>	HOCl	Cl <sub>3</sub> <sup>-</sup>
1.95	3.74	1.09	0.10	0.81
3.37	3.20	0.80	0.06	1.14
1.44	2.36	1.2	0.14	0.66
2.38	1.00	1.05	0.0004	0.95

the experiments [61, 85, 86]. The formation of the chlorine hydrate, the neutralisation of the NaOH and the HOCl + HCl reactions are exothermic, therefore intensive cooling is required. Reaction of the hypochlorites of calcium or other metals can also be performed [61, 85, 86]. The role of the by- reactions can be seen in the concentrated zinc chloride solution under acidic conditions (pH = 1), where the elementary chlorine is the predominant species, but the activity of the trichloride ion (Cl<sub>3</sub><sup>-</sup>) is strongly increased in the system [87]. The distribution ( $\times 10^2\text{M}$ ) of the species in the ZnCl<sub>2</sub>-Cl<sub>2</sub>-H<sub>2</sub>O system from which the hydrate is formed [87] is given in Table 8.

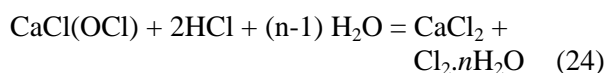
The Table 8 indicated that a decrease in pH decreases the amount of the hypochlorous acid significantly without changing the amount of the trichloride ion significantly. Further, the increasing amount of the dissolved zinc chloride decreases the relative amount of the free chlorine with the simultaneous increase in the trichloride amount [87].

The synthesis of the hydrate via the reaction of chlorine gas and aqueous metal chloride salt solutions can be used as well to avoid the hydrolysis of the chlorine [47, 61, 85]. Reaction of cold metal hypochlorite solutions with cold HCl solutions, equation (23), generated the metal chloride additive together with the free chlorine in situ, and the formation of the chlorine hydrate occurred at appropriate temperature and concentration [61, 86].



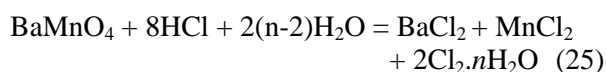
The chlorinated lime containing Ca(OCl)<sub>2</sub> and CaCl(OCl) can also be used, equation (24),

the temperature of the reaction is lowered up to -20°C or still lower because the presence of calcium chloride can decrease the freezing point of the water to -52°C; therefore the method could be useful for the synthesis of the chlorine hydrate at low temperatures [61].



This method has many advantages such as gaseous chlorine is not needed, the hydrolysis of chlorine is suppressed due to the presence of large excess of chloride salts and hydrogen ions, the concentration and temperature interval of the reactions are wide (the hypochlorite concentration can be adjusted to form 25% aqueous hypochlorous acid in the first step, and by using calcium hypochlorite the reaction temperature can be decreased to highly negative temperatures). The yield of the hydrate is high, chlorine does not evolve from the solutions, and the chlorine hydrate could be separated by an easy filtering procedure [85]. During the use of HCl for the generation of chlorine, however, the concentration of the formed chloride salts (e.g. KCl, NaCl or CaCl<sub>2</sub>) and the residual HCl should be considered. If the HCl is more concentrated than 1-2 M, there is no hydrate formation (probably due to formation of HCl<sub>3</sub>) [26, 45].

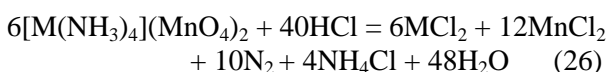
Contrary to HOCl other strong oxidizing acids, e.g. HMnO<sub>4</sub> or H<sub>2</sub>MnO<sub>4</sub> are of limited use for the preparation of the chlorine hydrate [23] because the MnCl<sub>2</sub> formed is easily oxidized by the chlorine hydrate to MnO<sub>2</sub>. Their salts, however, produce a mixture of chlorides of the appropriate cations of the starting permanganate or manganate salt and manganese(II) chloride as shown in equation (25).



The presence of another chloride compound, however, can stabilise the MCl<sub>x</sub>-MnCl<sub>2</sub>-Cl<sub>2</sub>·nH<sub>2</sub>O system [45]. For example, in the case of NaCl or KCl probably the complex of the MCl<sub>x</sub> and the MnCl<sub>4</sub> resist the hydrolysis to MnO<sub>2</sub> [27].

Various manganate and permanganate salts [88, 89, 90] are reacted with HCl under chilling conditions in the presence of the various metal

chlorides-manganese(II) chloride mixtures and elementary chlorine [23]. The various known permanganate complexes could also be used in this reaction [91, 92, 93, 94]. The complexes having chlorine sensitive ligands like ammonia [91, 93, 94] cannot be used due to the immediate consumption of the evolved chlorine by the ligand with the formation of HCl and nitrogen as shown in equation (26) where M is either Cu, Cd or Zn [23].



### 4.3. Formation from chlorine gas and ice

Chlorine containing gases in a closed system are brought in contact with ice between -80 and 9°C. At the surface of the ice a small amount of the hydrate is formed, thus the chlorine from the gas mixture could be recovered. By heating the hydrate the chlorine can be released. The efficiency of the chlorine removal is indicated in Figure 8 [79].

This method can be used for the removal of chlorine from dilute gas mixtures which do not form hydrate with water. Pressure increases the chlorine hydrate forming ability. Starting with pure chlorine in the reaction with ice, only 0.7% of the hydrate was formed related to the original amount of the ice at -9.3°C [79]. The use of snow

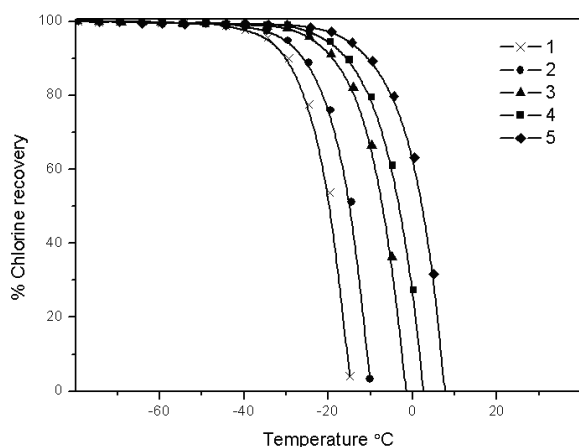


**Figure 8.** Removal of chlorine from gas mixtures at low temperature and at 689.5 kPa pressure. 1-0.5 vol % Cl<sub>2</sub>; 2-1 vol % Cl<sub>2</sub>; 3-3 vol % Cl<sub>2</sub>; 4-5 vol % Cl<sub>2</sub>; 5-10 vol % Cl<sub>2</sub>.

leads to only 0.1% yield in spite of the larger surface area. Sparging with chlorine containing gas may lead to the decomposition of the chlorine hydrate. Therefore, the next charge of the snow was put in contact with chlorine in a cold trap at -11.1°C, so that the surface area could be exposed for a longer time. For this experiment a chlorine hydrate yield of 11.8% was observed. Consequently, purging gases remove the chlorine hydrate formed on the ice surface by reason of the vapour pressure [79].

### 4.4. Preparation by the reaction of liquid chlorine and water

Since the chlorine can easily be liquefied at normal temperatures even by a slight overpressure, the reaction of the liquid chlorine and water is a well known and widely used reaction [6, 7, 9, 10, 12, 13, 17, 19, 14, 20, 33, 95] especially for the recrystallization of the hydrate when the liquid chlorine is prepared from the hydrate by thermal decomposition (>28.7°C) in a closed tube [13, 45].

The chlorine content of the hydrate prepared in this way is generally higher than the hydrates formed by other reaction route [20]. This phenomenon, however, may be of consequence because in this method large crystals are formed, which do not contain as much adsorbed water as the snow- or jelly-like hydrates formed directly e.g. from gaseous chlorine and water [20].

During the preparation of dense hydrate for zinc chlorine batteries, liquid chlorine is combined with an aqueous zinc chloride solution (10-40%) and the heat of the hydrate formation is removed at ambient temperature. The process requires no cooling of the aqueous solutions to the negative temperature range and the heat of the hydrate formation is passed to the surroundings by the evaporated chlorine which is then liquefied and recycled. The chlorine content is 0.32 g Cl<sub>2</sub>/g hydrate, while solution refrigeration provides only 0.15-0.17g Cl<sub>2</sub>/g chlorine hydrate concentration [57].

### 4.5. Formation in the reaction of liquid chlorine and ice

Only one example has been known for this type of reaction. Barrer and Edge found evidence for the

interaction of ice and condensed phase of chlorine at 90 K with the formation of the surface layer of hydrate [56].

#### 4.6. Manufacture of the hydrate

In the industrial scale preparation of the hydrate the engineers faced a lot of technical problems like adhesion of the formed hydrate on the walls of the cooled surfaces, problems of the chlorine injection pumps and so on. In order to solve these problems numerous technical solutions, apparatuses and *in situ* methods have been developed.

The first method for continuous preparation of dissolved hydrate was patented by De Vains [76]. A high surface area packed column was developed to contact the counter current stream of the  $\text{Cl}_2$  gas and water at the optimal temperature range (0-8°C). The formed and dissolved hydrate prepared in this way had a larger chlorine concentration than the product of the process using dissolution of chlorine gas [76] (see section 2.2). In this way, the dissolved hydrate can be prepared, but the isolation of the solid product raises technological questions. One of the most important among them is the adherence of the hydrate to the parts of the devices, thus causing clogging and decreasing the cooling efficiency.

##### 4.6.1. Devices to solve the chlorine adding problems

Extreme reactivity, corrosivity and harmful nature of the chlorine gas required the developing of simple and easy methods to feed it to the reactors during the hydrate synthesis. An apparatus consisting of a vacuum tube in which water serves both as solvent and liquid chlorine engine was fabricated to dissolve chlorine. The water arriving under pressure can access the device through a pipe. The chlorine injection pipe is filled via the chamber in which vacuum is created by passing water in a cone. This vacuum is filled by the arriving chlorine which is immediately dissolved in the water entering into the chamber. This chlorine solution can be crystallised completely at a temperature of 3°C. The chlorine content of the solution depends on the pressure at which the dissolution takes place. The longer the tube, the greater is the pressure, and thus the chlorine solution becomes more concentrated and larger amount of hydrate can be obtained [96].

A special hydrate tank was developed as a chlorine source for the Zn-chlorine batteries which does not require the chlorine gas pump as shown in Figure 9 and Figure 10. The tank (1) is provided with a hollow cylindrical ejector (9) attached to the hydrate containing liquid circulation pipe (17) and a chlorine introducing pipe (10) is fitted to the upper side surface of the ejector (9). An orifice (11) having an inverted conical hole (12) is attached to the inner surface of the upper end of the ejector (9). Thus, the pressure of the chlorine hydrate containing liquid is reduced at the exit (B) due to the calibre difference between the upper and the lower parts, and the hydrate containing liquid is atomised into a fog. Accordingly, the chlorine from the chlorine feeding pipe (10) is generated at an electric cell (5) which is well sucked and completely mixed with the hydrate containing liquid. By this mechanism, the mixing efficiency or the formation efficiency is increased, and the installation of a gas pump is unnecessary. In this way, 1 kW power of the battery is ensured by  $3.5 \text{ dm}^3 \text{ min}^{-1}$  chlorine streams and a circulation rate of  $10 \text{ dm}^3 \text{ min}^{-1}$  slurry at temperatures below 7°C and the reaction time is 8 h [97].

By using a special pump system a plugging and jamming resistant arrangement has been developed,

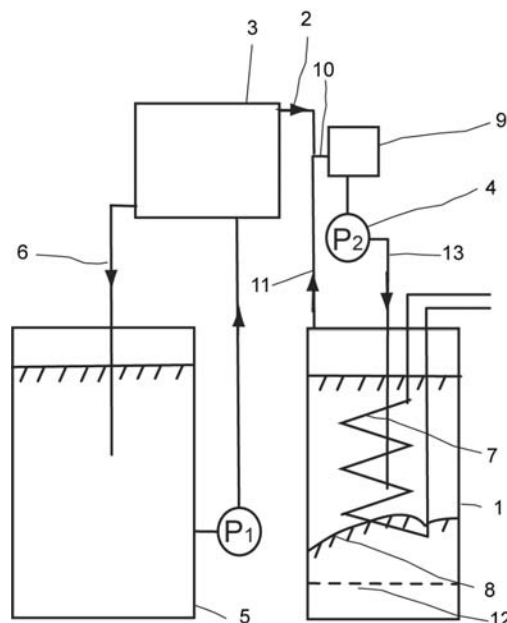
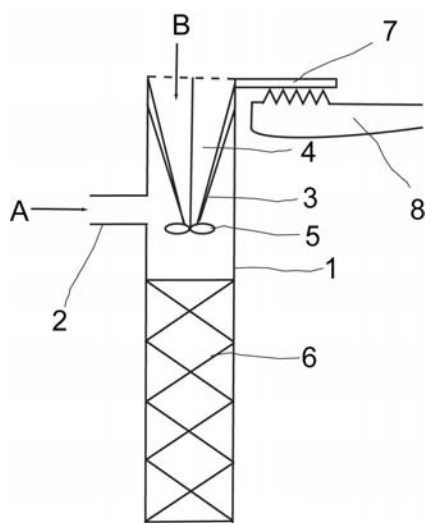


Figure 9. The chlorine hydrate tank.



**Figure 10.** The device shows the addition of chlorine gas to the chlorine hydrate tank, where 1 - The hollow chlorine hydrate manufacturing tank, 2 - gaseous chlorine inlet pipeline, 3 - Venturi tube to increase the speed of water, 4 - Mixer to distribute water into droplets, 5 - Propeller, 6 - Solid chlorine hydrate storage place, 7, 8 - Controller units, A - Chlorine gas inlet, B - Water inlet.

where the pump of the chlorine and the chilled water is located in the store. There was also an outlet conduit leading from the pump and being substantially straight and vertically disposed. It had an exit discharge into the gas phase above the liquid level in the store [98].

#### 4.6.2. Devices to solve adhering, clogging and jamming problems

Since sticking and adhering of the hydrate on the cooled surface cause insulation which decreases the heat transfer from the cooling surface to the solution, a hydrate tank, Figure 11, was developed which consisted of a hollow cylinder (2) with upper (4) and bottom (6) openings. The cooling (5) and heating (7) elements are placed at the upper and lower part of the tank respectively. Chlorine gas was introduced through a pipeline (3) placed at the centre of (2) so that it comes in contact with the water in the bottom part of the cylinder. The water is circulated in the hollow cylinder where it is mixed with the chlorine gas, then overflows to the outside part of the hollow cylinder via aperture 4 in the upper part of the

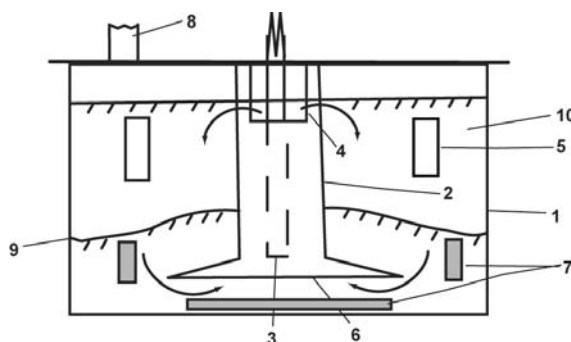


**Figure 11.** The chlorine hydrate tank arrangement, where 1 - The hydrate tank; 2 - Hollow cylinder; 3 - Chlorine gas introducing pipeline; 4 - Upper opening part of the hollow cylinder; 5 - Cooling elements; 6 - Bottom opening part of the hollow cylinder; 7 - Heating elements; 8 - Chlorine exit pipeline; 9 - Solid hydrate ( $\text{Cl}_2 \cdot 6\text{-}8\text{H}_2\text{O}$ ); a - aqueous solution is kept in equilibrium with solid hydrate/chlorine gas.

hollow cylinder. The aqueous solution is effectively cooled by the coolers (5) arranged at the upper part of the tank, and the formed chlorine hydrate crystals sink to the bottom (9).

The flowing chlorine water does not allow the accumulation and adhesion of the formed hydrate on the cooler plates. The shape of the upper opening of the hollow cylinder is such that it does not allow the accumulation of the hydrate crystals in the cylinder and clogging of the end of the chlorine gas pipeline. The special advantage of this equipment is its reversibility. The chlorine gas can be generated from the hydrate by supplying hot water through the heating elements (7), which are placed below the deposited layers of the hydrate so that the crystals of the hydrate get heated and decomposed to chlorine which escaped through the opening (8).

The aqueous solution, which comes in contact with the hydrate crystals, was saturated with chlorine so that the hydrate crystals and the solution were in equilibrium [78].

During the reaction of chlorine with chilled water, agitation was needed to ensure uniform distribution of the chlorine and the hydrate since the latter due to its high specific gravity precipitated at the bottom of the hydrate tank and frequently clogged the chlorine supply pipeline at the distant end.



**Table 9.** Dependence of the rate of chlorine absorption ( $\text{mol}/\text{m}^2/\text{h}$ ) on the vapour pressure.

Vapour pressure, Hgmm	$\text{H}_2\text{O}:\text{Cl}_2$ molar ratio	$\text{Cl}_2$ absorption $\text{mol}/\text{m}^2/\text{h}$
668*	8	High
230	0.44	27
150	0.245	20.5
97	0.165	15.7
58	0.084	7.6
32	0.044	4.9

\*The temperature could not be maintained at  $-6^\circ\text{C}$  due to the reaction heat of the large amount of hydrate formed [70].

the pressure depends on the amount of the consumed chlorine the cooling capacity of the coil is controlled by changing the amount of cooling medium in the coil following the pressure in the upper part of the tank. Since the solid hydrate deposited on the surface of the cooling coils, it was periodically removed with shaking and pumped out as slurry made from the concentrated electrolyte solution resulting from the evaporation of water [69]. Similarly, water or 15-35% aqueous zinc chloride solution was heated to control the  $\text{Cl}_2:\text{H}_2\text{O}$  ratio in the gas phase, and chlorine was introduced directly into the space above the solution through a perforated tube or a cooling tube or a coil located above the chlorine inlet tube. The amount of the solid hydrate deposited is dependent on the temperature of the solution and the cooling coil. The chlorine:  $\text{H}_2\text{O}$  ratio also affected the yield. The vapour pressure of a 35% aqueous  $\text{ZnCl}_2$  solution was 655 Hgmm at  $100^\circ\text{C}$ . The chlorine absorption rate at  $-6^\circ\text{C}$  [70] is given in Table 9.

#### 4.6.3. *In situ* manufacturing methods

The *in situ* methods do not use the elementary chlorine gas separately; it is prepared in the reaction mixture during the hydrate forming process.

A pressure of 110-120 bar compresses and stabilises the chlorine hydrate prepared in the reaction of a 10-15% aqueous  $\text{HCl}$  and chlorinated lime at negative temperatures. The

apparatus consists of a cooling block, a heating block, a compressor block, and a filter block which operated as a storage place for the solid compressed hydrate [61].

Electrolytically prepared chlorine was used as reagent to manufacture the hydrate *in situ* during charging of the high energy density zinc chloride batteries. The aqueous zinc chloride solution (25%) was immersed in a beaker of an ice-salt mixture at  $-5^\circ$  and a current of approximately 10 A was passed for 100 min through the battery, when gas evolution and deposition of a light yellow smooth microcrystalline chlorine hydrate was observed [63].

Manufacturing of hydrate in a similar chilled electrolytic process provided for the regeneration of leachants to recover zinc from scraps or  $\text{ZnO}$  and  $\text{ZnFe}_2\text{O}_4$  containing wastes. The formed  $\text{ZnCl}_2$  solutions having pH 2-3.5 were electrolysed at  $5-9^\circ\text{C}$  using a current density of  $1000 \text{ A}/\text{m}^2$  keeping the  $\text{ZnCl}_2$  concentration around 25% [29, 100]. Chlorine resistant graphite, platinized platinum or  $\text{RuO}_2$  or  $\text{La}_2\text{O}_3$  sensitised Ti anodes and diaphragms were used to separate the formed hydrate slurry which could be recycled easily into the leaching process, because the handling and pumping of the low viscosity slurry in  $\text{ZnCl}_2$  solution is safer and easier than working with the chlorine gas [29, 100].

#### 4.7. Accidental formation of the hydrate

In winter time, pipes carrying chlorine gas may become clogged by the formation of the hydrate [66]. Similarly, in extremely cold winter weather the concentrated chlorine solutions has to be heated to avoid the chlorine hydrate formation [101].

The hydrate, or “chlorine ice” as it is more popularly called, is formed as a deposit in the chlorinator devices when the water flowing through the chlorinator walls at low temperatures causes problems which can be manifested mainly in two ways: one among them is when the hydrate is deposited progressively around the glass metering tube which obliterates the calibration of the tube. The second one is the formation of deposits on the hard rubber ball floats which may cause cementation together which in turn causes

interference in the accuracy of the chlorine feed and reduces the automatic safety features for which these floats are designed. In order to avoid the hydrate formation, radiant heating is applied using electric light bulbs as heaters, or sometimes electric heating coils had been used directly. Solution of this problem was developed by warming the water supply which is attached to the chlorinator. This can be performed in a known way of water heating, e.g. by using electricity, or heat exchanger with steam or hot water [102].

The hydrate formation and its deposition on the walls of the industrial apparatus during the separation of the HCl and the chlorine gas in a counter-current aqueous extraction process at  $-2^{\circ}\text{C}$  was avoided by controlling the HCl concentration between 0-20%, and the temperature was controlled between  $-2$  and  $10^{\circ}\text{C}$  at 0.1 MPa. The pressure and the temperature could also be increased simultaneously to 0.55 MPa and to  $25.5^{\circ}\text{C}$  [68]. The formation of the hydrate could also be prevented by removing the larger part of the  $\text{H}_2\text{O}$  from the chlorine streams obtained from electrolysis of NaCl brine or the Deacon process at  $13^{\circ}\text{C}$  (the hydrate would be formed below  $10^{\circ}\text{C}$ ), and gaseous HCl was added in the weight ratio of 1:18.5 to the remaining  $\text{H}_2\text{O}$ . The mixture was then cooled between  $-25^{\circ}\text{C}$  and  $0^{\circ}\text{C}$  to remove the remaining water as an HCl solution without hydrate formation [67].

The possibility of the hydrate formation in seawater was studied because of an accident in which chlorine filled tank cars were lost at coastal waters. The surfacing of any gaseous chlorine was not expected in the temperature range of  $0$ - $30^{\circ}\text{C}$  if the pressure was above 9 bar ( $< 90$  m depth). Liquid chlorine drops were formed between  $8$  and  $11^{\circ}\text{C}$  without formation of any chlorine hydrate. However, at 90 meter depth liquid chlorine drops and fine white flakes of the hydrate were formed together. These flakes appeared to have almost neutral buoyancy neither rising nor falling at an observable rate. Around 45 meters, due to decrease in the pressure, coexistence of gaseous chlorine, liquid chlorine and the hydrate was observed for a short time [60]. Only a very small area exists where liquid chlorine and chlorine gas could be formed at  $8^{\circ}\text{C}$ , which is the typical temperature of the seawater at the site of the

accident in the month of the accident. It means that at the site of the chlorine spilling hydrate should be formed; however, it can be dissolved and diluted with the infinite amount of the seawater [60].

Starting from the exact composition of the hydrate, namely  $\text{Cl}_2 \cdot 6.2\text{H}_2\text{O}$ , liquid chlorine can be formed at large depths above  $27^{\circ}\text{C}$ ; however, the hydrate can be in equilibrium both with liquid chlorine and gaseous chlorine, which depends on the pressure, temperature and concentration relationships. The evaluation of the situation including the result of existing area of the hydrate in the seawater at 1 and 9 atm as the function of the temperature is also given [60].

## 5. The composition of the hydrate

The determination of the composition of the hydrate had attracted attention for a long time, because of its non-stoichiometric nature, dependence of its composition on the preparation method and conditions [14]. Furthermore, large number of problems such as the solubility of chlorine in water, instability of the crystals during weighing had caused difficulties in the analysis.

Based on the structural characteristics (section 6), the formula of the hydrate can be written as  $(8-x)\text{Cl}_2 \cdot 46\text{H}_2\text{O}$ , where  $x$  is the number of the unfilled cages in the elementary cell of the hydrate ( $Z=1$ ), or it could also be described as  $\text{Cl}_2 \cdot (5.75 + y)\text{H}_2\text{O}$ , where  $y + 5.75 = n$ ;  $n$  is the number of water molecules per chlorine molecule. Theoretically it meant that the hydrate, which is richest in chlorine, could be characterised with the formula derived from the maximal filling ratio. The experimental numerical values of the minimal filling ratios of voids by chlorine required to stabilise the clathrate cage have not been known.

The composition of the hydrate depends on many factors such as the reaction route ( $\alpha$ ), the presence and concentrations of the additives or metal salts ( $\beta$  and  $c_{\beta}$ ) or acids (pH). The temperature ( $T$ ), the pressure ( $p$ ), and the reaction time ( $t$ ) are the other important factors as expressed in equation (27).

$$n = f(p, T, t, \alpha, \beta, c_{\beta}, pH) \quad (27)$$

Only a few studies are available where some of the parameters were kept constant. Increasing pressure at the same temperature in the reaction of

water vapour and chlorine gas increased the occupancy of the voids in the clathrate cage. Similar effect was observed with decreasing temperature at a constant pressure [51, 52]. Generally, an increase in the metal chloride concentration in the aqueous solutions that reacted with chlorine gas results in the decrease of the chlorine content in the hydrate [37, 38, 41]. The use of liquefied chlorine generally gives higher chlorine content in the hydrate. It should be noted, however, that over the classical factors like temperature or pressure, the reaction time has more important effect on the occupancy and the composition [31, 32], especially, when chlorine gas is used in the reaction [85, 103].

### 5.1. Chemical analysis of the hydrate

The composition of the hydrate was first determined by Faraday in 1823 by reacting the hydrate with ammonia and leaving it for 22 h to decompose the primarily formed nitrogen chlorides and measuring the amount of the liberated ionic chlorides as AgCl. He found that the hydrate was  $\text{Cl}_2 \cdot 10.29\text{H}_2\text{O}$  and  $\text{Cl}_2 \cdot 11.05 \text{H}_2\text{O}$ , but he believed that the chlorine content is underestimated due to incomplete drying of the crystals and because of the imperfect decomposition of the nitrogen chlorides [5].

Maumene in 1883 reported that the number of the water molecules present in the hydrate depended on the experimental conditions under which the hydrate had been prepared [14]. The crystals of the hydrate, prepared by passing a stream of chlorine into different solutions around  $5^\circ\text{C}$  were dewatered in a funnel and then slightly compressed between two filter papers, were reported to have a composition of  $\text{Cl}_2 \cdot 12\text{H}_2\text{O}$ . The crystals formed in the presence of a significant excess of liquefied chlorine were found to have the composition of  $\text{Cl}_2 \cdot 4\text{H}_2\text{O}$ . These crystals were cubic and seemed to be just like those described by Ditte [13].

However, if the chlorine dissolved in a warm solution was placed in the large branch of a tube and the chlorine and the water vapour were allowed to escape slowly into the cooled small branch of the same tube, the hydrate was formed with a variable composition, but close to  $\text{Cl}_2 \cdot 7\text{H}_2\text{O}$  [14]. It was also remarked that the colour of the hydrate was deeper if more chlorine

was present in the compound [14]. The crystal size, however, caused important change in the composition of the hydrate as found by Roozeboom [20], who at the same dissociation pressure and similar composition found light yellowish white snow-like hydrate microcrystals, and large crystals for the deep yellow coloured hydrate [20].

In order to avoid the analysis errors observed by Faraday, the analyses were performed by the reaction of chlorine hydrate directly with aqueous potassium iodide solution and by determining the liberated iodine with sodium thiosulphate. Two hydrate samples were prepared from chlorine gas and water by cooling; the excess water was removed by pressing the snow like hydrate mass between filter papers. The  $n$  values found were very high, 20.1 and 13.58, which showed unambiguously that the dewatering was not complete. The use of a centrifuge for dewatering resulted in the decrease of the  $n$  value to 11.77.

By using liquid chlorine and water larger crystals were formed which were removed from the solution and analysed separately; the  $n$  values varied between 8.77 and 9.10. The use of pressure filtering of the large crystals prepared from the same method resulted in  $n$  values of 8.42–10.09. The various results are the consequence of the excess water content of the snow like or jelly like mass of the hydrate. Furthermore, the chlorine rich phases can be formed only after longer reaction time [20].

Villard studied the composition of various gas hydrates and pointed out that the chlorine hydrate had probably the same composition as the other hydrates [15, 16]. The presence of hydrochloric acid, however, affects the composition and it is rather difficult to avoid the formation of a little hydrochloric acid when chlorine is kept in the presence of water for a longer time. Even a small amount of hydrochloric acid can retain a relatively large amount of water which does not take part in the hydrate formation [16]. Since, the dissociation pressure of the hydrate formed in the presence of HCl increases [34] and when this pressure becomes equal to the pressure of the chlorine, the reaction stops and would never be completed [16].

Bouzat and Azinières developed simple analytical methods to determine the number of water molecules

**Table 10.** The effect of the reaction time on the composition of the hydrate.

Time	<i>n</i> value	Time	<i>n</i> value
10 min	8.8	3 d	7.55
1.5 h	9.6	5 d	6.35
3 h	8.2	1 w	6.44
24 h	5.90	20 w	6.30
24 h	6.08	20 w	6.12
2 d	6.8	39 w	5.97
2 d	7.05	39 w	6.10

present in one molecule of the hydrate [31, 32]. The method is based on the assumption that liquefied chlorine (vapour pressure  $p = 3.66$  atm at  $0^\circ\text{C}$ ) can evaporate from the hydrate crystals without leaving any residue, thus there is no need for “drying” or chlorine decontamination. Their results for water molecules per chlorine were found to be between 5.93 and 6.92, mostly greater than six. They supposed that the fractional value above 6 is the consequence of trapping of some uncombined water by the hydrate crystals or the hydrate crystals trapped some uncombined water containing only dissolved chlorine. Therefore, they concluded that the composition of the chlorine clathrate is  $\text{Cl}_2 \cdot 6\text{H}_2\text{O}$  [31, 32] which is consistent with the results of Villard [15] who determined the composition of the hydrates formed by reacting the water and the liquefied gas in a sealed tube. Anwar-Ullah [33] used the same preparation and analytical method and his analysis showed that the reaction time has remarkable effect on the composition of the hydrate formed, Table 10 [33].

The reaction time played a lesser role in the change of the composition when the synthesis was

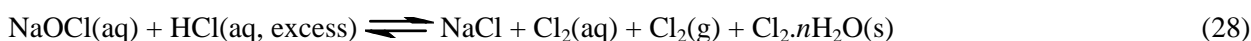
performed under chlorine pressure and the drying was performed under chlorine stream. In this case, the composition of the crystalline hydrates varied between  $n = 5.9$  and  $6.15$ , the average value was  $\text{Cl}_2 \cdot 6.02\text{H}_2\text{O}$ .

Using a known amount of copper(II) sulphate as an additive, Anwar-Ullah measured the amount of the free water. If it was subtracted from the initially used water, the amount of the water bound in the hydrate could be obtained. This analysis gave  $n$  values between 5.6 and 6.4, which indicated a larger uncertainty in the measurement, but the average value was  $\text{Cl}_2 \cdot 6.05\text{H}_2\text{O}$  [33].

Allen found higher water content ( $\text{Cl}_2 \cdot 7.27\text{H}_2\text{O}$ ) in the hydrate prepared in 5-14% calcium chloride solution. It could be expected that the chlorine content of the hydrate prepared in metal salt solution would be lower than in the hydrate prepared in pure water under the same conditions [23].

Since the kinetic viewpoint is one of the most important factors in the reaction of chlorine gas and aqueous solution, Kótai *et al.* studied the role of the reaction time on the value of  $n$  during the formation of the hydrate *in situ* via the reaction of sodium hypochlorite with excess hydrochloric acid under cooling [61, 85, 86, 103].

The reaction of sodium hypochlorite with excess hydrochloric acid, equation (28), is used to produce the chlorine hydrate *in situ*, and to determine the value of  $n$  (the number of water molecules bound to the hydrate). The concentration of the remaining hydrochloric acid is estimated by potentiometric titration. If the total amount of unreacted hydrochloric acid is  $y$  and the total amount of water present in the reaction mixture is  $z$  and the bonded is  $n$ , then the concentration of the hydrochloric acid  $c$  can be described by equation (29).



$$\text{Since, } c = a/(w - n) \quad (29)$$

Therefore,  $n$  can be calculated if the other quantities are known. The method is equally applicable to equilibrium or non-equilibrium system.

This method eliminates the errors due to the presence of intercalated mother liquor in the crystals, because the inclusions are taken into consideration as unbound solution [85, 103]. Since the crystals are not removed from the mother liquor for analysis, the errors due to

**Table 11.** Changes in the  $n$  value at different temperature as a function of time (in min).

T(°C)	15-30	30-60 $\Delta n$ values	15-60 min
-4.5	0.28	0.58	0.86
-3	0.33	0.53	0.86
-1	0.39	0.47	0.86
1	0.40	0.59	0.99

**Table 12.** Changes in the  $n$  values at various temperatures as the function of time (in min).

T(°C)	$n$ values	T(°C)	$n$ values
0	7.042	8	6.672
2	6.947	10	6.584
4	6.854	(15)	6.369
6	6.762	(20)	6.162

isolation and decomposition due to the isolation can be avoided as well. For the determination of the composition of the *in situ* formed hydrate, sodium hypochlorite is reacted with a known amount of excess HCl solution during cooling (equation 28).

The chlorine concentration in the reaction mixture is estimated iodometrically. In the knowledge of the total chlorine expected to be liberated according to equation (28), the difference in the two values is the amount of chlorine bound to the hydrate [85, 103].

The method can be used for other metal hypochlorites such as  $\text{Ca}(\text{OCl})_2$  or other oxidisable compounds to prepare water soluble gases and their gas hydrates. The salts used help to reduce the freezing point.

The results of the analysis as the function of time at different temperatures are shown in Table 11.

It can be seen from Table 11 that the reaction time is an important factor at any temperature. The changes in the composition during the first hour of the reaction can be seen in Table 12. Furthermore, the concentration of the chlorine in the solution also strongly influences the composition of the formed hydrate [23].

The minimal reaction time is one hour when the change in the composition becomes constant at negative temperatures [103]. This method gives a chance to measure systematically the composition of the chlorine hydrate formed in water or in various metal salt solutions by reacting HOCl and metal hypochlorites with HCl. The method avoids the errors due to the isolation and decomposition of the hydrate, and avoids the errors due to the inclusions in the hydrate crystals. The conditions (temperature, pressure, concentrations and likes are easily controlled), the reaction time can be adjusted, and the reaction proceeds even at very low temperatures due to the freezing point effect of the HCl used and to the metal chloride salts formed [85, 103].

The above mentioned method provides a chance for the exact analysis of the hydrate prepared in water or aqueous solutions under various conditions. The composition of the hydrate prepared from water vapour and chlorine gas, however, could not be determined with this method.

Cady [51, 104] developed a simple and correct technique to measure the composition of the hydrate formed from gaseous starting materials. A known amount of water vapour and excess of chlorine gas were reacted in a cold reactor where the hydrate deposited at the wall of the reactor. The chlorine content of the hydrate could be calculated from the known amount of water vapor at the start of the reaction and the weight of the hydrate deposited in the reactor. The temperature and pressure conditions could be adjusted easily and the method has sufficient accuracy. The results are given in Table 13.

The measured values unambiguously show that the occupancy of the hydrate increases with decreasing temperature at the same pressure, or also increases if the pressure increases at the same temperature.

## 5.2. Calculations based on experimental results

There are numerous methods for the calculation of the composition of the hydrate which are based on experimentally available data, e.g. heat of formation, dissociation pressure or density.

### 5.2.1. Calculation of the composition from the heat of formation

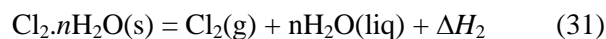
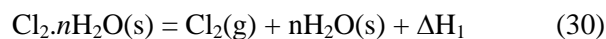
The values of the heat of dissociation are available from direct calorimetric measurements [44, 49] or

**Table 13.** The estimated values of  $n$  in the hydrate prepared at various temperatures and pressures.

$n$ value	T(°C )	Pressure atm
7.28	0	0.46
7.38	0	0.48
6.94	0	1.00
6.96	0	1.00
7.04	0	1.01
6.99	0	1.01
6.92	0	1.01
6.62	0	1.55
6.66	0	1.55
6.48	0	2.04
6.45	0	2.04
6.22	0	3.08
6.22	0	3.08
6.19	0	3.35
6.20	0	3.35
7.01	-10.7	0.48
7.04	-10.7	0.48
6.59	-10.7	1.00
6.29	-10.7	1.55
6.04	-10.7	2.50
6.05	-10.7	2.50
7.24	-21.1	0.20
7.16	-21.1	0.20
7.17	-21.1	0.20
6.67	-21.1	0.49
6.73	-21.1	0.49
6.24	-21.1	1.00
6.26	-21.1	1.01
6.36	-21.1	1.01
6.05	-21.1	1.52
6.10	-21.1	1.52
6.02	-21.1	1.55

can be calculated from the equilibrium dissociation curve by using the De Forcrand rule [105, 106] or the Clausius-Clapeyron equation including its modified forms [32, 47, 54, 107] as well.

De Forcrand determined the  $\Delta H_1$  and  $\Delta H_2$  values for the reactions given in equation (30) and equation (31) [105].



Thus the  $\Delta H_2 - \Delta H_1$ , obtained from subtracting (30) from (31), equals to the melting heat of  $n$  moles of water as given in equation (32).

$$n = \frac{\Delta H_1 - \Delta H_2}{\Delta H_{ice}^m} \quad (32)$$

of the hydrate formed from water;  $\Delta H_2$  is the molar heat of formation of the hydrate formed from ice, and  $\Delta H_{ice}^m$  is the molar melting enthalpy of the ice at 0°C.

The  $\Delta H_2$  was also expressed by equation (33).

$$\Delta H_2 = L + S + n \cdot \Delta H_{ice}^m + \frac{T' - T}{D} \cdot 1000 \quad (33)$$

where  $T'$  and  $T$  are the decomposition temperature of the hydrate and melting point of chlorine, respectively,  $L$  and  $S$  are the heat of liquefaction and solidification of chlorine, respectively and  $D$  is the heat of vaporization [108].

De Forcrand reported different  $n$  values depending on the methods used for the calculation. A value of  $n = 7.12$  was reported when the equation (31) with precise thermochemical parameters were used [108]. Another  $n$  value = 6.88 was reported using  $\Delta H_{ice}^m = 1.436 \text{ kcal/mol}^{-1}$  the latent heat of ice [105]. The use of the precise values of the dissociation enthalpy resulted in the  $n$  value as 6.91 [106].

Bouzat confirmed that the hydrate is close to the formula  $\text{Cl}_2 \cdot 6\text{H}_2\text{O}$  on using even more precise  $\Delta H_1$  and  $\Delta H_2$  values [109, 110].

According to thermochemical considerations [106, 108],  $n$  was found to be 6.90 [108]. The  $\Delta H_1$  and  $\Delta H_2$  values were determined by using the Clausius-Clapeyron equation, at the intersection point of the two dissociation curves ( $T_c = -0.24^\circ\text{C}$ ). The value of  $n = 7.97$  was obtained [111] from Roozeboom data [20]. Similarly, Kótai *et al.* [47]

found  $n = 8.34$ , which is the same as the average  $n$  value obtained by Roozeboom [20].

Since  $\Delta H_2$  is only slightly different for the various hydrates, it suggests that  $n$  is primarily proportional to  $\Delta H_1$  [49].

Wilms and Van Haute by using their own dissociation pressure values [41, 50] together with Roozeboom's [20] and Harris' [111] found  $n = 7.97$ . Having made adequate corrections for the heat of solution of the chlorine into the liquid phase and the heat of evaporation of the water passing into the gas phase, the corrected value was  $7.05 \pm 0.04$  [37, 39]. The uncorrected ( $n = 7.97$  and  $8.34$ ) values of Wilms and Kótai were close enough, but the corrected ones ( $n = 7.01$  and  $7.05$ ) agreed very well with the value  $7.05$  obtained by using the density data of Roozeboom [20].

### 5.2.2. Statistical thermodynamical considerations

Van der Waals and Platteeuw [50] considered the gas hydrates to be solid solutions, and described the occupancy at a given temperature by the Langmuir isotherm given in equation (34) [112].

$$\theta = \frac{KP}{1 + KP} \quad (34)$$

Since the chlorine is just able to fill the smaller voids, the chemical potential ( $\mu$ ) difference of the empty clathrate cage and the filled hydrate ( $\theta_1$  and  $\theta_2$  are the filling ratios in large and small cages) can be written as in equation (35) [51].

$$\Delta\mu^w = \mu_0^w - \mu_n^w = RT \left( \frac{6}{46} \ln(1 - \theta_2) + \frac{2}{46} \ln(1 - \theta_1) \right) \quad (35)$$

The  $\Delta\mu^w$  value could be considered as 265 cal around  $0^\circ\text{C}$  [51, 52] and the  $n$  value could be expressed by equation (36).

$$n = \frac{46}{6\theta_2 + 2\theta_1} \quad (36)$$

The occupancy,  $\theta_1$  and  $\theta_2$  could be calculated if the  $n$  values of hydrates prepared by various methods are known.

Using the  $\Delta\mu^w = 265$  cal given by Davidson [51, 52] at quadruple point and  $n = 7.503$  [52] at

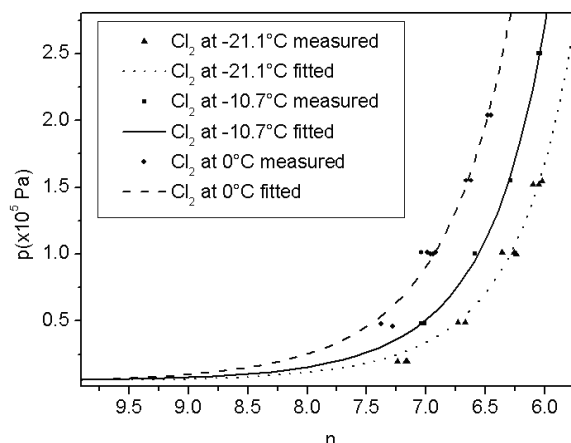


**Figure 13.** The composition and pressure relationships at constant temperatures for the hydrate prepared from water vapour and chlorine gas.

$T = 0^\circ\text{C}$  and  $p = 0.32$  atm, the occupancy  $\theta_1$  for small cavities are 0.140, and  $\theta_2$  for large cavities are 0.9751 [52]. It meant that there are 0.28 chlorine molecules in the small cavities, and 5.85 chlorine molecules in the large cavities. Therefore, the hydrate could be written as  $6.13\text{Cl}_2.46\text{H}_2\text{O}$ .

Starting from the  $\text{Cl}_2.7.47 \text{H}_2\text{O}$  at 0.316 atm equilibrium pressure at the lower quadruple point ( $-0.24^\circ\text{C}$ ), the results of the theoretical calculation performed in this way together with the experimental data for the hydrates prepared at  $-10.7$  and  $-21.1^\circ\text{C}$  are shown in Figure 13. It can be seen from the Figure 13 that all three curves cut each other around the hydration number of  $n = 9.5$  ( $p = 0.066$  kPa), which probably meant that the minimal chlorine content stabilised the clathrate lattice. The experimental values are sometimes higher than this value, however, all results after correction were below this value [23].

The composition-pressure relationships gave three equations (37), (38) and (39) ( $p$  in kPa) [23].

$$p(T = 0^\circ\text{C}) = 18.72 - 3.92n + 0.52n^2 \quad (37)$$

$$p(T = -10.7^\circ\text{C}) = 21.36 - 4.86n + 0.25n^2 \quad (38)$$

$$p(T = -21.1^\circ\text{C}) = 20.89 - 4.94n + 0.26n^2 \quad (39)$$

Since decreasing pressures, under isotherm conditions, decrease the occupation of the clathrate lattice, there is a pressure at any temperature when the chlorine built into the clathrate lattice reaches

the minimal level required to stabilise the empty lattice as a clathrate. Presuming that the stability effect of the occupation does not depend on the temperature, the decreasing pressure may reach a limiting value belonging to a limit of occupation which is the same in all isotherms. The intersection point of the isotherms drawn from the experimental pressures and composition relationships (Figure 13) should give this point where the minimal occupational level means that the energy is sufficient to compensate the energy difference between the empty clathrate lattice and the ice lattice.

### 5.2.3. Determination of the composition from the dissociation pressure

The calculation of the hydrate formula could be accomplished by applying the mass action to the water tensions as well. Equation (40) could be applied by using the activities of the reaction partners. Since the hydrate has a permanent stoichiometric composition, therefore the activity at a given temperature is constant. Since the activity of the gas is proportional to the pressure (if necessary, corrected according to the Van der Waals constants and decreased by the vapour pressure of the water), therefore the tension of the hydrate ( $p$ ) at constant temperature could be described by equation (41).

$$K = \frac{a_{Cl_2} \cdot a_{H_2O}^n}{a_{Cl_2, nH_2O}} \quad (40)$$

$$p \cdot a_{H_2O}^n = const. \quad (41)$$

A reduction in the activity of the water by a factor  $f$  causes the tension to increase by a factor  $f^n$ . Therefore, if salt is added to the water in an amount that would decrease the vapour pressure by 1%, then the tension of the hydrate would increase by  $n\%$ . Thus  $n$  could be determined. The change of the activity of the water in its various physical states is well documented. At a temperature below  $0^\circ\text{C}$ , where  $p^W$  and  $p^E$  are the vapour pressures of the water and the ice, and if  $P^W$  and  $P^E$  are the hydrate tensions in equilibrium with the super cooled water and ice then the relation between  $p$  and  $P$  are expressed by equation (42).

$$P_E \cdot P_E^n = P_W \cdot P_W^n \quad (42)$$

therefore  $n$  is expressed by equation (43)

$$n = \frac{\lg P_W - \lg P_E}{\lg p_E - \lg p_W} \quad (43)$$

The application of this method for the calculation of  $n$  is basically the same as the previous one [20] (both are related to the second law) and led to the same result [49]. In this calculation corrections were also taken into account.

### 5.2.4. Calculations from density

The density of the hydrate could be easily measured experimentally, therefore numerous methods have been developed for calculating the composition of the hydrate starting from simple pycnometric and dilatometric measurements by using the lattice constant values or the molar volume difference between the ice and clathrate lattice.

#### 5.2.4.1. Pycnometric method

A simple pycnometric method was developed by Wilms and Van Haute [40, 41] considering that at a specific temperature a mixture of the hydrate and the aqueous chlorine solution are in equilibrium. The total weight ( $G$ ), the total volume ( $V$ ) and the total weight of the chlorine ( $C$ ) could be written as in equations (44), (45) and (46).

$$G = g_s + g_l \quad (44)$$

$$V = g_s v_s + g_l v_l \quad (45)$$

$$C = g_s x_s + g_l x_l \quad (46)$$

where  $s$  refers to the hydrate phase and  $l$  refers to the liquid phase [40, 41]. The above equations lead to the expression in  $x_s$  by equation (47).

$$x_s = \frac{C v_l v_{x_1} - v_s \frac{C - G x_1}{G v_1 - V}}{G v_1 - V} \quad (47)$$

where  $v_s$  and  $x_s$  refer to the hydrate and are defined by equations (48) and (49). The others could be determined from the solution which is in equilibrium with the hydrate [40, 41].

$$v_s = \frac{1}{d_s} \quad (48)$$

$$x_s = \frac{M_{Cl_2}}{M_{Cl_2} + n \cdot M_{H_2O}} \quad (49)$$

Therefore  $n$  could be calculated from the measured density of the hydrate. Since equation (48) is a linear equation, the correlation between  $x_s$  and  $v_s$  could be written, by means of the experimental results of Roozeboom, as in equation (50).

$$x_s = 1.857517 - 1.856619v_s \quad (50)$$

The density ( $d$ ) obtained by Roozeboom was 1.237 [21], and the calculated composition calculated from this equation was  $\text{Cl}_2 \cdot 7.05\text{H}_2\text{O}$  [23].

Using the value of the lattice constant of the hydrate, a value of  $n = 6.97$  was obtained for the same hydrate. The method based on the constant difference between the dilatation of the clathrate and the ice lattice gave a value of 7.00 for the  $n$ , which is very close to the values found by the other methods [23].

#### 5.2.4.2. Dilatometric method

The dilatometric measurements provided exact results [40, 41]. Considering the equilibrium between the hydrate and the solution in a capillary tube at temperatures  $T_1$  and  $T_2$  so that the difference between the two temperatures was low ( $0.78^\circ\text{C}$ ), the total volume  $V_T$  could be written as in equation (51) [40, 41].

$$V_T = V + ah = g_1v_1 + g_s v_s \quad (51)$$

where  $a$  is the capillary constant ( $\text{cm}^3 \text{cm}^{-1}$ ) and  $h$  is the height (cm) in the capillary.

The total weight is expressed by equation (52),

$$G_T = g_1 + g_s \quad (52)$$

and, the total weight of the chlorine is expressed by equation (53)

$$W_{\text{Cl}_2} = g_1 x_1 + g_s x_s \quad (53)$$

Going from temperature  $T_1$  to  $T_2$ , the total weight of the mixture and the total weight of the chlorine remained unchanged. Since  $T_2 < T_1$ , thus  $x_{l_2} < x_{l_1}$  and an amount of the chlorine hydrate should be crystallised out. This lead to the decrease in the total volume because  $v_s < v_1$  [40, 41].

Supposing, that

$$x_{s_1} = x_{s_2} = x_{s_{12}} \quad (54)$$

and

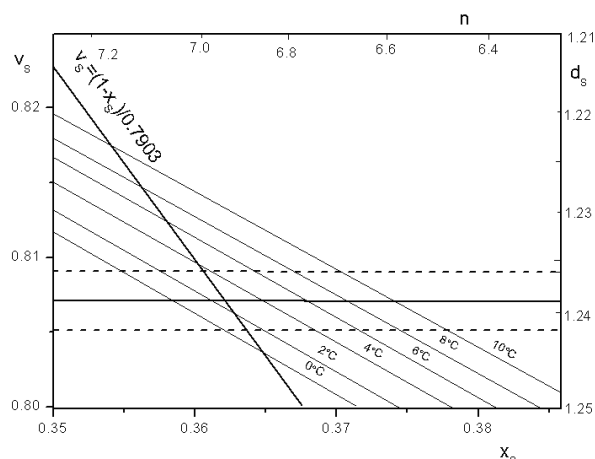


**Figure 14.** Relation between density and composition of the hydrate.

$$v_{s_1} = v_{s_2} = v_{s_{12}} \quad (55)$$

The equations (54) and (55) could be combined to give the equation (56).

$$x_{s_{12}} = \frac{x_{l_2} - \frac{\Delta V_{l_2}}{g_{l_2}} + (x_{l_1} v_{l_2} - x_{l_2} v_{l_1})}{\frac{\Delta V_{l_2}}{g_{l_2}} (v_{l_1} - v_{l_2})} - \frac{x_{l_1} - x_{l_2}}{\frac{\Delta V_{l_2}}{g_{l_2}} - (v_{l_1} - v_{l_2})} v_{s_{12}} \quad (56)$$

The equation (56) gives a linear relationship in the form of equation (57).

$$x_{s_T} = A_T - B_T v_{s_T} \quad (57)$$

with

$$T = \frac{1}{2}(T_1 + T_2) \quad (58)$$

The results calculated with the equation 57 are plotted in Figure 14.

The temperature dependence [40, 41] can be written as in equation (59).

$$x_s = (1.854928 + 0.008032t) - (1.854044 + 0.008017t)v_s \quad (59)$$

With the knowledge of the temperature and the density values, measured at the given temperature, the composition ( $n$  value) of the hydrate could be calculated as described in the previous paragraphs. Using the density, 1.237, measured by Roozeboom,

**Table 14.** Calculated composition of the hydrate from the density values.

T(°C)	<i>n</i> , value
0	7.042
2	6.947
4	6.854
6	6.762
8	6.672
10	6.584
(15)	6.369
(20)	6.162

the equation (58) resulted in the formula  $\text{Cl}_2 \cdot 7.04\text{H}_2\text{O}$  at 0°C [23].

Assuming that the density did not change between 0 and 10°C and the presence of  $\text{NaNO}_3$  had no effect on the density of the hydrate. The *n* values thus calculated at different temperatures using the experimentally determined value of  $d = 1.239 \text{ g cm}^{-3}$  are given in Table 14.

The *n* values in Table 14 are seen to decrease with increasing temperature which is inconsistent with the fact that the *n* values generally increase with increasing temperatures [51, 52, 103], therefore the above assumptions are incorrect.

#### 5.2.4.3. Calculation from the density and the lattice constant

The relationship between the lattice constant and the density of the hydrate is expressed by equations (60) and (61) [40, 41, 113].

$$d_s = \frac{46M_{\text{Cl}_2}}{a^3 N} \left( 1 + \frac{M_{\text{Cl}_2}}{nM_{\text{H}_2\text{O}}} \right) \quad (60)$$

$$d_s = d_\beta \frac{1}{1 - x_s} \quad (61)$$

Here, 46 is the number of water molecules in the unit lattice, *a* is the lattice constant in Å, *N* is the Avogadro number  $6.023 \times 10^{23} \text{ molecules mol}^{-1}$ ,  $d_\beta$  is the density of the metastable empty lattice ( $\text{g cm}^{-3}$ ). Since the most reliable lattice constant for the hydrate is  $a = 12.03 \text{ Å}$  [53], the  $d_\beta$  for the empty lattice is  $d_\beta = 0.7903$ . Therefore the formula in equation (62) could be deducted [40, 41].

**Table 15.** The density and lattice constant values for the hydrate as the functions of temperature.

T, °C	<i>n</i>	$d_s, \text{g cm}^{-3}$	<i>a</i> , Å
0	6.86	1.244	12.007
2	6.93	1.240	12.027
4	6.99	1.235	12.047
6	7.06	1.231	12.066
8	7.13	1.227	12.085
10	7.19	1.223	12.106

$$v_s = (1 - x_s) \times 0.7903 \quad (62)$$

The values of *n* and  $d_s$  were calculated at different temperatures and are collected in Table 15. Supposing that the density does not change with the temperature, the lattice constant could then be calculated.

The results show that the lattice constant gradually increased with the temperature and the occupancy *n* of the cavities. The linear expansion coefficients could be expressed as in equation (63).

$$a_t = a_0(1 + \alpha t) \quad (63)$$

where  $\alpha = 8.25 \times 10^{-4}$ . By comparing the linear thermal coefficient with the appropriate value of the ice at 0°C ( $\alpha = 9.2 \times 10^{-5}$ ), this value is higher with one order of magnitude [40, 41]. It could be the consequence of the erroneous assumption that the density was independent of the temperature. Expansion of the hydrate lattices (even in the case of the ethylene oxide hydrate) [114] was hardly 1.1% between 70 and 270 K, while the appropriate value for the ice was roughly 0.4% and 0.6% in the *a* and *c* axes, respectively which was below 1% [114]. This, however, gave a chance to calculate the formula of the chlorine and other gas hydrates from the knowledge of the experimental density without using the lattice constant with the assumption that the difference between the thermal expansion values of the ice and the clathrate lattice was constant [23]. The  $n_2$  values calculated by this method are in Table 14 wherein the composition calculated from Eqns. (59) and (60) by using the experimental *d* values are also given.

#### 5.2.4.4. Calculation from the density by using the molar volume of ice

The assumption about the small change in the lattice constant and the temperature was made on the basis of experimental and thermodynamical viewpoints [114, 115], which could be confirmed by a simple calculation. The average diameter of the hydrates of structure I is 12.0 Å, when the diameter ( $D_M$ ) of the hydrate is about 5.2 Å and it starts expanding, which is roughly 1% at the  $D_M = 5.7$  Å [114, 115]. Since the size of chlorine molecule is 5.5 Å [115], thus less than 1% expansion of the hydrate lattice can be expected [23].

Since the difference between the expansion of the ice and the hydrate is almost unchanged with the temperature, there is no significant increase in the volume of the clathrate lattice which depends on the filling ratios. Starting from the density of the ice and the hydrate at a given temperature, the composition of the hydrate could be expressed [23, 116, 117]. The volume of the 46 molecule of ice is expressed by the equation (64).

$$d = \frac{m}{d} = 46 \frac{M_{H_2O}}{d_{ice}} \quad (64)$$

The constant difference in the volume of the empty (or filled) clathrate cages and the ice is expressed by the equation (65).

$$\Delta V = V_e - V_{ice} \quad (65)$$

where  $V_e = 46M_{H_2O}/d_\beta$ , ( $d_\beta$  is the density of the empty clathrate unit and is equal to 0.7903) [40, 41]. The density of the filled clathrate could be expressed as in equation (66).

$$d = \frac{m_s}{v_s} \quad (66)$$

where

$$M_s = 46M_{H_2O} + mM_{Cl_2} \quad (67)$$

and

$$V_s = V_e = V_{ice} + \Delta V = 46M_{H_2O} / d_\beta \quad (68)$$

The occupancy ( $m$ ) could be calculated by the equation (69).

**Table 16.** Compositions of the hydrate calculated from experimental density values and the molar volume of the ice.

$d(\text{g cm}^{-3})$	$n_1$	$n_2$	Ref.
1.20	7.60	7.63	[5]
1.22	7.25	7.28	[20]
1.23	7.08	7.12	[25]
1.237	6.97	7.00	[20]
1.239	6.94	6.97	[40]
1.31	5.99	6.02	[24]

$$n = \frac{46}{m} \quad (69)$$

Equation (69) gives the number of the water/per chlorine molecule in the hydrate if the experimental density is available. The experimental values of the hydrate densities are given in Table 16, together with the appropriate  $n$  values calculated from the lattice constant by this method [23].

The calculated  $n$  values obtained by the methods using experimental density values were in good agreement considering these are within the accepted range of values measured directly by chemical analysis. The agreement between the results obtained by the method described in section 5.2.3.4 indicates the applicability of the method for other gas hydrates too, where only the density is known and no information about single crystal or powder X ray results about the lattice constant is available [23].

Some theoretical considerations about the expansion of the clathrate hydrate lattices supported the assumption used in the above mentioned calculations. The expansion of the clathrate lattice unambiguously showed that large changes due to the filling of the hydrate lattice with chlorine molecules could not be expected. If the cage compound from its normal volume ( $v_0$ ) is expanded to volume  $v$  by incorporating “too big” molecules, the expansion work is given by equation (70) [115].

$$E = \int_{v_0}^v P dv \quad (70)$$

The compressibility  $\chi$  is expressed by equation (71), and  $P$  is given by equation (72).

$$\chi = \frac{1}{v_0} \cdot \frac{dv}{dp} \quad (71)$$

$$P = \frac{v - v_0}{v_0} \quad (72)$$

Substitution of the value of  $\chi$  from the equation (71) and that of  $p$  from the equation (72) into the equation (70) and integration of the resulting equation gives equation (73) which is related to the expanded grid.

$$E = \frac{(v - v_0)^2}{2\chi v_0} \quad (73)$$

Equation (74) represents the correlation between  $a$  and  $a_0$  where  $a_0$  is the lattice constant of the elementary cell containing 8M.

$$a = a_0 + \Delta a \quad (74)$$

then

$$v_0 = \frac{1}{8} N_L a_0^3 \quad (75)$$

with  $N_L = 6 \times 10^{23}$

$$v = \frac{1}{8} N_L (a_0 + \Delta a)^3 \quad (76)$$

or roughly

$$v = \frac{1}{8} N_L (a_0^3 + 3a_0^2 \Delta a) \quad (77)$$

Therefore,

$$E = \frac{9N_L a_0^4 \Delta a^2}{8 \cdot 2 \cdot \chi \cdot a_0^3 \cdot 41} = 8.3 \cdot 10^{21} \frac{a_0^3 \Delta a^2}{\chi a^2} \quad (78)$$

where  $E$  is in cal, the factor 41 in the denominator is the conversion factor for the conversion of  $\text{cm}^3$  and atm into cal, and  $a$  should be used in cm and  $\chi$  should be used in  $\text{atm}^{-1}$ . From equation (78), with  $a_0 = 12.0 \times 10^{-8}$  cm, one could get equation (79).

$$E_I = 36 \times (100 \cdot \Delta a / a)^2 \quad (79)$$

for the type I of hydrates. These values are small compared to the variation of the Van der Waals

binding energies due to individual differences in the hydrate-forming molecules [115].

### 5.2.5. Miller and strong method

In the equilibrium involving chlorine-water-chlorine hydrate at constant temperature, the addition of a component to the liquid phase increased the equilibrium pressure because of the increase in the decomposition pressure of the hydrate. If the composition was not affected by the third component, then  $n$  could be given by equation (80).

$$n = \frac{\lg \frac{f_1}{f_2}}{\lg \frac{a_1}{a_2}} \quad (80)$$

where  $f_1$  and  $a_1$  are respectively the fugacity in the gas phase and the activity of the water in the aqueous phase in the absence of the third component, while  $f_2$  and  $a_2$  are the fugacity and activity in the presence of the third component [40, 41]. If the third component has no vapour tension, e.g. solid salts like NaCl, the  $f$  and  $a$  values must be calculated from the experimental results  $(p_1, c_1, z_1 = 0)_T = (p_2, c_2, z_2)_T$  where  $c$  and  $z$  are the concentrations of the chlorine and the salt in the liquid phase.

Bozzo found that  $n = 6.20$  for 5-15% of NaCl solutions between 14-20°C [37, 38, 39], while the  $n$  values given by Wilms and Van Haute for 2-15% NaCl solutions between 4 and 10°C are given in Table 17 [40, 41] contains the temperature, the pressure, the NaCl concentration and the dissolved  $\text{Cl}_2$  concentration together with the  $n$  values:

The accuracy of the calculation methods discussed in section 5.2, is based on experimental measurements, and depended on many factors. Since the experiments for the hydrate, which was not in dynamic equilibrium with its mother liquor, were repeated many times. The measured parameters were related to compositions which were valid at the time of the measurement.

## 6. Thermodynamics of the hydrate

The thermodynamical evaluation of the dissociation of the hydrate is a thoroughly studied area.

**Table 17.** The composition of the hydrate determined by the Miller and Strong method between 2-15% NaCl concentration and 4-10°C.

T°C	$p$ mmHg	$z_2$ , wt.%	$c_2$ , wt.%	$n$
3.90	810.6	14.560	0.6129	6.95
4.13	813.5	14.433	0.5975	6.82
4.45	693.6	13.369	0.6297	6.90
5.44	808.4	11.989	0.6181	6.78
5.88	813.2	11.079	0.6465	6.88
6.00	792.8	10.549	0.6587	6.74
6.71	787.1	8.861	0.662	6.76
7.96	799.5	6.204	0.714	6.74
9.28	787.6	2.322	0.829	6.61

The heat of formation roughly equals with the heat of dissociation or melting enthalpy, if the temperature dependence of the reaction heat, the solubility of the chlorine in water and the vapour pressure of the water are neglected. The values of the dissociation heat, the relationship between dissociation and reaction heat, heat of formation and the standard heat of formation have been discussed [118]. From the equilibrium dissociation pressures, not only the dissociation heats, but the Gibbs free enthalpy and entropy could also be determined. The role of occupancy could be evaluated by statistical thermodynamical approximations which explained the anomalies observed in the hydrate chemistry.

### 6.1. The heat of formation

Evaluation of the equilibrium conditions, the standard heat of formation ( $\Delta H^0$ ), the reaction heat ( $\Delta H^a$ ) at given equilibrium conditions, and the heat calculated from the dissociation curve (H) could be distinguished very well. Based on these enthalpy values, the entropy and free enthalpy changes of the reaction could be calculated as well. The hydrate formation reaction is an equilibrium reaction, and the value of the heat of formation ( $\Delta H_f^0$ ) equals the heat of dissociation ( $\Delta H_d^0$ ) as given in equation (81).

$$\Delta H_f^0 = \Delta H_d^0 \quad (81)$$

Since the dissociation of the hydrate produces only chlorine (including some water vapour), the

dissociation pressure equals the vapour pressure of the hydrate. Since this system is solid  $\leftrightarrow$  gas + liquid or solid  $\leftrightarrow$  solid + gas type univariant system [35, 110], most of the thermodynamic rules e.g. the Clausius-Clapeyron equation are valid for the decomposition of the hydrate.

#### 6.1.1. Experimental determination of the heat of formation

The heat of formation of the hydrate from chlorine gas and water was determined directly by following the reaction of the chlorine gas with saturated cold chlorinated water. The  $\Delta H_2$  was found to be 16.9 kcal [49].

De Forcrand measured the heat of dissolution of the hydrate in water and corrected the value by the heat of dissolution of the chlorine gas in water. Thus, the heat of dissociation of the hydrate  $\Delta H$  into water and chlorine gas was determined to be 18.36 kcal mol<sup>-1</sup> [105, 106, 119].

Le Chatelier also determined the heat of formation of the hydrate by measuring the heat of dissolution at 5°C, the dissolution heat of the chlorine gas was taken into consideration [44]. Dissolution heat of the hydrate  $\Delta H_d$  was found to be 14 cal at 5°C [44]. By taking into consideration the heat of dissolution of the chlorine gas in water (3 kcal/mol) [120], the heat of formation  $\Delta H_2$  was found to be 17 kcal mol<sup>-1</sup> [44].

For the hydrate formed from gaseous components as in equation (82),



The equation (83) or (84), given by Le Chatelier is valid [42, 119].

$$n \frac{dp}{p} + n_1 \frac{dp_1}{p_1} + n_i \frac{dp_i}{p_i} + \frac{Q}{0.542} 273 \frac{dT}{T^2} = 0 \quad (83)$$

or

$$\lg(p^n p_1^{n_1} - p_i^{-n_i} \dots) + \int_0^T \frac{Q}{0.542} 273 \frac{dT}{T^2} = \text{const.} \quad (84)$$

where  $p$ ,  $p_1$ ,  $p_i$  are the pressures of the gases involved in the equilibrium,  $n$ ,  $n_1$ ,  $n_i$  are the numbers of moles of each gas appearing in the equation of the chemical reaction,  $Q$  is the amount of the heat released by the reaction of  $n$ ,  $n_1$ ,  $n_i$ , molecules and  $T$  is the absolute temperature.

Substituting  $n_1 = 8$  since the formula given by Roozeboom was  $\text{Cl}_2 \cdot 8\text{H}_2\text{O}$ , Le Chatelier found that  $\Delta H_3 = 102 \text{ kcal mol}^{-1}$  for the reaction (82) [44].

### 6.1.2 Determination of the heat of formation by the Trouton rule

de Forcrand [105, 106, 121, 122] first used the Trouton rule to determine the heat of formation. If  $\Delta H_1$  is the heat of dissociation of the hydrate into gaseous chlorine and ice, and  $T$  is the temperature at which the dissociation pressure is 760 Hgmm, then  $\Delta H_1/T$  is a constant value near to 30. Since  $T$  was known from experimental dissociation pressures of the chlorine [20], an approximate value of  $\Delta H_1$  was found to be  $8.478 \text{ kcal mol}^{-1}$  [105, 106].

### 6.1.3. Determination of the heat of formation by Eucken theory

As a measure of first approximation for the formation of gas hydrate, it was assumed that the formation energy of the  $\text{H}_2\text{O}$ -lattice of the hydrate was about the same as it is in the case of ordinary ice [49, 123].

The incorporation of the gas atom into the cavities of the  $\text{H}_2\text{O}$  skeleton involves the liberation energy  $W$  due to the action of Van der Waals-London forces between the gas molecule and the  $\text{H}_2\text{O}$  molecules. Analogously the heat of physical adsorption,  $W$ , is given by the equation (85); where  $L$  is the heat of vaporisation of the hydrate and about 8 kcal is the heat of evaporation of the  $\text{H}_2\text{O}$  from the larger aggregates free from the intended water.

$$W = \sqrt{8000 \cdot L} \quad (85)$$

The value of  $W$  thus calculated was similar to the heat of the reaction of the chlorine gas with ice [49, 123]. A value of  $W = 7.3 \text{ kcal}$  was found for the hydrate by using the heat of vaporization at  $0^\circ\text{C}$ , which is practically the same as the heat of liquefaction,  $L_S = 7.3 \text{ kcal}$  [49, 123].

### 6.1.4. Determination by the Clausius Clapeyron equation

Le Chatelier first used the Clausius-Clapeyron equation (86), based on the variation of the dissociation pressure with the variation in the temperature for the hydrate [34].

**Table 18.** The heat of dissociation ( $\text{kcal mol}^{-1}$ ) of the hydrate ( $\Delta H_1$  (ice) and  $\Delta H_2$  (water)) formation.

$\Delta H_1$	$\Delta H_2$	Author	Ref. No.
8.478	18.360	De Forcrand	[105]
-	17.760	De Forcrand	[108]
6.413	17.870	Harris	[111]
-	17.0	Le Chatalier	[44]
6.0	14.3	Le Chatalier	[34]
6.8		Tamman	[36]
-	19.100	Iskenderov	[43]
-	16.550	Bozzo	[38]
-	16.03	Smirnov	[24]
-	18.15	Byk	[54]

$$\frac{E}{T} \frac{Q}{S - \sigma} = \frac{dp}{dT} \quad (86)$$

where  $Q$  is the amount of heat released, and  $(S - \sigma)$  is the volume change produced by processing of the same amount of material [34].

The calculated  $\Delta H$  value are shown in Table 18. By taking into consideration the magnitude of difference and the uncertainties due to the number of water molecules in the hydrate as well as the variation of the solubility coefficient of the chlorine which can affect both the  $Q$  and the  $S - \sigma$  values, the method seemed to be reliable [34]. Therefore, this method was used many times to calculate the exact dissociation heat or heat of formation of the hydrate [37, 38, 39, 40, 41, 43, 47, 49, 54, 111, 124, 125].

The Clausius Clapeyron equation (87) could be derived if  $S - \sigma$  is replaced with  $\Delta V = (V_1 - V_2)$ , and  $E \times Q$  with  $\Delta H$ . The volume change can be easily calculated by taking into consideration the molar volume of the ice, the water and the clathrate cage, which are 18.0, 19.6 and  $22.8 \text{ cm}^3$ , respectively [112].

$$\Delta H = T(V_2 - V_1) \frac{dp}{dT} \quad (87)$$

where  $V_1$  and  $V_2$  are the volumes of the hydrate and the hydrate forming gas. The change in

the molar volume of the hydrate during melting at the lower quadruple point was obtained as  $\Delta V = 17.20 \text{ cm}^3 \text{ mol}^{-1}$  [54].

By using this  $\Delta V$  value, the intercalation heat was found to be 7.3 kcal for chlorine assuming that the enthalpy of the ice-clathrate process was zero [112]. This intercalation heat value is very close to 7.6 kcal calculated by Eucken formula given in equation (88).

$$\sqrt{\Delta H_h \Delta H_{ice}} = 7.6 \text{ kcal} \quad (88)$$

where  $\Delta H_h$  and  $\Delta H_{ice}$  are the respective heat of condensation of gaseous chlorine to liquid and water vapour to ice [112]. Since neglecting the heat of transformation did not cause large deviation, therefore the of transformation of the ice into the empty clathrate cage is considered close to zero. The real value of  $\Delta H_T$  was  $265 \text{ cal mol}^{-1}$  [51, 52].

The Clausius Clapeyron equation (87) could be changed to equation (89) with the assumption that  $V_1$  is negligible and the volume  $V = RT/p$ .

$$H = \frac{RT^2}{p} \frac{dp}{dT} = RT^2 \frac{2.3d \lg p}{dT} \quad (89)$$

Equation (89) could be integrated to equation (90).

$$\ln \frac{p_2}{p_1} = \frac{H}{R} \left( \frac{1}{T_1} - \frac{1}{T_2} \right) \quad (90)$$

The H values were more precise when the compressibility factor ( $z$ ) was used. Iskenderov and Musaev used  $z = 1$  for chlorine in the absence of known compressibility value and obtained  $H = 19.100 \text{ kcal mol}^{-1}$  for the hydrate [43]. Since  $z = 1$  was used for the chlorine, this equation was the same as the one used by Harris [111], Ionescu [124], Wilms and Van Haute [40, 41], Bozzo [38, 39, 81] and Kótai [47, 85] to calculate the heat evolved during the hydrate formation.

The calculated heat of dissociation values, given in Table 18, were close to the heat of formation. However, these values were definitely equal to the heat of decomposition calculated from the  $\ln p-1/T$  curve, even if the authors generally took these values as the real heat of dissociation or the heat of formation. Since the  $\ln p-1/T$  curve for the chlorine hydrate were not completely linear,

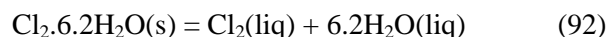
therefore the method required some refinement to provide accurate  $\Delta H_a$  or  $\Delta H_f$  values. Although the corrections were partly compensated, yet the results at higher temperature (with large  $p$ ) showed a significant deviation [49]. Therefore, several efforts were directed to solve this problem.

The numerical values of Q depend on the composition of the hydrate because the vapour pressure unambiguously depends on the hydrate composition [37, 38, 39, 40, 41]. For example, the heat of reaction for the equilibria presented in equations (9) and (12), were determined.

The heat of dissociation of the hydrate with unknown n vale, equation (91) had been obtained as  $\Delta H = 4.295 \text{ kcal mol}^{-1}$  [38].



However,  $\Delta H = 12.260 \text{ kcal mol}^{-1}$  was reported at  $28.3^\circ\text{C}$  for the dissociation of the hydrate with  $n = 6.2$  considered in equation (92) [37, 39].



In order to determine the heat of formation or the standard heat of formation, the H values calculated from the Clausius-Clapeyron equation had to be corrected with factors which could balance the effect of the above mentioned problems.

Stackelberg multiplied the H values from the Clausius Clapeyron equation by considering a correction factor  $f_1$  ( $<1$ ) because of the deviations of the chlorine from the ideal behaviour. This could be calculated from the equation (93) where a and b are Van der Waals constants of the gas and  $p$  is the dissociation pressure of the hydrate.

$$f_1 = \frac{V_{real}}{V_{ideal}} = 1 + P \left( \frac{b}{22400} - \frac{a \cdot 10^{-8}}{5.0} \right) \quad (93)$$

The  $f_1$  values at the invariant points and at  $9.6^\circ\text{C}$  where the dissociation pressure was 1 atm were close to 1 [23]. Using the fugacity values of the chlorine [126] instead of the pressure also returned the  $f_1$  factor with a value of 1 [23]. Further corrections in factors  $f_2$  and  $f_3$  resulted from the fact that the heat of formation was determined from the pure gas and pure water.

However, the gas was saturated with water vapour at the pressure of the measurement, (which increases the volume, therefore  $f_2 > 1$ ) and the water part contained dissolved gas (which decreases the volume, so  $f_3 < 1$ ). The factor  $f_2$  could be expressed by the equation (94).

$$f_2 = \frac{P}{P - p_{H_2O}} \quad (94)$$

where  $P$  is the tension of the hydrate,  $p_{H_2O}$  is the vapour pressure of the water (4.6 Hgmm) at 0°C.

Therefore  $f_2$  is significantly different from 1 when  $P$  is small which is the case in liquid hydrates but not in the chlorine hydrate ( $f_2 = 1.018$  [49]). The factor  $f_3$  could be expressed by the equation (95).

$$f_3 = 1 - L \quad (95)$$

Furthermore,  $L$  is the number of moles of gas dissolved in 6 mol of water ( $m_{\text{water}} = 108$  g) at pressure  $P$ . The value of the factor  $f_3$  for the hydrate is 0.992. However,  $f_3$  also happened to be a function of the composition; therefore equation (96) is more reliable.

$$f_3 = 1 - L \frac{n}{6} \quad (96)$$

where  $n$  is the number of water molecules in which one mole of the chlorine gas is encapsulated [23].

In addition to these three correction factors, two additive correction terms had to be taken into account. One is the heat of solution,  $H_L$ , of  $L$  moles of gas in 6 (or  $n$ ) moles of water which had to be added to the heat of formation calculated from the Clausius-Clapeyron equation. Conversely, the heat of vaporisation of the water which is present as vapour in the gas,  $H_D$ , expressed in equation (97) had to be deducted.

$$H_D = \frac{4.9}{P} \quad (97)$$

The value of  $H_D$  is expressed in kcal if the pressure is expressed in Torr at 0°C. Alternatively one could also write the equation (98).

$$\Delta H_a = Q \cdot f_1 \cdot f_2 \cdot f_3 + Q_L + Q_D \quad (98)$$

where  $H$  is the heat of formation determined from the Clausius-Clapeyron equation ( $\ln p - 1/T$  equation).

These factors for the chlorine hydrate are:  $H_L = 0.04$  kcal, and  $H_D = 0.2$  kcal. The value of  $Q_D$  is only 0.22 kcal if ice reacts with chlorine. In this case, corrections  $H_L$  and  $f_3$  lose their roles, and  $H_d$  is the heat of sublimation of the ice. It may be mentioned that the plot of  $\lg p$  against  $1/T$  is not linear, there is a steep at higher temperatures.

By subtracting the solidification heat of the chlorine and of the water from the heat of formation  $\Delta H_2$ , the heat of formation from solid chlorine and ice ( $\Delta H_3$ ) is obtained. It appears then that the formation of the hydrate from the solid components has no noticeable heat evolution. The actual hydrate formation occurs without significant energy exchange. The entropy in this reaction is very low.

The heat of formations obtained by means of correction factors  $f_1$ ,  $f_2$ ,  $f_3$ ,  $H_L$  and  $H_D$  were;  $\Delta H_1$  ( $\text{Cl}_{2g}$ ,  $\text{H}_2\text{O}_{\text{liq}}$ ) = 15.5 kcal mol<sup>-1</sup> [49],  $\Delta H_2$  ( $\text{Cl}_{2g}$ , ice) = 7.1 kcal mol<sup>-1</sup> [49], and  $\Delta H_3$  ( $\text{Cl}_{2s}$ , ice) = 0.5 kcal mol<sup>-1</sup> [49, 123].

Calculation of the  $H$  values, when the modifying factors were taken into consideration, could also be made. The real gas behaviour of the chlorine could be expressed when the pressure-temperature relationship is not presented in the usual form but in a modified form, as given in equation (99), was suggested by Peshkova [127].

$$\lg p = A - B/T \quad (99)$$

Introduction of a temperature dependent factor in the equation (99) leads to equation (100).

$$\lg p = A - B/T + C f(T) \quad (100)$$

Substituting equation (100) into the Clausius-Clapeyron equation and entering the compressibility  $z$ , the equation (101) is obtained.

$$H = 2.3RT^2 z \frac{d \lg p}{dT} = 2.3Rz \left( B + C \frac{df(T)}{dT} \right) \quad (101)$$

Peshkova supposed that  $z = 1$ , which is close to the real value 0.9867 at 1.013 bar and 15°C [126]. The temperature dependent heat of formation could be calculated and the results obtained by using compressibility factor  $z = 1$  are shown in Table 19.

Table 19 indicated that reaction heat decreased with the decreasing temperature. Similar trend

**Table 19.** The heat of formation of the chlorine hydrate.

$T, K$	$P, kPa$	$\Delta H_f, J mol^{-1}$
273.37	33.36	72697.2
278.15	57.62	74412.4
283.15	104.13	76206.0
288.15	182.99	78000.5
293.15	319.48	79794.5
298.15	553.03	81589.0

was observed by Kótai *et al.* [48], but an opposite trend was reported by Bozzo *et al.* [37, 38, 39]. In the calculations of Bozzo  $z$  was taken into account only with one factor decreasing with increasing temperature and pressure [43]; consequently  $z$  should be decrease with increasing temperature. Therefore, the  $H$  values should decrease as well. The consideration is that the  $dp/dT$  characterised the phase transition and increased by increasing temperature. Therefore the  $H$  values increased during the transition from the lowest to the highest point on the curve [43].

### 6.2. The Gibbs energy relations of the hydrate

The equilibrium constant of the reaction (9) could be expressed by equation (102) [124].

$$K_a = \frac{a_{Cl_2 \cdot nH_2O}}{a_{Cl_2} \cdot a_{H_2O}^n} \quad (102)$$

Assuming that the activities of the solid hydrate and the water are approximately one, the activity of the gas could be expressed by equation (103).

$$a = P \quad (103)$$

The equilibrium constant  $K_p$  could therefore be expressed by equation (104) [124].

$$K_p = 1/P_{Cl_2} \quad (104)$$

The standard Gibbs energy  $\Delta G_r^0$  is related to the equilibrium constant  $K_p$  by the equation (104) permitting the calculation of  $\Delta G_r^0(T)$  [124] as expressed in equation (105).

$$\Delta G_r^0(T) = -RT \ln K_p \quad (105)$$

**Table 20.** The thermodynamical functions of the decomposition reaction of the hydrate.

$T, K$	$\Delta H_r, kJ mol^{-1}$	$\Delta G_r, kJmol^{-1}$	$\Delta S_r^0, Jmol^{-1}K^{-1}$
272.91	30.45	2.57	121.0
272.15	30.56	2.66	122.1
271.15	30.52	2.76	122.8
270.15	30.42	2.86	123.2
269.15	30.37	2.95	123.8
267.15	30.18	3.14	124.7
265.15	29.29	3.31	125.5
263.15	29.51	3.46	125.3
173.16	19.64	8.24	161.0

The calculated  $\Delta H$ ,  $\Delta G$  and  $\Delta S_r^0$  values are shown in Table 20 [47].

### 6.3. The entropy relations of the hydrate

Bouzat suggested that the entropy change in the decomposition of the hydrate would result from the liberation of a molecule of gas, equation (106), under a definite pressure that has the same value for all similar systems [35, 110].



Stackelberg assumed that the the entropy change in the formation of gas hydrates from water and chlorine gas was zero. The entropy of the six freezing water molecules encapsulating the gas molecule was equated with the entropy of which was reduced by -5 eu assuming that the gas freely rotated in the cage [124].

A simple way to estimate the entropy change during the clathrate formation is to consider the entropy of condensation and solidification of the chlorine and the entropy of solidification of the water as expressed in equation (107).

$$\Delta S_r^0 = \Delta S_{Cl_2_{cond}}^0 + \Delta S_{Cl_2_{solid}}^0 + 6\Delta S_{H_2O_{solid}}^0 \quad (107)$$

The estimated  $\Delta S_r^0$  was -60.8 eu from the experimental value of the vapour pressure whereas the one calculated from the equation (106) was -56.4 eu. Ionescu attributed this difference to the fact that the entropy change

during the clathrate formation from the ice was not equal to zero [124]. It was also believed [23] that the assumption of six water molecules in the calculations could be another source for this difference.

The relationship between the entropy of the decomposition reaction and the enthalpy and the Gibbs energy could be expressed by equation (108). The calculated values of  $\Delta S_r^0$  are given in Table 20.

$$\Delta S_r^0 = \frac{\Delta H_r - \Delta G_r}{T} \quad (108)$$

#### 6.4. Statistical thermodynamical considerations

The difference in the chemical potential between the empty clathrate cage and the clathrate cavity filled with gas could be described by equation (34). Since the relation between the occupancy ( $\theta$ ) and the constant  $K$  at constant temperature is expressed by the Langmuir isotherm given in equation (33) [112], the values of the constants  $K_1$  and  $K_2$  corresponding to occupancy  $\theta_1$  and  $\theta_2$  were determined and found to be 0.518 and 125 respectively [52].

The use of equation (34) and changing occupancy  $\theta_2$  from 0 to 99.9% at various  $n$  values, the chemical potential differences show curves that have minima and are shifting towards higher values as it is shown in Figure 15.

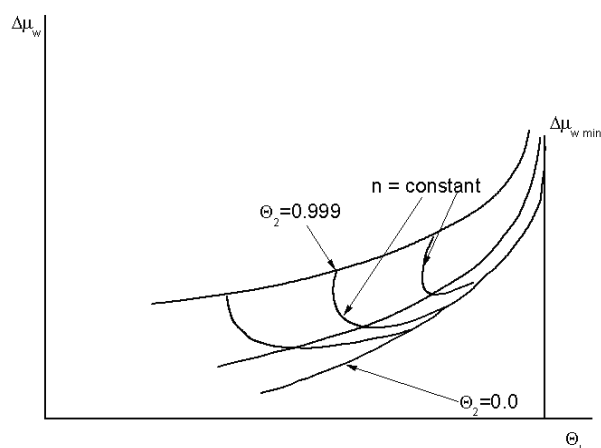


**Figure 15.** The changes in chemical potential and in the occupation of  $\theta_2$  cavities at various  $n$  values of the hydrate.

This minimal energy state allows the determination of the degree of the space occupation in small and big cavities [103].

#### 6.5. The role of the composition on the heat of the decomposition

With the knowledge of the  $n$  value at the invariant point, it is possible to calculate the heat of formation, by the Kirchoff equation (109).

$$H = H_0 + \Delta T \frac{dH}{dT} \quad (109)$$

where  $H_0$  is the heat of formation at the initial invariable point of the phase diagram, and  $dH/dT$  can be expressed as in equation (110).

$$\frac{dH}{dT} = (C_p + n18C_p^w)_T - (C_p + n18C_p^w)_0 \quad (110)$$

where  $C_p$  is the molar heat capacity of the gas under test conditions,  $C_p^w$  is the heat capacity of the water under the conditions of the hydrate formation,  $n$  is the number of the water molecules in the hydrate at the temperature of the formation of the gas hydrate [43].

Since the composition of the hydrate could be obtained experimentally at several temperatures [51, 52, 103] and synthesis conditions, the heat of formation could be calculated for different temperatures for various hydrates.

The difference between the two values of the heat of formation, calculated by the Kirchoff equation (109), for the hydrate having the similar composition at the invariant point, and the other for the hydrates formed at the same temperature is equal to the intercalation heats of the chlorine content differences between the two hydrates as is given in equation (111).

$$\Delta H = (n\delta_1 - n^*\delta_1) + (m\delta_1 - m^*\delta_2) \quad (111)$$

where  $n$  and  $n^*$  are the occupancy in the type I cavities of the two different hydrates,  $m$  and  $m^*$  are the occupancy of the type II cavities, and  $\delta_1$  and  $\delta_2$  are the average intercalation heats in the cavities of type I and II respectively. These calculations have been published [23, 116, 128].

#### 7. Molecular and crystal structure of the hydrate

Davy [1] and Faraday [5] realised that the hydrate was a compound of the elementary chlorine with

water. Although several theories were developed about the coexistence of HCl and HOCl in the hydrate to explain its composition and properties, yet the exact knowledge of the crystal structure, the occupancy of the cavities, and the freedom of rotation within the cavities remained essential questions of the hydrate chemistry [53, 95].

### 7.1. Chemical structure of the hydrate

Schönbein, shortly after the discovery of the hypochlorous acid, suggested that the chlorine in the hydrate existed in its hydrolysed form as HCl and HOCl, because these two acids were found in the dilute aqueous solutions of the chlorine or the chlorine hydrate [129]. Since, the reaction of HOCl and HCl in the formation of chlorine did not stop at 0°C, Göpner excluded the coexistence of HCl and HOCl in the hydrate. The reaction of the hydrate with elementary mercury, however, resulted only in the mercury(II) chloride which was believed to be the decomposition product of mercury oxychloride formed from HOCl and elementary Hg [28].

Schiff investigated the possibility of the coexistence of HOCl and HCl in the hydrate structure very precisely [8]. First of all, the concentration of the formal “HOCl content” of the hydrate is comparable with the concentration of the concentrated hypochlorous acid solution, and the differences in the properties of the HOCl solutions and the chlorine hydrate are unambiguous. While a concentrated solution of HOCl decomposes very quickly even in scattered light, the same concentration of the hypochlorous acid was supposed “to build” into the hydrate along with HCl and H<sub>2</sub>O (HOCl + HCl + 9H<sub>2</sub>O) and remained unchanged for a long period of time. The assumption that the HCl, which rapidly disintegrates the concentrated HOCl at 20°C, would just act in the contrary at a slightly lower temperature (about 10°C) and would contribute to the durability of HClO proved to be invalid [8].

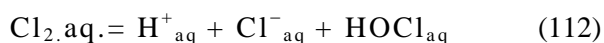
The reaction with elementary mercury, performed by Göpner [28], is not specific because the HOCl and the Cl<sub>2</sub> also give HgCl<sub>2</sub> as the main product. In the first case HgCl<sub>2</sub> is formed from the decomposition of the primarily formed mercuric oxychloride, and in the second case it is formed due to the strong chlorination effect of the highly

condensed chlorine in the hydrate toward the primarily formed Hg<sub>2</sub>Cl<sub>2</sub> [8].

Faraday emphasised that the hydrate acted on organic substances just as the free chlorine did [5]. Likewise, it also acted on the epidermis without staining or etching as would be expected if the crystals contained hypochlorous acid [8]. Contrary to the hypochlorous acid, the chlorine hydrate showed no tendency for deflagration even in hot concentrated sulfuric acid. Since, neither the HOCl nor the HCl form a hydrate by themselves, therefore these may not be present as HCl and HOCl in the hydrate without changing [8].

Jakowkin suggested an unambiguous solution for this problem by measuring the conductivity of the hydrate solutions and studying the distribution of the elementary chlorine present in the hydrate between water and carbon tetrachloride [26, 27]. Distribution of the chlorine between the water and the carbon tetrachloride is possible only if the chlorine is not hydrolysed, and the chlorine could go from aqueous layer into the carbon tetrachloride. However, the carbon tetrachloride dissolves neither the HCl nor the HOCl from dilute aqueous solutions. The distribution coefficient refers to the whole amount of the chlorine (hydrolysed and the unhydrolysed form) which changes significantly with the concentration, viz., the distribution coefficient is 20 for concentrated solutions and zero for very dilute solutions [26, 27].

Similarly, the conductivity ( $\mu$ ) of the dilute aqueous chlorine solutions at 0°C, considered in equation (110), is almost equal to that of the hydrogen chloride solutions at the corresponding levels. However, the conductivity of the chlorine in more concentrated solutions is significantly lower [26]. The conductivity of the chlorine in aqueous solution is due to H<sup>+</sup> and Cl<sup>-</sup> ions as shown in equation (112).



The ratio of  $\mu_d/\mu_\infty$  ( $\mu_d$  and  $\mu_\infty$  are respectively the conductivity at dilution  $d$  and at infinite dilution) at 0°C were determined. It was found that in aqueous solution the hydrate at low concentrations dissociated into hydrochloric acid and HOCl. In more concentrated solutions, however, the dissociation was not observed because the formed

HCl autoinhibited the process. By adding 0.05-0.1 M hydrochloric acid to the solutions, the hydrolysis of the chlorine could be completely prevented. Therefore, under the same conditions, the observed distribution coefficient ( $\sim 20$ ) for the unhydrolysed chlorine was observed [26, 27].

## 7.2. Molecular structure of the hydrate

Comparing the results of the experiments that produced orthorhombic and other irregular (non-cubic) crystals of the hydrate [11, 12], and accepting Maumene results about the existence of a very dark yellow hydrate formed in a chlorine rich environment with a  $\text{Cl}_2 \cdot 4\text{H}_2\text{O}$  formula [14] (analogous  $\text{BrCl} \cdot 4\text{H}_2\text{O}$  was isolated and analyzed [130]), the existence of various not only crystallographically but molecularly and structurally different hydrates of chlorine can not be excluded [23].

In the case of type I clathrate, depending on the composition, the filling ratio of the large and small voids could be different. In the  $\text{Cl}_2 \cdot 7.27\text{H}_2\text{O}$  formed from water-rich solution as the chlorine must fill a minimum of 16% of the pentagonal dodecahedral sites [82]. In a more chlorine rich hydrate,  $\text{Cl}_2 \cdot 6.04\text{H}_2\text{O}$ , the minimum occupancy of the dodecahedra was (81%) [131].

### 7.2.1. NMR spectroscopic investigations

Proton NMR line width of the hydrate lattice was determined as a function of the temperature. The line width of the rigid lattice decreased with the temperature and the widths were similar to that of the ice. The chlorine rotates rapidly in the cavities and the activation energy for the motion decreases probably by a combination of the rotational and the diffusion processes. It had a value of 7.7 kcal/mole [75, 132].

In the structure of the hydrate, the captured chlorine atoms completely fill the tetrakaidecahedron type cavities and partly fill the dodecahedron type cavities as well. Despite the stabilization effect of the encaged chlorine molecule on the clathrate framework, there is an increase in the melting point compared to that of the ice, and the mobility of the protons in the framework is so great that the line width is less than 0.1 G at 260 K as is shown in Figure 16 [132].

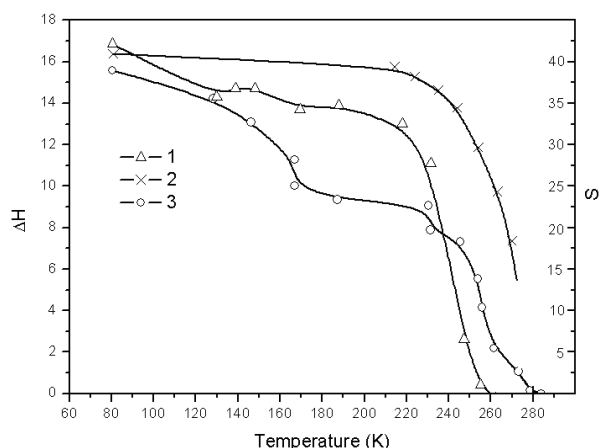


**Figure 16.** The relationship is observed between the line width ( $\Delta H$ , G) and the temperature for the  $\text{Cl}_2 \cdot 5.75\text{H}_2\text{O}$  (1) and for the ice (2). The relationship between the second moment ( $S$ ,  $\text{G}^2$ ) and temperature for  $S(T)$  for the  $\text{Cl}_2 \cdot 5.75\text{H}_2\text{O}$  (3) is also shown.

It is seen from Figure 16, that the  $\Delta H$ - $T$  curve for the hydrate clathrate above 100K is located below the appropriate curve of the hexagonal ice. Furthermore, a very sharp decrease starting from 220K is also observed which is lower by 80K than the melting point of the clathrate. It is obvious from the comparison of the  $\Delta H$  value of the hydrate with the appropriate value of ice at  $-40^\circ\text{C}$  ( $\Delta H_{\text{ice}}$  at  $-40^\circ\text{C}$  is 15 G), and that the mobility of the protons in the hydrate framework is higher than in the hexagonal ice.

Since the  $S$  value decreased with the increasing mobility of each atom at the lattice points, the intramolecular contribution of isotropically rotating atoms to the  $S$  value is zero. Thus the  $S$  value ( $\text{G}^2$ ) could be calculated only from the intermolecular contributions by the equation (113).

$$S = 358.6 \sum_k R_{jk}^6 \quad (113)$$

where  $R_{jk}$  is the distance (in  $\text{\AA}$ ) between the centres of the rotating molecules, and  $k$  is the index of protons in the neighbouring molecules.

If the water molecules could be isotropically rotated in the hydrate frame, the  $S$  value would be roughly  $6.8 \text{ G}^2$ ; however, the observed  $S$  value at 283 K was approximately  $1.3 \text{ G}^2$ . Since the diffusion of the molecules further decreases the

second moment, therefore it is probable that the observed low value of the second moment is due to the increasing number of the diffusing water molecules or protons. This diffusion can start around 230-240 K was confirmed by the sharp decrease in the line width in this temperature range. Although the closest neighbours contribute little to the value of  $S$  in the hydrate than in the ice, yet the experimental value of the second moment in the hydrate was a bit higher than that of the ice. This could be attributed to the fact that the protons are not located along the O-O line, but they enclosed in a tetrahedral angle [133].

The relation between the second moment and the temperature is complex. By not considering the temperature range near the melting point ( $\sim 300$  K), there are two temperature ranges where the  $S$  value plots decrease fairly fast: 120-140 K and 240-260 K. Calculation of the activation energy of the motion is expressed by equation (114) [19].

$$E_a = 37T_n \quad (114)$$

where,  $T_n$  is the starting temperature (in K) of the fast decreasing value of  $S$ .

The  $T_n$  values 130 and 250 K gave  $E_a$  values of 5 and 9 kcal mol<sup>-1</sup> respectively. These energies are very close to the dissociation energies of one or two hydrogen bonds. Decrease in the value of the second moment between 120-140 K may be explained by the beginning of the proton hopping from one bond to another or in the direction of the bond. This kind of hopping is very probable when large number of defects exist in the frame. The decreasing second moment around 250 K is obviously the consequence of the simultaneous transition of both protons of the water molecules from one bond to another [133].

A sharp signal component in the <sup>1</sup>H NMR spectrum of the hydrate above 77 K together with the wide bands was also observed which merged with the wide band above 260 K. This sharp signal component might belong to the trapped water molecules in the small cavities of the frame which do not form hydrogen bond with the frame and consequently rotate isotropically [133].

The value of the second moment for the isotropically rotating water molecules located in the dodecahedral void gave  $\sim 4$  G<sup>2</sup> value. The experimental  $S$  value of the sharp component at

77K is roughly  $\sim 2G^2$  which, taking into consideration the error of the arbitrary selection of the signal component, seems to be a very close value [133]. This signal is the first experimental evidence of the possibility of the enclathration of water in the small cavities supposed by Pauling on the basis of the X-ray studies of the hydrate [95].

### 7.2.2. Vibrational spectroscopic investigations

Isotopic effects on the vibrational frequencies, mean amplitudes of the vibration and force constants in solid, liquid, and isotopic gaseous chlorine species were compared with the similar parameters for the hydrate. It could be seen that these parameters for <sup>35</sup>Cl<sub>2</sub>, <sup>37</sup>Cl<sub>2</sub> and <sup>35</sup>Cl<sup>37</sup>Cl molecules in the gas phase are almost the similar to that of the hydrate [81]. The isotope effect on the mean vibrational amplitudes is low becoming insignificant with increasing temperature and practically diminishes above room temperature. From the values of the force constants 3.161, 3.144 and 3.150 dyne/Å for <sup>35</sup>Cl<sub>2</sub>, <sup>35</sup>Cl<sup>37</sup>Cl and <sup>37</sup>Cl<sub>2</sub> respectively, it is unambiguously shown that the Cl-Cl bond is stronger in the hydrate than in the liquid or solid chlorine [134].

Three bands at 538, 545 and 554 cm<sup>-1</sup> are observed in the Raman spectra of the hydrate with relative intensity 1:6:9 were recorded at -196°C. These agreed with the calculated ones for the stretching frequencies of the <sup>37</sup>Cl-<sup>37</sup>Cl, <sup>35</sup>Cl-<sup>37</sup>Cl and <sup>35</sup>Cl-<sup>35</sup>Cl molecules. The calculated isotope shift between the <sup>35</sup>Cl<sub>2</sub>, <sup>35</sup>Cl-<sup>37</sup>Cl and <sup>37</sup>Cl<sub>2</sub> molecules are 8 and 15 cm<sup>-1</sup> respectively, which agreed very well with the observed ones at 9 cm<sup>-1</sup> and 16 cm<sup>-1</sup> [81].

The band observed at 103 cm<sup>-1</sup> may be due to the external vibration of the water lattice because the translational bands of the chlorine are not active in the Raman spectrum according to the point group symmetry of the chlorine in these crystal structures. Comparing the band positions and intensities of Br<sub>2</sub> and BrCl hydrates having analogous structures, the observed line cannot be a band belonging to hindered rotational motions of the chlorine guest in the cavities [81].

### 7.2.3. X-ray studies of rotation

The free rotation of the molecules forming the hydrate in the cavities show the powder X-ray because of the following reasons

a) X-ray reflection intensities do not give any evidence of the location of the chlorine in a given position. The intensities could be interpreted in a way, that the nuclear form factor attributes of which suffered from a very rapid decrease by increasing the angle of reflection in accordance with the statistical distribution of the scattering centres on the large volume of the cavities [53], and b) The energetic considerations ensure that no forces are present that could fix the molecules in a certain situation. So it is really rotation, not just “rotation accept” [53].

#### 7.2.4. UV-VIS spectroscopic investigations

UV-VIS spectra of the chlorine hydrate crystals, prepared from water vapour and chlorine gas at 0.5 atm pressure [135] was studied. It was found that most of the chlorine in these crystals was located in the larger  $5^{12}6^2$  cavities [52, 61]. The solid state spectra were recorded at 200 K and 77 K and compared with the spectrum of the dissolved chlorine hydrate in aqueous NaCl solution [135]. Practically the same peak intensities were observed in all the three spectra. The spectrum recorded at 200 K was similar to that of the gas phase chlorine, while that of the aqueous chlorine solution shifted from  $500\text{ cm}^{-1}$  to higher energy. When the temperature of the chlorine hydrate was lowered to 77 K there was a  $500\text{ cm}^{-1}$  shift in the spectrum so that it was much closer to that of the aqueous solution in position but retained the narrow width of the spectrum at 200 K.

The similarity between the spectra of the hydrate at 200 K and that of the gaseous chlorine indicated that the guest host interaction was quite weak. The narrowness of the peak ( $\omega_{\text{max}} = 30300\text{ cm}^{-1}$ ) was a strong evidence to indicate that the chlorine was located in one type of cavity. On average, the chlorine atoms were in the centre of the cavity, and on average  $3.45\text{ \AA}$  far from the surrounding oxygen atoms. Thus the excited states of chlorine may not be perturbed by the walls of the cavity. Similar situation might be valid at 200 K due to the thermal motion, which randomizes the position of the chlorine molecule within the cavity. So there is no direct interaction between the cavity walls and the chlorine LUMO orbital. At 77 K, the blue shift of the peak might indicate

**Table 21.** Calculated energies ( $\text{kcal mol}^{-1}$ ) for the hydrate clathrate unit.

H <sub>2</sub> O	20	24	26	28
$E_{\text{vdw}}$	-9.2	-7.65	-7.31	-4.93
$E_{\text{strain}}$	-8.14	-5.14	1.41	0.53
$\Delta G$	-11.93	-8.93	-2.38	-3.26

the settling of the chlorine molecule near to the cavity wall and the wall could perturb the excited state.

#### 7.2.5. Quantum chemical calculations

Semiempirical calculations of the number of water molecules in the first layer of the hydrate type clathrates in crystalline state showed that the most stable arrangement consists of a 20-water-molecule dodecahedron, and the second most stable possibility is a water layer consisting of 24 water molecules as tetrakaidecahedron.

The shapes containing 26- or 28-water-molecule are less stable for the hydrate. The Van der Waals stabilization, the strain energy of the clathrate unit and the entropy term of the motional freedom have been taken into account during the calculation of the free energy change for the formation of the water clathrate. The Van der Waals energies, the strain energies and the free enthalpy changes during the clathrate formation are presented for the four geometric arrangements in the Table 21 [136].

The strain energy counteracts the van der Waals energy in case of the larger cages, which is in accordance with the experimental results obtained about the existence of only 20 and 24 membered cages in the chlorine hydrate structure. A theoretical UV-VIS study using RICC2 methods about the hydrate, and calculation of the electronic absorption spectrum of a chlorine molecule trapped in  $(\text{H}_2\text{O})_{20}$ , dodecahedral, and  $(\text{H}_2\text{O})_{24}$ , hexakaidecahedral cages was made [137].

The low occupation of the  $5^{12}$  cages was considered to be steric interactions. Experimentally all the  $6^25^{12}$  cages, but only about 30% of the  $5^{12}$  cages of the hydrate were occupied with  $\text{Cl}_2$  molecules [138]. Since the chlorine molecule encapsulated within the water cage has relatively little effect on

its low-lying valence transitions, therefore a large number of solvent to solute charge-transfer transitions occurred at energies starting near  $48000\text{ cm}^{-1}$ . CC2 and CC3 methods have been used to calculate the excitation energies of the low-lying excited states of the isolated  $\text{Cl}_2$  molecule in a  $(\text{H}_2\text{O})_{20}$  dodecahedron having inversion symmetry ( $C_i$  point group). The chlorine molecule was located at the centre of the cage and the geometry of the  $\text{Cl}_2(\text{H}_2\text{O})_{20}$  system was optimised by retaining inversion symmetry with the RIMP2 method.

The  $\text{Cl}_2(\text{H}_2\text{O})_{24}$  cluster structure was optimized by using the base geometry of the  $(\text{H}_2\text{O})_{24}$  cage and the oxygen atom positions were considered from a proton disordered experimental CS-I type hydrate structures. The positions of the hydrogen atoms were randomised as per Bernal-Fowler rules. The  $\text{Cl}_2$  molecule was located at the centre of the cage and oriented along the long axis using the experimental gas-phase bond length. The CC2 and CC3, RIMP2 and RICC2 calculations were performed with the frozen core approximation in all calculations. The RICC2 method was used to calculate the electronic absorption spectra of  $\text{Cl}_2$ ,  $\text{Cl}_2(\text{H}_2\text{O})_{20}$  and  $\text{Cl}_2(\text{H}_2\text{O})_{24}$ , indicated that in all the three species the low-lying transitions near  $30000\text{ cm}^{-1}$  were due to the  $\text{Cl}_2\ \pi_g \rightarrow \sigma_u$  transition. In  $\text{Cl}_2$ , the next group of transitions was also valence-like and occurred near  $50000\text{ cm}^{-1}$ . However, in  $\text{Cl}_2(\text{H}_2\text{O})_{20}$  and  $\text{Cl}_2(\text{H}_2\text{O})_{24}$  there was a dense manifold of charge transfer states starting near  $45000\text{ cm}^{-1}$ . The charge transfer states involved excitation of an electron from the lone-pair orbitals of the  $(\text{H}_2\text{O})_{20}$  and  $(\text{H}_2\text{O})_{24}$  cages to the  $\sigma_u$ -like orbital of the chlorine, and had oscillator strengths up to 300 times greater than the most intense valence transitions of the isolated  $\text{Cl}_2$  molecule. The UV-VIS spectrum of the  $\text{Cl}_2$  in a clathrate hydrate environment is shown in Figure 17.

### 7.3. Crystal structure of the hydrate

Stackelberg, Claussen and Pauling studied the structure of the gas hydrates independently from each other practically at the same time [48, 49, 138, 139, 140, 141, 142, 143]. Based on the refinement of the results of structural characteristics, the gas hydrates belong to the cage-compounds

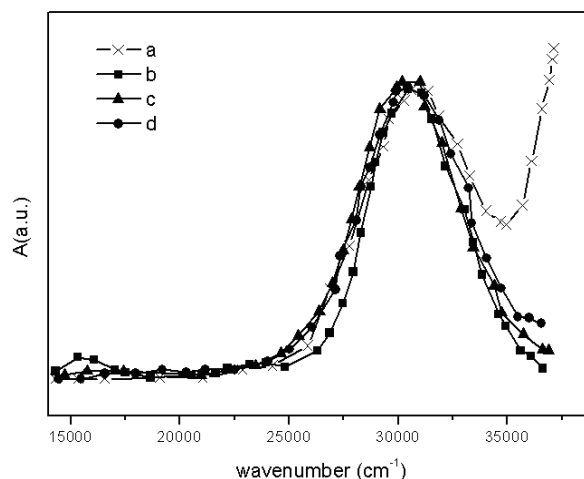


**Figure 17.** Calculated UV-VIS spectra of chlorine hydrate, aqueous chlorine solution and gaseous chlorine. (a) the curve for an aqueous solution of the chlorine; (b) the curve for the gaseous  $\text{Cl}_2$ ; (c) the curve mainly due to the chlorine in  $5^{12}6^2$  cages at 200K and (d) the curve for the same sample but at 77K.

and the gas molecules are stored in their crystal lattice cavities without any crystallographic orientation. The hydrates of the smaller molecules, such as chlorine, contain 46 water molecules in a cubic elementary cell with a lattice constant of about  $12\text{ \AA}$  [142]. The chlorine hydrate is isomorphic with the other type I gas hydrates [53].

Stackelberg and Müller first suggested that the unit cell in the structure of the hydrates of small molecules such as  $\text{Cl}_2$  had 48 water molecules and 8 void spaces that were filled by the hydrating molecules. The cell constant was given about  $12\text{ \AA}$  [140].

Claussen, however, criticised the bondangles of about  $60^\circ$  between the water molecules which were much smaller than the tetrahedral angle present between the water molecules in the ordinary ice [139, 141].

Claussen found a slight deformation of a regular dodecahedron, so that the angles around the two opposite molecules were exactly tetrahedral (a structure which could be packed into a diamond-like cubic cell) [139]. This arrangement causes a new hole of void, a hexakaidecahedron containing 4 hexagonal and 12 pentagonal faces [139]. The structure of the hydrate is a body-centered cubic lattice having a pentagonal dodecahedral array of

20 water molecules at each corner and in the centre of the cube. The dodecahedra at the corners of the cube are joined to adjacent corners of dodecahedra by two additional water molecules to form hexagons of water molecules. The body centered dodecahedron is attached to all of the 8 corners of dodecahedra through single hydrogen bonds and is attached also to the 12 of the added "hexagon" type water molecules. The resulting structure has another type of voids, besides the pentagonal dodecahedron, namely a tetrakaidecahedron (24 water molecules). This structure has two opposite hexagonal and 12 pentagonal faces. The volume of this cavity is slightly larger than the volume of the dodecahedron [139]. The obvious advantage of such a structure is the presence of the hydrogen bond angles of about  $108^\circ$  in the dodecahedra and in the twelve pentagonal faces of the hexakaidecahedra; the other hydrogen bond angles (in the four hexagonal faces of the hexakaidecahedra are about  $120^\circ$ ) [142].

Stackelberg re-evaluated the powder X-ray diffractometric results of the chlorine hydrate, and modified the bond angles and the lattice constant. The smaller cavities in the 48 membered cage were given regular pentagonal dodecahedron structure with  $5.01 \text{ \AA}$  diameter. The modified one was  $5.2 \text{ \AA}$  in the 46-membered cage [143]. The six large cavities in the 48-membered cage had  $5.8 \text{ \AA}$  diameter, which changed to  $5.9 \text{ \AA}$  for the 46-membered structure [53, 143]. The shapes are tetradecahedral in the 46-membered cage. The space group is  $O_3^h\text{-Pm}3n$ , and the lattice constant is  $11.98 \text{ \AA}$  with X-ray density  $1.37 \text{ g cm}^{-3}$  calculated for the idealized formula  $8\text{Cl}_2.48\text{H}_2\text{O}$ . The refined structure of the hydrate resulted in the formula of  $8\text{Cl}_2.46\text{H}_2\text{O}$  or the formula of  $\text{Cl}_2.5.75\text{H}_2\text{O}$ .

The experimental analyses showed roughly 96% saturation of the cavities in the structure. The re-determined X-ray density ( $1.32 \text{ g cm}^{-3}$ ) had good agreement with the pycnometric value  $1.29 \text{ g cm}^{-3}$  [143]. For an idealized structure it could be assumed that all the  $\text{H}_2\text{O}\text{-H}_2\text{O}$ -distances between adjacent water molecules are the same. In the case of a lattice constant of  $12.00 \text{ \AA}$  this distance was  $2.81 \text{ \AA}$ . The cavities enclosing a pentagondodecahedron have 20 corners ( $\text{H}_2\text{O}$

molecules) and are made up of 12 pentagons. It is shown as a regular polyhedron in which the angles of all pentagons are  $108^\circ$ . The centres of these cavities are, as stated above, in the corners and in the middle of the elementary cell at the positions  $\frac{1}{2} \frac{1}{2} \frac{1}{2}$  and are rotated by  $90^\circ$  relative to the others [53].

There are  $2 \times 20 = 40$  water molecules located in the elementary cell, 24 locations are at positions (k) and 16-locations are at positions (i). The remaining  $6\text{H}_2\text{O}$  molecules are at locations (c) and form connecting bridges between the pentagonal dodecahedron springs. Each of these molecules has 4 neighbours (k) and is located as the fourth neighbour of the (k) molecules [53].

This framework has cavities ( $\text{H}_{II}$ ) consisting of 2 opposite hexagons and 12 pentagons that form a double belt ( $2 \times 6$  pentagons) and are surrounded between the hexagons. These polyhedral have 24 corners (water molecules). Considering that polyhedral ( $\text{H}_I$ ) and ( $\text{H}_{II}$ ) consists of spherical water molecules touching each other (radius =  $1.4 \text{ \AA}$ ), the internal free spaces can be built up [51]. The chlorine hydrate has relatively weak X-ray reflections and a strong background blackening. The latter is probably due to lattice defects and strong thermal vibrations of the soft crystals [53].

Pauling's single crystal X-ray diffraction studies resulted  $11.88 \text{ \AA}$  lattice constant. Pauling supposed inclusion of free water molecules into the cavities [95]. The crystal structure of the hydrate is shown in Figure 18 [95].

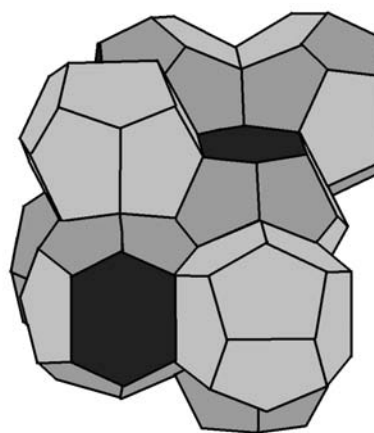


**Figure 18.** The crystal structure of the chlorine hydrate.

The O-H...O distance is 2.75 Å, the pentagons deviated slightly from planarity, while the hexagons were a bit planar not equiangular. The O-O-O angles on the pentagon faces ranged from 106.1° to 114.8°, while each hexagon had angles of 109.6° and 125.2° [95].

## 8. Miscellaneous uses of the hydrate

Faraday observed that the hydrate acted upon substances like chlorine itself and suggested its use as a source of elementary chlorine [5]. Ditte pointed out that the hydrate crystals decomposed dynamically and re-formed in a closed tube. Thus, the hydrate can be stored in this state for months [11]. Since the hydrate has high chlorine content (100 times more chlorine compared to the amount of gas at the same volume), it has comfortable properties as solid without technical problems which are incident on liquid or gaseous chlorine. The chlorine hydrate is a preferential candidate as solid chlorine source for various industrial purposes.

### 8.1. Storage of chlorine in the hydrate at a controlled temperature

A hydrate storage tank having uniform temperature storage unit for high energy density batteries was developed. There were four storage tanks for the hydrate based electric-power storage system of 20 MW for 8 h consisting of 300 Zn-Cl battery modules (200 V, 340 A), which were kept at within  $8 \pm 0.5^\circ$  with a separated loop-shaped main cooling circuit built by using R21 cooling fluid (CHClF<sub>2</sub>). Each hydrate tank had its own cooling cycle, and the working fluids of each circuit were attached to the appropriate branch (cool or warm) of the circuit of the heat dissipaters. The common circuit was located above the tanks and was attached to a heat-releasing tank, where the evaporated R21 working fluid was condensed and sent back to the circuit [144]. The assembly of the storage tank is shown in Figure 19.

### 8.2. Chlorination reactions with chlorine hydrate

The chlorine hydrate prepared from chlorinated lime and hydrochloric acid and compressed under 100-110 bar pressure could be stored at room temperature as a filter cake in the filtration unit of the apparatus kept at constant pressure (~10 bar).

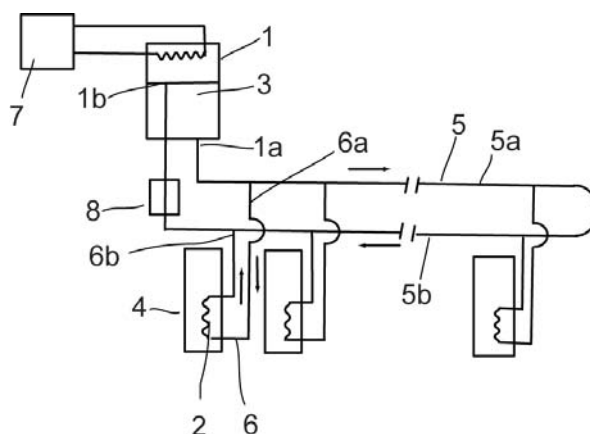


**Figure 19.** Uniform temperature chlorine hydrate storage tank. (1) cooling condensator tank, (1a) cool stream, (1b) warm stream, (2) coolers of sub-cooling circuits, (3) R21 working fluid, (4) the hydrate tank, (5) loop-shaped main cooling circuit, (5a) cool stream, (5b) warm stream, (6) sub-cooling circuits, (6a) cool stream, (6b) warm stream, (7) cooler equipment, (8) heater.

The chlorine liberated from this solid hydrate by depressurizing the filter chamber at room temperature or above could be used in situ for chlorination reactions in aqueous media [61].

#### 8.2.1. Chlorination of poly(vinyl chloride)

The hydrate prepared in this way was closed into an autoclave together with poly(vinyl)chloride granules, optionally with a radical forming catalyst like azo-bis(isobutyronitrile), and the mixture was heated above the decomposition point of the hydrate ( $>30^\circ\text{C}$ ). The heterogeneous mixture containing liquid chlorine, water and solid poly(vinyl)chloride and is suitable for high pressure aqueous phase post-chlorination of the PVC. Instead of azobis(isobutyronitrile), UV light illumination could also be used and the pressure of the system was controlled by temperature [145].

#### 8.2.2. Disinfections with chlorine hydrate

The hydrate could be used as a source of chlorine for disinfecting air and water. Its use eliminates the safety problems associated with the use of liquefied chlorine or other problems of operational efficiency. The disinfecting effect could be lowered by shifting the pH to the alkaline range in case of sodium hypochlorite.

Water and air could be disinfected by an apparatus in which the hydrate dissolves or decomposes in water or in air forming dissolved or gaseous  $\text{Cl}_2$  respectively at normal temperature or above [146]. In order to inject and distribute the solid hydrate in water pipeline systems, a special apparatus was also developed. Using a static mixer built into the pipeline system, the hydrate is pumped out from a storage tank as slurry which is easily and quickly dissolved in water at  $35^\circ\text{C}$  giving liquid chlorine and water. The liquefied chlorine could be used only at 0.3 MPa pressure [147].

### 8.2.3. Metallurgical applications

Platinum metals (Pt, Pd, Rh, Ir, Os, Ru) and Au, Ag or Hg could be removed from roasted ( $750^\circ\text{C}$ ) ores or concentrates of strong acidic HCl or  $\text{NH}_4\text{Cl}$  solutions with the chlorine hydrate via oxidative leaching [148]. The leaching solution contains chloride salts like  $\text{ZnCl}_2$ ,  $\text{CrCl}_3$ ,  $\text{FeCl}_3$ ,  $\text{MgCl}_2$ ,  $\text{AlCl}_3$ ,  $\text{FeCl}_2$  or  $\text{CaCl}_2$  in a concentration of 6-10 M. The optimal temperature of the leaching solution is supposed to be above  $100^\circ\text{C}$  [148].

The hydrate reacts selectively with non sulfide ores of Zn, Cu, Sn, Ni and Pb including  $\text{ZnFe}_2\text{O}_4$ . It does not react with oxides of iron(III), aluminium and manganese. It can be used for selective hydrometallurgical leaching of the above mentioned elements, ZnO and  $\text{ZnFe}_2\text{O}_4$  containing industrial wastes, Zn containing scraps or deep sea nodules. The latter may be leached well only after grinding and pre-reduction with CO at  $650^\circ\text{C}$  for 4 h [29].

Leaching of the zinc from its ferrite ore (21.2% Zn, 8.2% Pb and 30.4% Fe) proceeds rapidly with the removal of only in a small proportion. The results could be represented by the shrinking core model [30]. Comparison of the leaching by chlorine hydrate (100% of Zn and 3% of iron was extracted after 180 min, all the lead went into solution and the iron came down as  $\text{Fe}_2\text{O}_3$ ) and the leaching by 40% aqueous sulphuric acid (80% zinc and substantial amount of iron is leached but the lead did not get into solution) indicated that the latter is not as economical, and additionally there are difficulties due to  $\text{Fe}(\text{OH})_3$  formation [30].

The separation of zinc and the iron(III) oxide could be attributed to the free energy  $\Delta G_{298}^0 = 25.6$  and  $51.6 \text{ kJ mol}^{-1}$  respectively for the reactions given in equations (115) and (116).



More iron was removed as FeO from the blast furnace at 0.025M chlorine content, since FeO reacted with the chlorine hydrate; the  $\Delta G_{298}^0$  for the reaction in equation (117) was  $58.2 \text{ kJ mol}^{-1}$ .



The hydrate slurry is formed during low temperature chlorination ( $<9^\circ\text{C}$ ) and leaching of low grade zinc ores at higher chlorine concentrations. The hydrate formation has some advantages; it does not cause any problem during pumping of the slurry [149] and ensures much higher concentration of the dissolved chlorine than the chlorine gas. This is an important factor, because the chlorine concentration has enormous effect not only on the mechanism and rate of the leaching but also on the productivity of the process as well [149].

Mainly  $\text{Zn}_2\text{SiO}_4$ ,  $\text{ZnSiO}_3$  and ZnO containing ores and arc-furnace dust (mainly  $\text{ZnFe}_2\text{O}_4$ ) were leached with the hydrate at  $4^\circ\text{C}$  at a 0.002-0.04 M dissolved chlorine concentration [149]. The dissolution rate strongly depended on the chemical nature of the Zn containing compound, concentration of the dissolved chlorine and the size of the starting zinc particles. The concentrations ( $\text{mg L}^{-1}$ ) of the leached main metal components at a 0.04 M dissolved chlorine concentration (except  $\text{ZnFe}_2\text{O}_4$  where 0.025 M chlorine concentration was used) at  $4^\circ\text{C}$  are presented in the Table 22.

The starting ores are generally not homogeneous in their zinc content and chemical nature.

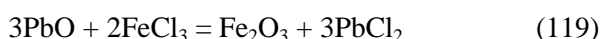
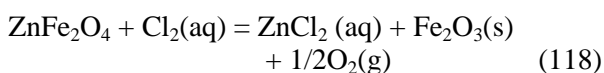
**Table 22.** The leached amount of elements from each zinc compounds by the hydrate.

	$\text{ZnFe}_2\text{O}_4$	$\text{ZnSiO}_3$	$\text{ZnSi}_2\text{O}_4$	ZnO
Zn	104.8	141.0	148.3	240.0
Fe	9.1	2.01	4.5	3.1
Pb	20.8	60.0	58.3	60.3

Furthermore their particle sizes and shapes are also different. The particle size plays an important role in the dissolution rate, because most of these reactions are controlled by the surface diffusion or by a combination of the surface diffusion and the diffusion of the reactant chlorine to the surface.

In case of the spherical particles, the primary reaction rates decreased with time because of the diffusion of chlorine through the reacted layer to reach the unreacted core, and the soluble products have to come back in the same layer from the opposite direction. The surface area, where the reaction proceeds, also decreases with the dissolution of the outer part of a spherical particle. The activation energies of these reactions are high enough, which is in agreement with the diffusion through a series of pores and veinlets.

Furthermore, in the 0.002 MCl<sub>2</sub> solutions the reaction is mainly controlled by the diffusion of the chlorine to the surface, and in the case of particles that are rich in SiO<sub>2</sub> and Fe<sub>2</sub>O<sub>3</sub> the leaching does not take place through a reacted shell [147]. The chemical reactions in these systems are the reactions described by the equations (118) and (119).



Due to oxygen evolution, the oxygen content of the leaching agent affects the reactions. The dissolved oxygen has a large effect on the iron leaching, e.g. the leaching of the iron by oxygen saturated leaching agent decreased by 36.5% and the rate of dissolution of ZnFe<sub>2</sub>O<sub>4</sub> also decreased by 3%. Recovery of the accompanying elements is, however, dependent on the presence of other reactions. For example, 100% of the lead, manganese and copper are leached together with 30% of the iron, 75% of the Co and 25% of the Al within 2h from ZnSiO<sub>3</sub> ores. The lead is completely leached within 1h (due to the presence of PbO and FeCl<sub>3</sub>).

These by-reactions may influence the low leaching level of iron even at high iron containing ores as ZnFe<sub>2</sub>O<sub>4</sub> [149].

Various binary alloys, such as Zn-Sn, Zn-Pb, Zn-Mg, Zn-Al and Zn-Cu, or polymetallic such as die

casting alloys and die-metal (Sn-Cu-Pb-Al-Mg-Fe alloy), brass (Cu, Pb, Zn) or welding alloy (Cu-Al-Mg) could be leached with the chlorine hydrate at 0.11 M chlorine content at 3.3°C. The dissolution rate of the zinc was proportional to the circulation rate of the leachate, and the rate of the reaction was controlled by the diffusion of the chlorine onto the surface at low concentrations [133]. The dissolution was independent of the flow rate if it exceeded 0.2 dm<sup>3</sup> min<sup>-1</sup>.

Since the dissolved chlorine hydrate decreased the viscosity of the solution, the relationship was not linear [55], and the activation energy was 16.55 kJ mol<sup>-1</sup>. The reaction occurred preferentially at the grain boundaries and twin defects, the layer formed was porous and the magnitude of the reaction rate did not decrease [148]. The leaching rate was roughly 100 times higher than that with HCl. The effect of alloy addition to zinc did not increase the leaching via galvanic effect, or alternatively a surface film could hinder the chlorination reaction [30].

In the case of the Zn-Fe, Zn-Al and Zn-Pb alloy the dissolution of zinc was selective, Fe, Al or Pb were not detected in the solution. The leaching rate was a bit slower in the case of Zn-Fe than in the case of pure zinc [55]. Lead accelerated the corrosion of the zinc in Zn-Pb, and 2PbO.PbCl<sub>2</sub> was formed. The treatment of the Zn-Al residue gave Al and Al<sub>2</sub>O<sub>3</sub>. In the leaching of Zn-Mg and Zn-Sn only traces of Mg and Sn could be detected in the solution [55].

Die casting alloy and Cu-Zn released a trace amount of copper together with zinc, however, the dissolution rate was lower by 17% compared to that of pure zinc [55]. After a long term action on the die-metal alloy a spongy residue of Al and Al<sub>2</sub>O<sub>3</sub> was left behind and a minimal amount of Al and Fe were leached out (6-6 ppm, respectively). The dissolution rate of the die-metal alloy was much higher than the die casting alloy, though the only difference between the two alloys was in their copper content.

The welding alloy dissolved very slowly, only zinc and trace concentration of Mg was found in the solution. The 60/40 leaded brass initially showed extremely fast rate of Zn dissolution, the Zn/Cu dissolution rate after twenty minute was 10:1.

After 2 h, the ratio of the Zn and Cu in the solution was almost the same as in the residual material (roughly 40:60). The overall rate coefficient was,  $k_{Zn} + k_{Cu} = 0.44 \times 10^{-4} \text{ kg m}^{-2} \text{ s}^{-1}$  [55].

The leaching of the BS1004A zinc die cast alloy was typically performed around 4°C in 10% ZnCl<sub>2</sub> solution at 0.025M chlorine concentration. The dissolution rate was found to be 0.40 mg cm<sup>-2</sup> at 4°C, and the formed zinc chloride solution contained only 12 ppm aluminium and 8 ppm iron. The ZnFe<sub>2</sub>O<sub>4</sub> containing flue dust showed 92 % leaching efficiency after 90 min at 3.5°C, but only 6.8% of the iron was dissolved out. The amount of iron can be decreased by aeration of the solution. The chlorine concentration in the hydrate slurry was 0.03 M [29].

#### 8.2.4. The hydrate in batteries

In the metal-chlorine type batteries the chlorine electrode is made of the hydrate [63, 64, 65, 150, 151, 152, 153]. The hydrate allows the concentrations of chlorine and electrolyte to be controlled easily, and is regenerated during charging of the secondary battery with a simple cooling [63, 64].

A single cell battery was constructed from thick graphite plates drilled to allow an even distribution of the electrolyte. No diaphragm was used to separate the cell into compartments and a 25% aqueous ZnCl<sub>2</sub> solution was used as electrolyte. A potential of 2.1 V was observed between the battery plates [63]. Not only zinc, but magnesium, aluminium, tin, nickel or copper could also be used as anode materials. The best results were given by zinc and magnesium, but the aluminium, despite of its electropositive character, did not give the expected results due to the formation of aluminium hydroxide on the surface of the metal [64]. The voltage current densities on discharge are indicated in Table 23.

During the charge and discharge processes the deposition and the dissolution of the anode metals, mainly zinc, are reversible and proceed at 98% efficiency. The rate of dissolution of the deposited zinc is greater than the cast zinc due to a greater reactivity and an increased surface area of the freshly electrodeposited zinc [154, 155].

The concentration of the zinc chloride during the discharge increased from 0.5 M to 1.5 M at

**Table 23.** Voltage (V) and current densities (mA cm<sup>-2</sup>) on discharge with various metals.

Voltage(V)	Zn	Mg	Al
0	2.1	2.7	1.85
10	1.85	2.28	1.45
20	1.77	2.15	1.35
30	1.6	1.98	1.17
40	1.55	1.87	1.05
50	1.45	1.75	0.95
60	1.4	1.65	-
70	1.32	1.55	-
80	1.25	1.45	-
Voltage(V)	Sn	Ni	Cu
0	1.6	1.12	1.2
10	1.15	0.8	0.987
20	0.95	0.65	-
30	0.81	-	-

1.4-2.4 mA cm<sup>-2</sup> current density in the case of rod electrodes of the cast zinc, while in the case of the electrodeposited zinc this value was between 2.2-6.2 mA cm<sup>-2</sup> [154].

During charge, the metal chlorides are electrolysed into metal and free chlorine. The liberated chlorine forms the hydrate if the temperature and pressure conditions are favourable [64, 81]. The liberated chlorine reacts with the metal electrolyte which carries it to the electrode reaction. A separated water/electrolyte solution tank is used for the formation of the hydrate during the charge; the discharge process required that the chlorine is recovered from this tank. Thus the chlorine can bubble out through the electrolyte by replenishing its chlorine content to a constant and required level [156]. This solution minimises the chlorine excess to avoid a direct reaction (not electrochemically) between the chlorine and the zinc electrode [156].

During the discharge of either primary or secondary batteries the electrolyte solution is pumped to the electrode compartment to dissolve the hydrate. Chlorine at the positive electrode

combines electrochemically with the metal to produce electric energy resulting in the decomposition of the hydrate [63, 64].

The heat generated during the battery charging (the hydrate formation) is stored in a heat storage tank. This stored energy is used as source of energy during liberation of  $\text{Cl}_2$  from the hydrate when the battery discharges. This arrangement decreases the energy required for the operation of the batteries to generate chlorine. It consists of 96 cells and operates with  $25 \text{ mA cm}^{-2}$  current density for 8 h and for another 8 h with  $22.5 \text{ mA cm}^{-2}$  current density. There is  $750 \text{ dm}^3$  of electrolyte solution in the electrolyte tank which is attached to the hydrate tank of  $1000 \text{ dm}^3$  and a heat storage tank ( $2200 \text{ dm}^3$ ).  $540 \text{ dm}^3 \text{ min}^{-1}$  was the rate of circulation [157].

The electrolyte, 2 M  $\text{ZnCl}_2$ , 1 M  $\text{KCl}$  and 2 M  $\text{NaCl}$  at pH 1, is circulated by a pump (3) from the electrolyte vessel (2) to the electrode section (1) comprising a negative zinc electrode and a positive chlorine electrode.

During charge, the liberated chlorine at the cathode is sent to the hydrate tank (6) by the chlorine gas pump (4) through the valve (5) where it immediately reacts with water and forms the solid hydrate. The hydrate tank (6) has a chiller (7) which is coupled to a heat storage liquid tank (8). The heat liberated during the hydrate formation is absorbed by the compressed coolant circulated in the chiller (7) by the pump (9) through the valve (10). The absorbed heat is taken by the coolant to the heat storage liquid tank (8).

During discharge, the hydrate tank (6) is warmed by the heat storing liquid supplied by the pump (9) through the valve (11). These and the resultant chlorine gas blows into the electrolyte vessel (2) through a valve. The chlorine gas dissolves in the electrolyte and the process starts again [157]. The details are shown in Figure 20.

A simple, trouble-free method and apparatus was also developed for controlling the chlorine feed to a metal-chlorine battery from a chlorine hydrate source. The aqueous electrolyte is circulated from the electrode compartment to hydrate container from which chlorine and water are released. The released chlorine increases the pressure in the container there by controlling the flow-rate of the

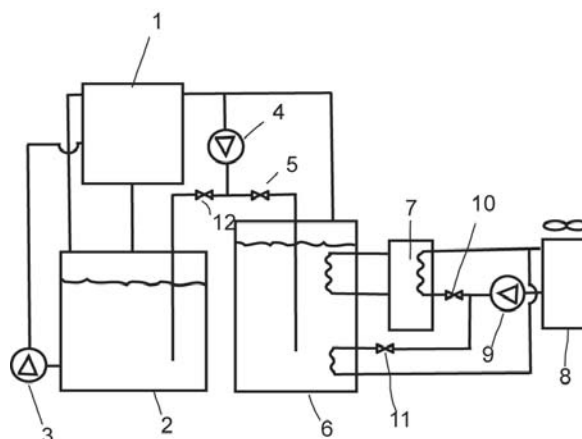


**Figure 20.** The arrangement in Zinc-chlorine hydrates battery. electrode section (1), electrolyte tank (2), electrolyte pump (3), chlorine gas pump (4), valve (5), hydrate tank (6), chiller (7), heat storage liquid tank (8), pump (9), valve (10) and valve (11).

electrolyte from the container to the recycle line and back to the electrode compartment. This diminishes the pressure in the container. These steps are repeated during the discharge of the battery. Between the pump and the hydrate container a check valve prevents the admission of the electrolyte to the container [158].

The automatic replenishment of the batteries with chlorine from the hydrate tank is maintained by circulating the warm solution of the metal halide through the chlorine hydrate to release and carry chlorine back to the battery where it reenters through the pores of a carbon electrode. The flow is regulated by a valve that closes when the pressure in the storage tank reaches a predetermined level. Since the electrolyte is the heat source for decomposing the solid  $\text{Cl}_2 \cdot 6\text{H}_2\text{O}$  (at  $-5$  to  $5^\circ\text{C}$ ), therefore the chlorine flow ceases when the electrolyte flow is shunted around the tank. A suitable detector in the battery determines when more chlorine is required and opens the valves on the tank line and partially closes the shunt [114].

The energy-specific power relationship is an especially significant factor in vehicle applications. The limiting specific energy in the Zn-chlorine hydrate batteries was  $165 \text{ W/h}$  for 2 h duration at  $80 \text{ W kg}^{-1}$  of one fourth of the maximum power. During 6 h charge and 4 h discharge at half of the maximum power, this battery can attain 71.5%

energy efficiency at 38 W kg<sup>-1</sup> [152]. A 50 kWh battery having 500 kg weight for use in vehicles was also developed [153]. The battery life is 1,000 deep cycles which ensures more than 100,000 km in a typical suburban car. During charge at 75 A (27 A cm<sup>-2</sup>) at 137 V for 8 h, the zinc chloride concentration decreased from 22 to 5% and 36 kg of zinc was plated out on the zinc substrate and 39 kg chlorine was stored in the hydrate form. Discharge capacity is about 400 Ah, the energy density is 71 Wh kg<sup>-1</sup>, discharge voltage is 110 V, coulombic efficiency is 67%, electrochemical energy efficiency is 54% [153]. Test of a 1.7 kWh system for 1000 h showed that there is a slight (2%) loss in electrochemical energy efficiency during the test period [151]. The battery efficiency is calculated by the equation (120).

$$E(t) = E(i) \times E(e) \quad (120)$$

where  $E(i)$  is the coulombic efficiency depending highly on the operational conditions,  $E(e)$  is the voltaic efficiency that depends mainly on the activation of the electrode [159]. The zinc electrode base is made of dense graphite and the chlorine electrode is made of porous graphite. Chlorine reacts when the electrolyte containing the chlorine flows through the porous graphite electrode. This electrode is etched for increasing the surface area and activation as well. The potential of the zinc electrode hardly changes, even if the electric current increases during the charge and discharge. The potential of chlorine electrode, however, does not change. The activated electrode shows reduction of the overpotential with 60 mV during charge and 50 mV during discharge, which results in 5.5% increase when it is converted to the voltaic efficiency [159]. The fall in the voltage during charge and discharge is due to the overpotential of the battery itself and of the voltage loss due to electrolyte and contact resistance. The results are shown in Table 24 for a 10 kW (80 kWh) battery.

The main cause for the fall in the coulombic efficiency is that the deposited zinc on the zinc electrode is dissolved by the chlorine in the electrolyte, because there is no membrane in the battery and the chlorine contacts the zinc directly. It is desirable to decrease the amount of the

**Table 24.** Parameters of a 80 kWh zinc-the hydrate battery.

	Charge V	Discharge V	Voltage eff. %
OV	2.12	2.12	100
OP	0.04	-0.06	95.4
Cl <sub>2</sub> OP	0.02	-0.02	93.6
Zn IR	0.05	-0.05	89
VL	2.23	1.99	89

where OV = overvoltage, OP = over-potential, Cl<sub>2</sub>OP = chlorine electrode overpotential, ZnIR = decreasing at Zn electrode due to inner resistance, and VL = voltage loading state.

dissolved zinc and chlorine concentration in the electrolyte. During the charge and discharge these should be kept at as low level as possible. A 0.5% of the current loss may belong to hydrogen production [159]. Some of the parameters are given in Table 24.

### 8.2.5. Paper and cellulose bleaching

Bleaching of paper and cellulose with chlorine is a well known process, and easy handling of the hydrate has provided an opportunity for using it as an alternate chlorine source [160].

The chlorine is a favorable separating agent for the incrustations of the cellulose plant fibers. There are numerous technical difficulties when unbound chlorine is used even in gaseous form or in aqueous solution. However, the chlorine hydrate proved to be a safe and effective bleaching agent. It has given the best quality end product in the pulp manufacturing process compared to the use of chlorine either in the gaseous or solution form. The black liquor in the latter processes is extremely dark and concentrated and contained a lot of hydrochloric acid which affects the raw materials and the devices in the system making the manufacturing process expensive [161, 162].

### 8.3. Refrigeration with the hydrate

The refrigeration system using the endotherm decomposition of the hydrates is energetically more favourable than the classical compression methods. The decomposition temperature and

pressure of the hydrate is in a very comfortable range [163]. The chlorine hydrate could be used for cooling at positive temperature by melting the hydrate which absorbs a lot of heat from its environment [24]. This method requires 4-5 times less chlorine compared to a simple liquefaction and thermomechanical compression. Since the decomposition of the hydrate could be performed at temperature  $<40^{\circ}\text{C}$  with the formation of liquid chlorine, which can produce cooling by its evaporation. Thus, chlorine has two-fold role in this process, forming hydrate and acting as a refrigerant [24].

The ambient night air also acts as a secondary cooling media. A cooling tower is filled with water and chlorine in the appropriate ratio to form the hydrate and the reaction heat is absorbed by the cool night air when its temperature is below  $8^{\circ}\text{C}$ . During the day the hydrate absorbs the heat from its warm environment to decompose and thus this cooling could be used to cool the ambient air or water. This method could be used to produce cooling between 0 and  $8^{\circ}\text{C}$  [164]. The details are given in Figure 21.

The chlorine gas at 4.14 bar enters into the crystalliser (1) and is mixed with water. At about  $21^{\circ}\text{C}$  when the crystalline hydrate is formed and the heat evolved is absorbed by the cold water

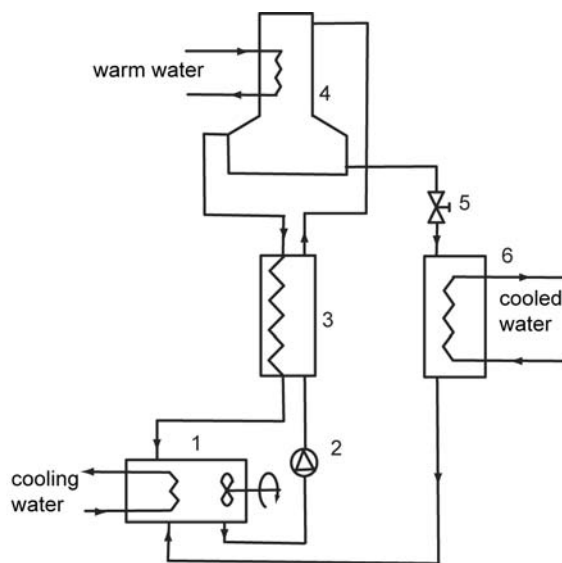


**Figure 21.** The hydrate refrigeration unit.

circulating in a coil. This cooling ensures a temperature which is needed for the formation of the chlorine hydrate and the crystalline hydrate slurry consists of 15-20% w/w solid hydrate. Water is pumped (2) from the crystalliser (1) through a heat exchanger (3) where it is heated to  $28^{\circ}\text{C}$  to decompose it in a melter-decanter (4) to make about 8.83 bar working pressure [24].

In a smelter device melting of the hydrate on the grid acts as a refrigerant toward low-grade heat (hot water, low pressure steam, thermal water). The hydrate melts at a temperature of about  $30^{\circ}\text{C}$ , forming liquid chlorine and water. The separation of the formed mixture takes place due to the density difference between the liquid chlorine and water. Having had its heat content recovered, the water is recycled to the crystallizer. The liquid chlorine is sent to the evaporator (6) where it boils at  $4^{\circ}\text{C}$  and provides a cooling effect [24]. The chlorine gas returns to the hydrate forming reactor by the pressure difference due to the pressure drop during hydrate formation. The process occurring in the hydrate refrigeration unit including their nodal points are shown in the Figure 22 [24].

The driving force of the chlorine hydrate formation is the temperature difference  $\Delta T_1$  (A-K) between the equilibrium temperature of hydrate formation and the temperature of the suspension in the crystalliser under the same pressure. The equilibrium temperature depends on the pressure. The driving force of the melting process is the  $\Delta T_2$  (L-B) temperature difference between the decomposition temperature of the hydrate in the melter decanter and the equilibrium temperature of the hydrate formation at the same pressure [24]. If  $\Delta T_1$  is not below  $4^{\circ}\text{C}$ , it is sufficient for the producing cold water with a temperature of  $8-10^{\circ}\text{C}$  or suitable for the needs of air conditioning.

The heat balance of the installation in specific units can be expressed by equation (121).

$$q_0 + q_m + q_n + q_{mes} = q_{kr} \quad (121)$$

where  $q_0$  is the cooling capacity of 1 kg of refrigerant;  $q_m$  is the heat in summarized form conveyed from the hot source to the chlorine hydrate in the melter;  $q_n$ ,  $q_{mes}$  are the heat equivalents of pumping and mixing of the



where  $G_v$  is the weight of the initial water,  $G_g$  is the weight of the water in the hydrate,  $G_r$  is the weight of the remaining brine,  $\zeta_v$  is salt concentration in the source water,  $\zeta_g$  is the zero salt concentration in the hydrate,  $\zeta_r$  is the salt concentration in the brine.

The amount of water in hydrate is expressed by equation (123).

$$G_g = G_v - G_r \quad (123)$$

or, after expressing  $G_r$  and substituting it into the equation 122 one gets the equation (124).

$$G_g = G_v [1 - \zeta_v / \zeta_r] \quad (124)$$

The results shown, in Figure 23, demonstrate the change in the duration of the fresh water release, the temperature difference and the solute concentration in the reactor as well as the change in the equilibrium temperature of the hydrate formation and the freezing of the solution. As it can be seen, the yield of the fresh water is very high (80%) if the operations are performed even at 8°C, thus the process is easy, simple and cost effective [58].

### 8.5. Other fields of application

There is a strict correlation between the dissociation tension of the hydrate and the vapour tension of

the water in contact with the hydrate, and an approximate change of 40 Hgmm in the hydrate ( $\text{Cl}_2 \cdot 8\text{H}_2\text{O}$ ) tension at 0°C is proportional with the 0.1 Hgmm change in the water tension [44]. The measurement of the change in hydrate can be used for the determination of very small changes in water tension, e.g. during the determination of the molecular weights of dissolved materials in aqueous solutions [165]. Since the stoichiometric coefficient ( $n$ ) of the water in the formula of  $\text{Cl}_2 \cdot n\text{H}_2\text{O}$  is used in the equation (125), therefore the productg quotient and the ratio of the two pressures strongly depend on the value of  $n$ .

$$P_{\text{Cl}_2} P^n = \text{const.} \quad (125)$$

The hydrate formation can also be used as a versatile tool for the separation of chlorine from chlorine containing gases e.g. from mixtures of HCl,  $\text{Cl}_2$ ,  $\text{H}_2\text{O}$ ,  $\text{O}_2$ ,  $\text{N}_2$  and  $\text{CO}_2$  formed in Deacon process of chlorine manufacture [80]. Since the conversion of HCl by oxidation is around 80-90%, the residual amount of HCl gas has to be removed by water and the aqueous HCl solution can be cooled to low temperatures without freezing. Thus the highly cooled solution of alkali and alkaline earth metal chlorides as NaCl, KCl or  $\text{CaCl}_2$  can be used as reactants for hydrate formation. The hydrate forms as a yellowish green amorphous/crystalline mass suspended in the water [80].

This 10-30% hydrate containing slurry is recovered from the equipment and can be used as cooling media to absorb the reaction heat of the exothermic hydrate forming reaction of the next charge. It is an advantage of the process that the hydrate formation is reversible and can be easily decomposed by swinging the temperature/pressure. During the removal of the reaction heat of the hydrate formation, the hydrate slurry formed in another charge is warmed up and decomposed into chlorine and water [80].

In order to transport chlorine gas in tank cars or other thick-walled containers, the method of the hydrate formation is designed to produce solid hydrate before transportation, and liberation with warm water at the site of use. The wall thickness of a 45 m<sup>3</sup> tank car can be reduced from ~30 mm to ~10 mm. The conditionally stable hydrate or "hydrate ices" containing more than 9 moles of

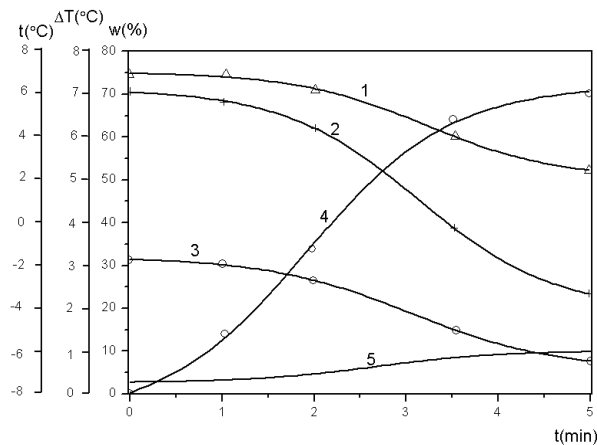


**Figure 23.** The results of the kinetics experiments showing the equilibrium temperature for the chlorine hydrate formation (1), temperature difference (2), freezing temperature of the solutions (3), yield of fresh water (4), concentration change on the solution in wt.% (5).

H<sub>2</sub>O per mole of chlorine are easily and safely transported between 0 and 14°C [166].

### 9. Safety considerations of the hydrate

The most widespread use of the chlorine hydrate is its use as electrode material of batteries in cars. Therefore the risk of this chlorine source in car ruptures has to be taken into consideration. Hydrogen evolution, rupturing, chlorine spills and evolution rate of chlorine from spills and other accidents were modeled and evaluated in detail.

Zinc hydrate batteries are usually condemned from an environmental point of view, due to the toxic nature of chlorine. This fear is usually overly emphasised. The efficient design [167] minimises the chances of any chlorine spill. The best way to encase the zinc chlorine batteries is a thin hollow shell filled with concentrated ammonia solution in water. This would make any rupture in the battery case highly visible because of the white cloud of ammonium chloride. A large amount of the escaping chlorine would be absorbed in this process [151, 167].

Since a fully charged battery for cars contains about 40.9 kg of chlorine in the form of hydrate, the potential accident situations were modeled [107] to study the distribution and the environmental hazards of the chlorine spills due to leaking, explosion, physical damage, and likes, and the effect of the heat transfer to environmental goods as pavement, wind and solar radiation on the evolution rate of chlorine from the spilled hydrate [107].

There are only a few liters of free chlorine gas in the batteries, therefore accidental leaking does not cause long term chlorine contamination which is affected by wind velocity and other meteorological conditions e.g. fog, cloud cover, solar radiation, temperature and its distribution around the car [107].

The decomposition rate of the hydrate depends very much on the outer temperature. Below 0°C, the water formed due to decomposition is essentially frozen onto the surface and prevents further decomposition, but increasing temperature increases the decomposition. The effect of main heat sources such as wind, solar radiation and pavement can be seen in Figure 24.

The total rate of the heat transfer to the hydrate is given in equation (126)

$$Q_T = Q_R A_R + Q_{cv} A_{cv} + Q_{cd} A_{cd} \quad (126)$$

where  $Q_T$  is the total rate of heat transfer to the hydrate,  $Q_R$  is the rate of heat transfer due to radiation per unit area of hydrate exposed to the radiation source,  $A_R$  is the area of hydrate exposed to the radiation source,  $Q_v$  is the convective heat flux to the surface,  $A_{cv}$  is the convective heat transfer area,  $Q_{cd}$  is the conductive heat flux to the hydrate from the floor, and  $A_{cd}$  is the area of contact between hydrate and floor.

The details of calculations and evaluations of each of the values in an accidental spill have been presented in detail [107]. Based on these calculations, the rates of chlorine release under normal conditions (I) and strong sunlight (II) are given in Table 26.

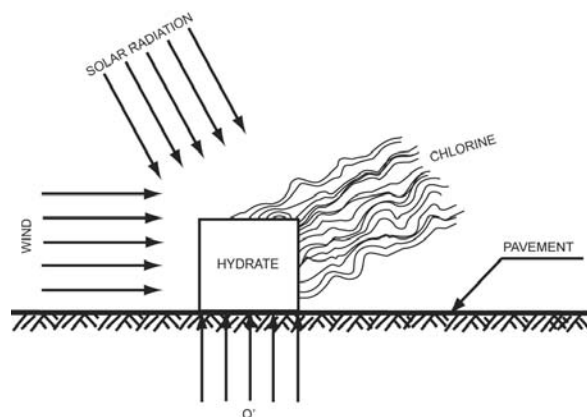


**Figure 24.** The effect of main heat sources on the hydrate spills.

**Table 26.** The rate (ml s<sup>-1</sup>) of release of chlorine gas from the hydrate.

Time after spilling min	Conditions	
	I	II
0	109	147
10	105	143
20	104	142
30	102	140

Suppose that the battery case is ruptured without an accident. Thus chlorine gas would leak without spilling of the hydrate. The total rate of heat transfer to the store is given by equation (127).

$$Q_T = Q_a + Q_s + Q_c \quad (127)$$

where  $Q_a$  is the heat transfer from the ambient,  $Q_s$  is the heat transfer from the sump, and  $Q_c$  is the heat transfer from the stack.

The detailed calculations were made by considering the heat transfer coefficients for all the system. The values of  $Q_a = 89.2$ ,  $Q_s = 7.634$  and  $Q_c = 20.6 \text{ kJ h}^{-1}$  sum up to  $117.39 \text{ kJ h}^{-1}$ . If  $\Delta H_l$  is the latent heat of the hydrate, the rate of chlorine release is expressed by equation (128).

$$V = \frac{QT}{\Delta H_l} = 10.5 \quad (128)$$

Thus equation (128) indicates that the amount of the chlorine released is less than  $11 \text{ cm}^3 \text{ s}^{-1}$  if the battery was completely ruptured [107].

Consequently, the use of the hydrate would not cause potential health and environmental hazard in the immediate vicinity of accidental spill. The solid hydrate does not spread along the ground like liquid chlorine and exposes much less surface area to ambient heat transfer sources.

Since the latent heat of the hydrate is 3.8 times higher than that of the liquid chlorine, therefore the smaller thermal driving force significantly reduces the rate of release of chlorine gas under all ambient conditions. In practical terms it means that the risk in case of the chlorine release is less by two orders of magnitude.

Experimental tests were carried out using a 50.4 kWh battery containing 41 kg of hydrate having a volume of  $126 \text{ dm}^3$  for the hydrate storage,  $28 \text{ dm}^3$  of vapour space in the cell stack and  $4 \text{ dm}^3$  vapour space in store. The overpressure was 0 and 17.2 kPa and the flow-rate of the chlorine gas was  $28 \text{ dm}^3 \text{ min}^{-1}$  and  $40 \text{ dm}^3 \text{ min}^{-1}$  respectively during charge and discharge [65].

The accidents of hydrate spill, the direct releases of chlorine vapour from the battery or hydrate decomposition within breached battery (by rupturing in the store wall due to collisions, piercing or uncontrollable increase in pressure),

hydrogen-chlorine explosion, and fire (electric fire, gasoline or diesel fuel fire) near the battery were tested. The accident places were outdoor road, road tunnel and garage or vehicle passenger compartment.

A special apparatus and detailed conditions for testing the hydrate formation in zinc chloride solutions had been published [65]. A number of laboratory spill tests were studied and the results were compared with the results of model calculations. Experimental field tests considered the ambient temperature, wind velocity, slab temperature, initial zinc chloride concentration, the weight of the chlorine in the battery, state of charge and [65].

The results showed that the major chlorine hazard associated with future widespread use of the chlorine hydrate batteries is large if the hydrate spills due to collisions. The extent of the downwind danger zone in this scenario depends upon the state of the battery charge, road and air temperatures, wind speed and turbulence level, local topography and the size of spill. The maximal dangerous distance from the site of the spill was 23 m downwind, with a subtended angle of about  $30^\circ$  around the mean wind direction.

The probability of a large hydrate spill is 2-7% in a collision at  $50 \text{ km h}^{-1}$ , which is same as the probability of fires or asphyxiations, but the fatality depends on the climate. The accidental chlorine release due to hydrogen-chlorine explosion or direct discharge of chlorine vapour from a partially breached battery should not cause any serious injuries. In road tunnel accidents at ventilation above  $6 \text{ m sec}^{-1}$  no dangerous cross section for an average chlorine concentration was produced [65].

The evolution of hydrogen as by-product at the zinc electrode could be an explosion hazard. However, it could be solved by installing a hydrogen chlorine reactor in the gas line, which slowly combines the hydrogen and the chlorine into hydrochloric acid under ultraviolet light [83, 167].

## ACKNOWLEDGEMENT

Thanks are due to various Journals for the permission to reproduce and use various figures in this review.

## REFERENCES

1. Davy, H. 1811, *Philos. Trans. Royal Soc. London*, 101, 155.
2. Scheele, C. W. 1774, *König Vetens, Akad. Stockholm*, 25, 89.
3. Gay-Lussac, L. J. and Thenard, L. J. 1809, *Memoires de Physique et de Chimie de la Societe d'Arcueil*, 2, 339.
4. Thenard, L. J. 1821, *Traite de Chimie, Theoretique and Practique*.
5. Faraday, M. 1823, *Quart. J. Sci.*, 15, 71.
6. Faraday, M. 1823, *Philos. Trans. Royal Soc. London*, 113, 160.
7. Faraday, M. 1823, *Philos. Mag.*, 62, 413.
8. Schiff, H. 1875, *Ber.*, 8, 419.
9. Biewend, E. 1838, *J. Prakt. Chem. [1]*, 15, 440.
10. Wöhler, F. 1853, *Liebig's Ann.*, 85, 374.
11. Nordenskjöld, A. K. 1874, *Bihang till Kongl. Svenska Vetenskaps-akad., handlingar*, 2, 3.
12. Rammelsberg, K. F. 1881, *Handbuch der Krystallographisch-Physikalischen Chemie*, p.19.
13. Ditte, A. 1882, *Comp. Rend.*, 95, 1283.
14. Maumene, G. 1883, *Bull. Soc. Chim. Fr.*, [2], 39, 397.
15. Villard, P. 1897, *Ann. Chim. Phys.*, [7], 11, 382.
16. Villard, P. 1894, *Compt. Rend.*, 119, 368.
17. Gay-Lussac, L. J. 1839, *Ann. Chim. Phys. [2]*, 70, 407.
18. Meyerhoffer, W. 1904, *J. Phys. Chem.*, 8, 571.
19. Isambert, F. 1878, *Compt. Rend.*, 86, 481.
20. Roozeboom, H. W. B. 1884, *Rec. Trav. Chim. Pays-Bas*, 3, 59.
21. Roozeboom, H. W. B. 1888, *Z. Phys. Chem.*, 2, 452.
22. Winkler, L. 1907, *Matematikai és Természettudományi Értesítő*, 25, 86.
23. Kótai, L., Balint, S., Gacs, I., Lakatos, Gy., Angyal, A. and Mehrotra, R. N. 2012, *Z. Anorg. Allgem. Chem.*, 638, 279.
24. Smirnov, L. F. and Kleshchunov, E. I. 1973, *Kholodil'naya Tekhnika*, No. (8), 19.
25. Bjorkman, H. K. and Symons, P. C. 1973, *Ger. Offen. DE 2313450*, 12 pp.
26. Jakowkin, A. A. 1897, *Ber.*, 30, 518.
27. Jakowkin, A. A. 1901, *Zhurnal Russkago Fiziko-Khimicheskago Obshchestva*, 32, 673.
28. Göpner, C. 1875, *Ber.*, 8, 287.
29. Fray, D. J. and Thomas, B. K. 1981, *Eur. Pat. Appl. EP 021809*, 12 pp.
30. Thomas, B. K. and Fray, D. J. 1982, *Chloride Electrometall., Proc. Symp.*, 21. Ed.: Parker, P. D., Publisher: Metall. Soc. AIME, Warrendale, Pa.
31. Bouzat, A. and Azinieres, L. 1923, *Compt. Rend.*, 177, 1444.
32. Bouzat, A. and Azinieres, L. 1924, *Bull. Soc. Chim. Fr.*, 35, 545.
33. Anwar-Ullah, S. 1932, *J. Chem. Soc.*, 1172.
34. Le Chatelier, H. 1884, *Compt. Rend.*, 99, 1074.
35. Bouzat, A. 1903, *Compt. Rend.*, 137, 322.
36. Tammann, G. and Krige, G. J. R. 1925, *Z. Anorg. Allgem. Chem.*, 146, 179.
37. Bozzo, A. T., Chen, H. S., Kass, J. R. and Barduhn, A. J. 1975, *Desalination*, 16, 303.
38. Fernandez, R., Carey, W. W., Bozzo, A. T., Barduhn, A. J., Gillam, W. S. and Johnson, S. 1967, *U. S. Dep. Interior, Office Saline Water Res. Develop. Progr. Rep.*, No. 229, 70 pp.
39. Bozzo, A. T., Chen, H.-S., Kass, J. R., Barduhn, A. J. and Editor: Delyannis, A. 1973, *Proc. Int. Symp. Fresh Water Sea*, 4<sup>th</sup>, 3, 437. Publisher: Work. Party Fresh Water Sea, Amaroussion, Greece.
40. Wilms, D. A. and Van Haute, A. A. 1973, *Desalination*, 12, 379.
41. Wilms, D. A., Van Haute, A. A. and Editor(s): Delyannis, A. 1970, *Proc. Int. Symp. Fresh Water Sea*, 3<sup>rd</sup>, 3, 117. Publisher: Work. Party Fresh Water Sea, Amaroussion, Greece.
42. Roozeboom, H. W. B. 1885, *Rec. Trav. Chim. Pays-Bas*, 4, 65.
43. Iskenderov, S. M. and Musaev, R. M. 1970, *Gazov Delo*, No. 12, 6.
44. Le Chatelier, H. 1885, *Compt. Rend.*, 101, 1484.
45. Goodwin, W. L. 1882, *Ber.*, 15, 3051.
46. Roozeboom, H. W. B. 1886, *Rec. Trav. Chim. Pays-Bas*, 5, 380.

47. Kotai, L., Bodi, F., Sebestyén, A. and Harfouch, S. 1991, *Hung. J. Ind. Chem.*, 19, 63.
48. Stackelberg, M. 1949, *Naturwiss.*, 17, 327.
49. Stackelberg, M. 1949, *Naturwiss.*, 17, 359.
50. Van der Waals, J. H. and Platteeuw, J. C. 1959, *Adv. Chem. Phys.*, 2, 1.
51. Cady, G. H. 1981, *J. Phys. Chem.*, 85, 3225.
52. Cady, G. H. 1983, *J. Phys. Chem.*, 87, 4437.
53. Stackelberg, M. and Müller, H. R. 1954, *Z. Elektrochem.*, 58(1), 25.
54. Byk, S. Sh. and Fomina, V. I. 1972, *Dokl. AN SSSR*, 204, 123.
55. Thomas, B. K. and Fray, D. J. 1981, *Metall. Trans. B.*, 12B, 559.
56. Bernal-Uruchurtu, M. I., Kerenskaya, G. and Janda, K. C. 2009, *Int. Rev. Phys. Chem.*, 28, 223.
57. Bjorkman, H. K. Jr. and Carr, P. 1984, *Ger. Offen. DE 3409411 A1*, 22 pp.
58. Kostyuk, V. I., Kopusov, V. I. and Levanyuk, T. A. 1966, *Vodosnab. Sanit. Tekhn. No. 5*, 15.
59. Karsten, C. J. B. 1846, *Karstens's Archiv*, 20, 45.
60. Macdonald, R. W. 1977, *J. Hazard. Mater.*, 2, 51.
61. Kotai, L., Harfouch, S., Bodi, F., Sebestyén, A., Müller, Zs., Papp, Gy. and Hung. Teljes, 1992, *HU 60455 A2*, 4 pp.
62. Allen, K. W. 1960, *J. Chem. Soc.*, 3162.
63. Symons, P. C. 1971, *Ger. Offen. DE 2128198*, 45 pp.
64. Symons, P. C. 1976, *US 3935024*, 14 pp. Continuation-in-part of U.S. 3, 713, 888.
65. Zalosh, R. G., Bajpai, S. N., Short, T. P. and Tsui, R. K. 1980, *Report, DOE(ET) 24-405-1*, pp.167.
66. Lunge, G. 1896, *Handbuch der Soda Industrie, Braunschweig*, 3, 271.
67. Dunning, C. L. 1951, *US 2553557*.
68. Mori, Y. and Suzuta, T. 2003, *Jpn. Kokai Tokkyo Koho, JP 2003261306 A*, 5 pp.
69. Bjorkman, H. K. 1973, *Ger. Offen.*, DE 2252224, 28 pp.
70. Symons, P. C. and Bjorkman, H. K. 1973, *Ger. Offen.*, DE 2255939, 35 pp.
71. Behling, H. L. 1978, *US 4115529*, 10 pp.
72. Redcay, A. K. 1957, *US 2785055*.
73. Nikitin, B. A. 1936, *Z. Anorg. Chem.*, 227, 81.
74. Nikitin, B. A. 1956, *Izb. Trudy, Izd. AN SSSR*, p.104.
75. Kislovskii, L. D. 1968, *Dokl. AN SSSR*, 183, 825.
76. de Vains, A. R. 1925, *Canadian Patent No. 24,616*.
77. Yabumoto, T. and Fujiwara, K. 1984, *Eur. Pat. Appl. EP 120491 A1*, 13 pp.
78. Yabumoto, T., Fujiwara, K., 1985, *Jpn. Kokai Tokkyo Koho, JP 60211780 A*, 3 pp.
79. Zeller, R. L., Fritts, S. D., Johnson, D. L., Carlson, K. J., Orosz, P. J. and Kaplin, R. B. 1999, *US 5985226 A*, 7 pp.
80. Bulan, A., Weber, R., Zank, J., Eble, A. and Werner, K. 2007, *PCT Int. Appl. WO 2007134720 A1*, 36 pp.
81. Anthonsen, J. W. 1975, *Acta Chem. Scand., Ser. A: Phys. Inorg. Chem.*, A29, 175.
82. Allen, K. W. 1959, *J. Chem. Soc.*, 4131.
83. Pelouze, J. 1843, *Ann. Chim. Phys.* [3], 7, 176.
84. Cournaux, M. and Guigues, P. 1891, *J. Pharm. Chim.*, [5], 23, 238.
85. Sebestyén, A., Szalkai, I., Bódi, F. and Kótai, L. 1992, *Proc. 42<sup>nd</sup> Can. Chem. Eng. Conf., Toronto, Ontario, Canada*, 277.
86. Kotai, L., Nagy, A., Bodi, F. and Sebestyén, A. 1999, *Hung. J. Ind. Chem.*, 27, 25.
87. Kim, J. T. and Jorne, J. 1978, *J. Electrochem. Soc.*, 125, 89.
88. Kótai, L. and Banerji, K. K. 2001, *Synth. React. Inorg. Met.-Org. Chem.*, 31, 491.
89. Kótai, L., Keszler, Á., Pató, J., Holly, S. and Banerji, K. K. 1999, *Indian J. Chem.* 38A, 966.
90. Kotai, L., Sajó I. E., Gacs, I., Sharma, P. K. and Banerji, K. K. 2007, *Z. Anorg. Allgem. Chem.*, 633, 1257.
91. Sajó, I. E., Kótai, L., Keresztury, G., Gács, I., Pokol, Gy., Kristóf, J., Soptrayanov, B., Petrusovski, V. M., Timpu, D. and Sharma, P. K. 2008, *Helv. Chim. Acta*, 91, 1646.
92. Kótai, L., Sajó, I. E., Fodor, J., Szabó, P., Jakab, E., Argay, Gy., Holly, S., Gács, I. and Banerji, K. K. 2005, *Transition Metal Chem.*, 30, 939.

93. Kótai, L., Banerji, K. K., Sajó, I. E., Kristóf, J., Sreedhar, B., Holly, S., Keresztury, G. and Rockenbauer, A. 2002, *Helv. Chim. Acta*, 85, 2316.
94. Kotai, L., Gacs, I., Sajo, I. E., Sharma, P. K. and Banerji, K. K. 2009, *Trends Inorg. Chem.*, 11, 25.
95. Pauling, L. and Marsh, R. E. 1952, *Proc. Natl. Acad. Sci. USA*, 38, 112.
96. Electrochlore, S. A. 1932, FR 752897.
97. Furukawa Electric Co., Ltd. Japan. 1984, *Jpn. Kokai Tokkyo Koho*, JP 59174504 A, 4 pp.
98. Fong, W. L., Catherino, H. A. and Kotch, R. J. 1983, *Fr. Demande* FR 2514569, 13 pp.
99. Behling, H. L. 1974, *Ger. Offen.* DE 2322568, 28 pp.
100. Fray, D. J. and Thomas, B. K. 1981, *Eur. Pat. Appl.* EP 22324, 10 pp.
101. Krusmann, B. H. 1929, *GWF, das Gas- und Wasserfach*, 77, 1046.
102. Wolfe, E. E. 1941, *Water Works and Sewerage*, 88, 40.
103. Kotai, L., Nagy, A., Bodi, F. and Sebestyen, A. 1999, *Hung. J. Ind. Chem.*, 27, 27.
104. O'Keeffe, K. F. R. and Braz. Pedido PI, 1982, BR 80-05767 A, 9 pp.
105. De Forcrand, M. 1901, *Compt. Rend.*, 133, 1304.
106. De Forcrand, M. 1903, *Ann. Chim. Phys.* [7], 29, 5.
107. Kodali, S., Henriksen, G. L., Whittlesey, C. C., Warde, C. J., Carr, P. and Symons, P. C. 1978, *US Department of Energy, Report COO-2966-2*, 60 pp.
108. de Forcrand M. 1902, *Comp. Rend.*, 134, 991.
109. Bouzat, A. 1905, *Ann. Chim. Phys.* [8], 4, 145.
110. Bouzat, A. 1923, *Compt. Rend.*, 176, 253.
111. Harris, I. 1943, *Nature (London, United Kingdom)*, 151, 309.
112. Barrer, R. M. and Stuart, W. I. 1957, *Proc. Roy. Soc.*, 243A, 172.
113. Saito, S. and Sadanaga, K. 1964, *Nihon Shiyo Gakkaishi*, 18, 180.
114. Tse, J. S., McKinnon, W. R. and Marchi, M. 1987, *J. Phys. Chem.*, 91, 4188.
115. Stackelberg, M. and Jahns, W. 1954, *Z. Elektrochem.*, 58, 162.
116. Lakatos, Gy., Sharma, P. K., Sharma, V., Balint, S. and Mehrotra, R. N. 2012, *Eur. Chem. Bull.*, 1, 4.
117. Korvezee, A. E. and Pieroen, A. P. 1962, *Rec. Trav. Chim. Pays-Bas*, 81, 385.
118. de Forcrand, M. 1902, *Compt. Rend.*, 135, 959.
119. Berthelot, M. A. 1875, *Ann. Chim. Phys.* [5], 5, 322.
120. Le Chatelier, H. 1886, *Compt. Rend.*, 103, 253.
121. De Forcrand, M. 1903, *Ann. Chim. Phys.* [7], 28, 384.
122. De Forcrand, M. 1903, *Ann. Chim. Phys.* [7], 28, 531.
123. Stackelberg, M. 1954, *Z. Elektrochem.*, 58, 104.
124. Ionescu, L. G. 1978, *Rev. Roum. Chim.*, 23, 45.
125. Kótai, L., Balint, S., Gacs, I., Lakatos, Gy., Angyal, A. and Mehrotra, R. N. 2012, *Z. Anorg. Allgem. Chem.*, 638, 648.
126. Martin, J. J. and Longpre, D. M. 1984, *J. Chem. Eng. Data*, 29, 466.
127. Peshkova, L. V. 1978, *Kholod. Tekhn. Tekhnol.*, 26, 64.
128. Bernal-Uruchurtu, M. I., Keresnkaya, G. and Janda, K. 2009, *Int. Rev. Phys. Chem.*, 28, 223.
129. Schönbein, C. F. 1847, *Pogg. Ann.*, 72, 450.
130. Anwar-Ullah, S. 1932, *J. Chem. Soc.* 1176.
131. Glew, D. N. and Rath, N. S. 1966, *J. Chem. Phys.*, 44, 1710.
132. Browstein, S., Davidson, D. W. and Fiat, D. 1967, *J. Chem. Phys.*, 46, 1454.
133. Afanas'ev, B. L., Klividze, V. I. and Malenkov, G. G. 1968, *Dokl. AN SSSR* 183, 360.
134. Sanyal, N. K., Verma, D. N. and Dixit, L. 1977, *Ind. J. Pure Appl. Phys.* 1977, 242.
135. Janda, K. C., Kerenskaya, G., Goldscheleger, I. U., Apkarian, V. A. and Fleischer, E. B. 2008, *Proc. 6<sup>th</sup> Int. Conf. Gas Hydrates, Vancouver, Canada*.
136. Tabushi, I., Kiyosuke, Y. and Yamamura, K. 1981, *Bull. Chem. Soc. Jpn.*, 54, 2260.

137. Schofield, D. P. and Jordan, K. D. 2007, *J. Phys. Chem. A*, 111, 7690.
138. Claussen, W. F. 1951, *J. Chem. Phys.*, 19, 259.
139. Stackelberg, M. and Müller, H. R. 1951, *J. Chem. Phys.*, 19, 1319.
140. Claussen, W. F. 1951, *J. Chem. Phys.*, 19, 662.
141. Stackelberg, M. and Müller, H. R. 1952, *Angew. Chem.*, 64, 423.
142. Claussen, W. F. 1951, *J. Chem. Phys.*, 19, 1425.
143. Müller, H. R. and Stackelberg, M. 1952, *Naturwiss.*, 39, 20.
144. Fujiwara, K. and Yabumoto, T. 1985, *Jpn. Kokai Tokkyo Koho*, JP 60160582 A, 4 pp.
145. Kótai, L., Bódi, F., Szelicsán, I., Szilágyi, R., Müller, Zs. and Sebestyén, A. 1991. HU 9101436A1, C07B-039/00.
146. Kótai, L., Harfouch, S., Sebestyén, A., Bodi, F., Bicskey, T., Papp, Gy. and Hung Teljes, 1992, HU 60440 A2, 4 pp.
147. Fukada, S. and Ono, M. 2005, *Jpn. Kokai Tokkyo Koho* JP 2005330192, 8 pp.
148. Letowski, F. K. and Guthrie, R. E. 1993, *S. African*, ZA 9200939 A, 14 pp.
149. Thomas, B. K. and Fray, D. J. 1981, *Metall. Trans. B: Process Metall.*, 12B(2), 281.
150. Whittlesey, C. C., Symons, P. C., Warde, C. J. and Brummet, B. D. 1979, *Proc. Intersoc. Energy Conversion Eng. Conf.*, 14<sup>th</sup> (Vol. 2), 2059.
151. Blevins, C. M. 1981-1982, *J. Power Sources*, 7, 121.
152. Will, F. G. and Spacil, H. S. 1977, *Proc. Electrochem. Soc.*, 77-6 (Proc. Symp. Electrode Mater. Processes Energy Convers. Storage), 713.
153. Carr, P., Chi, C. H. and Symons, P. C. 1978, *Proc. Power Sources Symp.* 28<sup>th</sup>, 23.
154. Begum, S. N. and Rao, P. V. V. 1985, *Bull. Electrochem.*, 1, 447.
155. Begum, S. N., Rao, P. V. V. and Udupa, H. V. K. 1981, *Proc. Seminar on Lead, Zinc and Cadmium Restrospect and Prospect*, Organized by ILZIC, Delhi.
156. Carr, P., Symons, P. C. and Aller, D. J. 1979, US 4146680, 5 pp.
157. Fujiwara, K. and Yabumoto, T. 1987, *Jpn. Kokai Tokkyo Koho*, JP 62002470 A, 4 pp.
158. Symons, P. C. 1977, US 4020238, 5 pp.
159. Horie, T., Ogino, H., Fujiwara, K. and Watakabe, Y. 1986, *Proc. Electrochem. Soc.*, 86-10 (Load Leveling Energy Conserv. Ind. Processes), 48.
160. Schacht, W. 1923, *Papier-Papierfab-rikant*, 21, 521.
161. Greene, U. T. 1973, US 3759784, 5 pp.
162. Fournier, R. 1923, *Papeterie*, 45, 374 and 418.
163. Smirnov, L. F. and Kleshchunov, E. I. 1972, SU355459.
164. Smirnov, L. F. and Rashkovskii, V. M. 1974, SU438, 848, Cl. F25D1/00.
165. Rosset, G. 1899, *Bull. Soc. Chim. Fr.*, 21, 361.
166. Mitchell, W. A., Barnes, H. M. and Kremzner, L. T. 1965, US 3217503, 5 pp. Continuation-in-part of US. 2975603 and 3086370.
167. Mitra, S. 1982, *J. Power Sources*, 8, 359.